(Ref: MoES/PAMC/H&C/45/2013-PC-II Dated 5th June, 2018)

IMPACT OF LU/LC AND CATCHMENT CHARACTERISTICS ON RUNOFF AND GROUNDWATER DYNAMICS OF WESTERN GHATS, KARNATAKA

NATIONAL INSTITUTE OF HYDROLOGY

HARD ROCK REGIONAL CENTER

BELAGAVI

2018-2022

COMPLETE STUDY TEAM

NIH Team

Dr. B.K.Purandara (PI)
Dr. B. Venkatesh
Dr. S.K.Jain

NIE Team

Dr. Yadupati Putty
Dr. Javeed M

TERI Team

Dr. Veerabasawant Reddy

COLLEGE OF FORESTERY Team

Prof. H. Shivanna

ABSTRACT

The present research is a unique attempt made to understand the linkages between land-use/land-cover (LU/LC) changes and hydrological responses of catchments located in Western Ghats mountain ranges, India. This region is the origin and primary catchment of many river in peninsular India. The lives of the majority of the rural population in the four southern states are thus critically dependent upon the watershed services provided by the Western Ghats Mountains forests. It is reported that, there has been an increased anthropogenic activities in this region, a rapid change in variety of land-use and land cover are taking place, which could have very significant impact on the water regime of the region, which include the soil-moisture storage, peak flow, ground water recharge, dry season flow. Therefore, there is need to understand the linkages between the change in land-use and land cover and components of the hydrological regime of the Western Ghats Mountains.

In order to understand the behavior of these linkages, a meso-scale watershed namely Biligi hole (catchment area of 28km^2) was selected at Kodigibil village in Siddapur taluk of Uttara Kannada district in Karnataka. Further three experimental watersheds with homogeneous land covers of natural forest, degraded forest and acacia plantation were selected within this meso-scale watershed. These watersheds were instrumented for measuring rainfall, evaporation, and temperature. The flows from these watersheds were measured by installing the notches. The soil moisture dynamics were captured by installing the soil moisture probes upto a depth of 1.50m. These instruments were measured at daily time step except the soil moisture probe which is read once a week.

The data collected were subjected to various analyses to understand the impact of land cover changes on the hydrologic regime of the region. The results obtained from the analyses of runoff show that, runoff was higher from degraded forests and did not last much longer whereas acacia watershed had runoff till the end of October. It is also observed that, despite the differences in the annual rainfall quantity, the percentage of precipitation converting into runoff remains consistent during the study period within each of the land covers. The cumulative plots of rain and runoff show a rank of degraded forest<acacia<forest in runoff generation. However, the residual cumulative plots (rainfall – runoff) indicate the reversal of the rank, i.e., forest<acacia<degraded forest. This indicate the quantity of water available as a catchment storage for the processes such as evapotranspiration and ground water storage

Soil moisture data were used to study both temporal and spatial variations. The temporal variation of soil moisture was influenced by rainfall and peak soil moisture generally preceded by peak rainfall. Degraded watershed responded relatively steeper for the rainfall events, whereas acacia and forest responded slowly and soil moisture built up was slower. The vertical profile soil moisture variation indicate that the soil moisture below 1.0m depth are higher under acacia plantation in comparison with the pattern observed under forest and degraded watersheds. This suggests the notion that the acacia

trees do have a shorter root system and utilize the soil moisture available within the top soil layer. Further, conceptual soil moisture model was used to explore the adoption of exotic plants. The results of the sensitivity analysis were indeed very encouraging to note that acacia species are able to successfully manage the inter-annual variability of climate along with the native forest in the region.

A Physically based Semi-Distributed rainfall-runoff model, namely Soil Water Analysis Tool (SWAT) was calibrated and validated for the selected watersheds under forest, degraded forest and acacia plantation using the observed flow series. This calibrated model was then used to simulate the impact of changing land cover on the daily flow in a meso-scale watershed namely, Biligi hole. The impact of land cover change was analyzed by steadily varying the % of land cover which leads to replace one land cover with another. The flows were characterized using the flow duration curve and by defining the indices such as low flow index (Q_{90}/Q_{50}) and high flow index (Q_{10}/Q_{50}). The results reveal that, the Biligi hole stream may flow only for 35% of time with increased peak flows, when the entire catchment is completely degraded. On the contrary, the combination of forest and acacia plantation can sustain the flow upto about 85% of the time with a moderated peak discharge. Further, information regarding the groundwater recharge under different land use was also obtained from the model. The result show that, the rate of groundwater recharge follows Forest>Acacia>Degraded land uses. However, these results were for first order stream and are verified by up-scaling the results to bigger catchment.

The up-scaling of the results obtained through hydrological modeling specially, rate groundwater recharge was verified through MODFLOW model. The up-scaling exercise was carried out for 2 catchment, namely Barchi catchment (<50 Km2) and Malaprabha (452 Km2), having similar morphological characteristics and rainfall regime. The rate of groundwater recharge obtained through hydrological modeling with the observed groundwater levels in these two catchments. The error of groundwater level matching was around 5%-10%.

Based on the results obtained through the analysis of runoff, soil moisture series from natural forest, degraded forest and acacia plantation and by using the conceptual rainfall-runoff model for predicting the impact of land cover changes, it can be concluded that, the acacia plants can help in restoring the hydrological processes which were lost due to the deterioration of the landscape. Also, the results suggest that the exotic species such as acacia plants can be an alternative replacement to the natural forest from the hydrologic perspective.

TABLE OF CONTENTS

SECTION- II

STUDIES FROM SOUTHERN WESTERN GHATS - KODAGU

LIST OF FIGURES

List of Tables

CHAPTER-I INTRODUCTION

1.0 INTRODUCTION

In the past few decades man made changes created havocs all over the world. One of the most conspicuous changes observed is with regard to land use land cover change which occur due to the population explosion, industrialization and agriculture revolution (Verbesselt et al., 2010; Vogelmann et al., 2016) and agriculture expansion is a major cause of the extensive changes in LULC thereby reducing the rate of percolation to groundwater (Scanlon et al., 2005). Groundwater-fed irrigated agriculture can have detrimental effect on groundwater, including a reduction in recharge and declination of water table (Han et al., 2017; Mojid et al., 2019).

The land area of the humid tropics includes a wide range of geological build which interacts with the prevailing climate to produce distinctive geomorphological features and hydrogeological regimes. The spatial variation of precipitation in the humid tropics can be very high, with variation in altitude and in distance from the ocean, for example. Rainfall and excess rainfall (groundwater recharge in areas of highly permeable soil) can also exhibit marked temporal variation. In the humid tropics, the mechanism of groundwater recharge and discharge are often closely interrelated and exert a strong influence on the overall surface water behavior of a catchment in terms of rainfall-runoff response. Throughout most of the non-alluvial areas of the humid tropics, thick lateritic soil profiles have developed as a result of deep weathering and strong leaching by infiltrating meteoric water. Although the characteristics of the residual mantle of alteration vary significantly with underlying geology, this layer normally includes some horizons of low vertical permeability. Given the frequent occurrence of high intensity precipitation, excess rainfall often exceeds the soil profile infiltration capacity and results in temporary soil-water perching. In consequence, a variable (and often high) proportion of the excess rainfall generates shallow soil interflow or overland flow to land surface depressions, from it either evaporates or runs off in surface water courses. This phenomenon further complicates the estimation of diffuse aquifer recharge in many hydrogeological environments of the humid tropics.

The natural vegetation of the humid tropics is equatorial or tropical rainforest, or the more richly-vegetated type of savannah grassland. All these vegetation groups include phreatophytic species which, at least in part, draw their moisture from the water table and as a result, evaporate large quantities of groundwater. Phreatic evapotranspiration is a very common process throughout areas with groundwater table depths of less than 5m, and can continue when it is at a substantially greater

depth. It is this process which keeps these areas green during the dry season, when the available shallow soil moisture has been exhausted. The rate of aquifer discharge via this route can be difficult to calculate, however, because of uncertainties and inaccuracies in the overall hydrological balance of such areas. If the natural forest vegetation is cleared for agricultural activities, excess rainfall will in general, increase as a result of reductions in evapotranspiration and perhaps also by excess supplementary irrigation in the dry season. Whether this, in turn will result in an increased rate of groundwater recharge will depend upon the overall soil-profile infiltration capacity and on the depth to the groundwater table.

Through history, intense human activities, including industrialization, mining, urbanization, agriculture, damming, etc., have resulted in significant and clear changes in the landscape with impact on the water balance of surface and groundwater systems. Land use change also has a direct influence on the catchment hydrology. This influence can be determined by a change in river discharge, or may be predicted by hydrological modeling studies. If a fully distributed model is used and combined with land use change scenarios, it allows for assessing the impact of the change on groundwater recharge, baseflow and total river discharge. Land use/land cover significantly influences the amount of precipitation that reaches the ground due to man made changes and interventions. In the earlier studies, the land-use change impact on groundwater has mainly focused on the change in water quality thereby neglecting changes in quantity.

It is reported that, currently the rate of deforestation is nearly 30 ha per minute (Myers, 1993). Therefore, both the rate and magnitude of water movement through trees and the forests they compose is being significantly altered (Bruijnzeel, 2000). In order to address the issue of removing the trees on local and regional water balances, we need to understand the physiology, ecology and environmental factors that influence water loss from trees and forested lands. In addition, as stands are reforested, either by tree planting or by the process of forest succession, it is necessary to relate the tree age with water use efficiency which will have significant influence on the water use estimates of a given tree during the course of a day, growing season, and a life time. In the presence of forest, water movement and water action are different because of the canopy, forest floor and organic rich soils. Forest on one hand due to their deep rooting system and added contribution to organic matter content of the soil have been generally found to improve the soil structure resulting in better surface recharge conditions. On the other hand the evapotranspiration requirements of the forest have been found relatively higher than other land uses. Therefore, the net effect of forests on

ground water regime becomes an important issue for investigation by hydrologists which in turn is useful for water resources planners and environmentalists.

Estimation of recharge is of importance for the assessment of ground water resources of an area. In temperate and tropical regions, rainfall is the main source of groundwater recharge. In addition to this, other important sources of recharge are influent seepage from rivers and canals, inter-basin groundwater flow and return flow from irrigation. The estimation of groundwater recharge in crystalline and other hard rocks is faced with greater problems as compared with sedimentary rock aquifers, on account of their heterogeneity. The groundwater residence time in the crystalline rocks may vary from only a few years in shallow weathered horizons to as much as several thousand years in deep fractures.

The recharge in volcanic rocks can be estimated by the same methods as in other rocks. The main source of recharge is the direct infiltration from precipitation, seepage from streams and return flow from irrigation. Recharge in old volcanics is generally low which is attributed to weathering effects and low permeability of rocks resulting in high runoff. In the Deccan traps, based on water balance and water-table fluctuation methods, groundwater recharge is estimated to vary from 10% to 20% of the rainfall (Adyalkar and Rao, 1979). Even in high rainfall areas, recharge is low due to the high relief and impervious nature of the Deccan traps. In arid regions of different parts of the World, the groundwater recharge in basaltic terrains is reported to be about 10% of the annual rainfall (UNESCO, 1975). Deeper confined and semi-confined aquifers may be recharged by leakage from shallow horizons through vertical fractures, and partly by lateral subsurface flow from outcrop areas.

Currently, mathematical models are used in all branches of science and engineering. In hydrogeology, by contrast, we deal with systems that were designed by nature. These natural systems are nearly always highly complex in their composition and arrangement of component materials. We can test these systems and materials by drilling holes, testing cores, analyzing water samples, measuring water levels and applying geophysical techniques. Even then it is merely a small window of information, a limited picture of the real world that extends beneath our feet (Kumar, 1996).

The mathematical model is an important tool in water resources planning and management. Surface water and groundwater models have been used to estimate water balance managing and allocating. According to the convenience of the model development, classical surface

and groundwater models were mostly simulated separately and supposed to use simple interaction of surface-subsurface water in their model boundary. When groundwater use was hugely rising and hydrological elements of whole water system are needed to fully manage, the coupling simulation of both surface and subsurface simulation was then developed. Coupling approach has been applied in specific case studies (Charles and Peter, 2004) surface and subsurface models have been joined, including fully-coupling of SWAT and MODFLOW (Il-Moon Chung, 2006). However the fully-coupling of surface and subsurface models are still complicated for practical application and data preparation. The semi-coupling is another approach for practical simulation (Bejranonda, 2008). In this study, SWAT and MODFLOW are used together and applied to various basins in the hard rock regions of Karnataka. Visual MODFLOW is highly capable and user-friendly model for sub-surface modelling whereas SWAT model has great surface modelling capabilities. However, these models are completely different in nature from each other, yet, if used together, the hydrology of the entire basin can be represented and studied efficiently. The basic idea of semi-coupling of SWAT and MODFLOW in this study was to use groundwater recharge and evapotranspiration as the coupling parameters. The SWAT model was applied for estimation of groundwater recharge and evapotranspiration. The output obtained from SWAT (recharge and ET) was then used as input for Visual MODFLOW. As a result, the surface and sub-surface hydrology of the basins of the hard rock regions can be studied.

The humid tropics cover one fifth of the Earth's land surface and generate the greatest amount of run-off of any biome globally (Fekete, Vörösmarty, & Grabs, 2002; Wohl et al., 2012). Three billion people worldwide live in humid tropical regions and depend on available water resources of tropical watersheds (State of the Tropics, 2014). Therefore, we need to properly manage watershed “services,” defined as the benefits that humans obtain from ecosystems at the scale of single watersheds or that are derived from processes occurring within the physiographic boundaries of a watershed. These services are essential to humans and range from water supply (e.g., for municipal, agricultural, or environmental uses) to water-risk mitigation (e.g., flood reduction and regulation of erosion) to cultural benefits (e.g., religious and recreation) and ecological functions (e.g., ecological flow regimes, contribution to the nutrient cycling, or habitat creation).

1.1 Groundwater use Pattern India

India is the largest user of groundwater in the world. Total annual groundwater abstraction in India was estimated to be about 245 km^3 in 2011 (CGWB, 2014a), out of which about 90% was consumed for irrigation (Saha et al., 2018). This high usage defines the groundwater irrigation economy on which India's national food security depends (Hira, 2009, Shankar et al., 2011, Smilovic et al., 2015, Zaveri et al., 2016, Cao and Roy, 2020). Expansion of irrigated agriculture and increased reliance on groundwater abstraction for irrigation has led to marked exploitation of this aquifer system, thus threatening the sustainability of the aquifer and agricultural productivity for current and future generations (Gleeson et al., 2020).

1.2 Placing the Western Ghats of India in the Context of the Degraded Land Cover and Implication of Reforestation

The Western Ghat region is the origin and primary catchment of many rivers (west and east flowing) in peninsular India. The lives of the majority of the rural population in the four southern states (Kerala, Tamil Nadu, Andhra Pradesh and Karnataka) plus parts of Maharashtra are thus critically dependent upon the watershed services provided by the Western Ghat forests. The portion of the Western Ghat that lies in Karnataka state, (locally named as Sahayadri Mountains, from here on it is referred as Sahayadri Mountains) contains the major portion of the forests. It is reported that, there has been an increased anthropogenic activities in the Sahayadri mountain region, a rapid change in variety of land-use and land cover are taking place, which could have very significant impact on the water regime of the region, which includes the baseflow and groundwater recharge.

In contrast to the Amazon basin where there has been a recent concentration of hydrological studies, no such studies have been carried out in Sahayadri mountain region. The Sahayadri mountain region is undergoing degradation of forests at *multi-decadal to century time scales* (Blanchart and Julka, 1997; Menon and Bawa, 1998; Pomeroy *et al*, 2003; Pontius and Pacheco, 2004) resulting a mosaic of complex land cover scenario. Patches of remnant forest, which are less disturbed and less used by people are at one end of the disturbance

gradient and at the other end are a heterogeneous category of disturbed and heavily used forest which consist of open forest, grassland and savannah woodlands. Livestock grazing, fuel wood and fodder extraction, fire as well as extraction of leaf-manure are major land-uses in these highly disturbed or degraded sites which provide local communities with substantial provisional ecosystem services (Millennium Ecosystem Assessment, 2005) and sustain many livelihoods (Lele, 1993; Rai, 2004). Further within the humid tropics, Rai (1999) estimated that nearly 80% of forestation using both native and exotic species was taking place in India in general and in Sahayadri mountain range in particular. Many degraded patches of land cover have been reforested with *Tectona Grandis* plantations, pre-1980 and exotic *Acacia Auriculiformes* plantations, post-1980 (hereon referred to as *'Acacia'*) (Pomeroy *et al*, 2003; Pontius and Pacheco, 2004; Ramachandra et al 2004). Consequently the Sahayadri mountain range offers an opportunity to evaluate the impact of land cover change on hydrologic regime arouse due to (i) forest land use and degradation and (ii) forestation over previously degraded land, relative to less used native forest.

There have been few sparse attempt made to understand the impact of land cover changes on hydrologic regime in Western Ghat. In one such attempt Samraj, et al., (1998) observed reduction in annual water yield of the order of 16% to 25.4% in the eucalyptus watershed over natural grassland watersheds located in Glemorgan in Nilgiris, India during the first and second rotation. The maximum reduction in runoff was observed during the July to October. Later Sikka, et.al., (2003) reported a reduction in the low flow volume as well as peak flow using longer period data from the same watersheds referred above. The significant reduction in low flow as a result of decline in base flow could be predicted with LFI decreasing by 2.0 and 3.75 times in the first and second rotation respectively. The studies reported above have examined the impact of eucalyptus on hydrologic regime of the region. There are no comprehensive studies carried out to evaluate the impact of acacia plants on the water availability in the region in general and in particularly from the Sahayadri mountain part of Karantaka and in particularly from Uttara Kannada district wherein acacia species have been used for large scale afforestation activities.

Hence, the main objective of this study is to understand the potential groundwater response to land use change, particularly with respect to an increase in forest cover within well capture zones. Due

to the long time scales involved in land-use change from short-rooted vegetation to mature trees, this study will adopt a modelling approach to enable a quantitative comparison of different forest cover/land-use change scenarios. A regional groundwater flow model will be developed to represent the groundwater flow system under different forest covers/land covers (natural forest, degraded lands and plantation forests) in a selected watershed of Western Ghats region (Belgaum and Uttara Kannada districts, Karnataka, India).

1.3 Uttarkannada District and Its Significance To The Present Study

Uttara-Kannada district is situated in the north-western sector of Karnataka state. Topographically the district could be divided into three distinct zones; the coastal belt, the central belt consisting of the hills and valleys of the Sahayadri range and the transition zone consisting of eastern table lands. The district being a forest rich region, its farming systems have been adopted to the local conditions. The main crops being Arecanut and Paddy. Due to the integration of Uttara Kannada with the wider market economy, most of the forest area was cleared and brought under the commercial crop. While the commercial pressure has mounted, so have the local demands of the rural population which resulted in depletion of minor forest. The degraded land, so created was considered for the plantation activities under social forest scheme. Initially, these areas were planted with the eucalyptus trees. During the early 1990's, when the local media reported that the eucalyptus trees are mining the ground water (Vandana Shiva & Bhandopadyaya, 1983) and proved by the experiments carried out by the Calder and his group in Karnataka (Calder, et.al., 1992), the Karnataka state shifted its afforestation strategy by adopting another exotic species such as Acacia auriculiformis and Casuarina. The early experiments have shown the survival rate of these exotic species as high as 90% in this region (Saxena et al., 1997 and Bhat, et al., 2002b). This has encouraged the Karnataka Forest Department to adopt and implement this as common species. The Uttarakannada was one of the major district in which the acacia auriculiformis was planted at almost all degraded lands. The economy of the rural people is dependent of the commercial crops such as Arecanut and Paddy. In the recent past, it has been reported by the media about the scarcity of water during the summer months and its effect of the summer paddy being grown in the region. And at times, the reduction of

water is reasoned as the result of excessive plantation of acacia in the district. But there are no scientific studies to comprehend the impact of the acacia plantation on the hydrologic regime in the area. The region provides the contrasting climate, physiographic setup and the complex land cover and the necessity of the study to understand the impact of exotic species on the hydrological regime of the area.

Keeping in view of the above issues, the present research is proposed to examine the poorly understood link between land-use/land cover changes on watershed services at local and at meso scale in the Sahayadri mountain region. The study will be undertaken in the Uttara Kannada district of Karnataka, where grass land and degraded land have been replaced by the monoculture forest. The hydrological implication of such an extensive plantation has not been studied. Therefore, a comprehensive study is proposed to look into possible changes in the hydrologic regime in the area due to exotic species plantation with the following objectives;

1.4 Research Objectives:

1. To investigate the influence of catchment characteristics - physiographic and climatic, on the dynamics of runoff and groundwater and establish the major controls in a region where Horton's overland flow is only a minor component of stream runoff;
2. To quantify hydrologic responses such as rainfall-runoff and evapo-transpiration under different forest covers/land covers (natural forest, degraded land and acacia plantation) at larger spatial and temporal scales including the impact of forestry on peak-flows and base-flows.
3. To understand the effects of evapotranspiration on base flow to changes in forest landscapes and interacting responses (surface and groundwater) to forest management and disturbance.
4. To quantify the infiltration capacity and saturated hydraulic conductivity under different land covers which will give an account of the impact of afforestation and deforestation on soil hydrologic regimes. This will help in understanding the role of preferential flow path-ways in ground water movement and recharge characteristics,

5. To estimate the groundwater recharge under different land use/land covers using conventional techniques (based on field and laboratory investigations carried out during the study period).
6. To assess the association between forest cover/land use and the groundwater system quantitatively and in a spatially distributed manner using Wetspass and MODFLOW
7. To "scale up" findings from small spatial and short time scales to larger spatial and longer time scales

The advantage of landscape perspective on forest hydrology is because it links scientific principles from plot, process, and small watershed scales with indirect and interacting hydrologic responses at larger spatial scales (i.e., within drainage basins and across large climatic and physiographic regions) in forest landscapes that are changing over long time scales. Within watersheds, forests are located in headwaters and hill slopes and it fulfil different water-related functions in the downstream areas including riparian zones depending on their location. A key unresolved issue in forest hydrology is how to "scale up" findings from one part of a watershed to larger areas or the whole watershed. Keeping in mind the main objectives of the present research, it was decided to identify a catchment of smaller size (in few hectares) in parts of Sahyadri mountain and upscale the characteristics to a more dynamic catchment such as Malaprabha or any other catchment having similar hydrological characteristics as that of the experimental catchment. The study is proposed mainly on the detailed hydrological investigations and observations at both landscape scale and watershed/catchment scale. Since experimental studies at the catchment scale is time-consuming and expensive, three smaller watersheds (5-10 ha size) were identified within a Biligihole catchment having about 28 sq. km area (a part of Aghanashini catchment).

CHAPTER –II LITERATURE REVIEW

2.0 Literature Review

2.1 International Scenario

Although many researchers around the world have been working on land use change and its impact on groundwater recharge, as far as the author is aware, very little study has been conducted on this issue in the context of Bangladesh. Groundwater is the primary, and often the only, safe source of drinking, industry and agricultural water in Bangladesh, as surface water is scarce and inconsistent (Qureshi et al., 2015; Mustafa et al., 2017). In particular, the use of groundwater is higher in the north-western region compared to other regions of the country (Shahid and Hazarika, 2010). For example, the amount of groundwater irrigation is 11 km^3 in the northwestern region compared to around 14 km^3 for all the remaining regions combined (CSIRO et al., 2014). However, this precious resource is under constant threats of overexploitation and pollution in this region. Notably in the last decade, this area has seen a substantial decline in the water table with 35 out of 36 groundwater monitoring wells in Rajshahi District showing falling water table trends, threatening the sustainability of irrigation water use (Jahan et al., 2010; Mustafa et al., 2019; Mojid et al., 2019). Due to excessive and inefficient use, the water table has fallen and depleted beyond an exploitable depth in some part of the north-western region of Bangladesh (Habiba et al., 2012). The reason behind the declining north-western water table and the role of anthropogenic factors, such as climate change, in the decline is currently unclear (Mojid et al., 2019). Recently, Mustafa et al. (2017) reported that groundwater levels in the area decreased by almost 5 m between 1979 and 2007 and inferred that climate change was not a significant factor in the groundwater level drop. They also examined the influence of land cover changes between 1990 and 2010 on groundwater recharge and found that the effects were not significant at the large basin scale. However, they identified land cover changes due to urbanization as one of the influencing factors for groundwater drought and depletion, along with groundwater abstraction, and outlined the importance of further study at the regional level. Urbanization dominated land use change has been observed to have a significant influence on groundwater recharge, even greater than climate change in a few studies (Ghimire et al., 2021). In recent decades, rapid economic growth and unprecedented urbanization have caused significant changes in LULC patterns. Shi et al. (2018) reported that the LULC change in recent decades is significantly higher than in previous decades. Dey et al. (2021) found a 15% increase in urbanized settlements in Rajshahi city between 2000 and 2020 and predicted a 30% increase in urbanization by 2040, compared to the city in 2000. Mojid and Mainuddin (2021) suggested that increased urbanization might have an effect on declining groundwater recharge. However, the effect of this unprecedented urbanization in recent years on the groundwater

system of north-western Bangladesh is still unknown but is thought to be important for ensuring the sustainable management of the overexploited aquifer. Moreover, identification of the effects of regional land cover changes, considering spatial, long-term temporal and seasonal effects, is vital. Huq et al. (2019) reported that land use and land cover in southern Bangladesh significantly change between the dry and wet seasons because of the non-uniform rainfall distribution of the tropical climate. However, the details of seasonal land cover changes in the north-western part of Bangladesh and their effect on the groundwater system are still largely unknown. To the best of the authors' knowledge, limited study has been done so far on seasonal land cover changes and their effect on groundwater recharge in north-western Bangladesh. Hence, the reliable assessment of human induced land use change and its influence on groundwater recharge is necessary for understanding groundwater flow dynamics.

The integration of long-term temporal and seasonal inconsistencies in land cover is important for estimating groundwater recharge, considering the sensitivity of recharge to varying land types (Dragoni and Sukhija, 2008). Recharge is also dependent on a spatially varied climate as well as hydrogeological factors like rainfall, soil and topography (Batelaan and De Smedt, 2007). Thus, consideration of the spatially distributed physical characteristics of a basin is important for recharge computation to increase the reliability of the simulated value (Gebremeskel and Kebede, 2017). To achieve this, a number of hydrological models have been developed based on concepts such as water balance and water table fluctuation (Ahmadi et al., 2012). WetSpass (Water and Energy Transfer between Soil, Plants and Atmosphere under a quasi-Steady State) is a widely used spatially distributed water balance model (Batelaan and De Smedt, 2001). It has been successfully applied across the world in different climates (Pan et al., 2011; Dams et al., 2013; Zomlot et al., 2015; Armanuos et al., 2016; Gebremeskel and Kebede, 2017; Salem et al., 2019). The original model can only support seasonal temporal resolution. To implement monthly support, WetSpass-M was developed (Abdollahi et al., 2017), which has been used previously in north-western Bangladesh (Mustafa et al., 2017, 2018, 2019, 2020).

The use of such models requires spatially distributed input data in raster form. The resolution of the input data can play a key role in analyses (Arnone et al., 2016) as the degree of raster data detail is dependent on the raster resolution. A number of studies have found that raster cell resolution can be a significant determinant for model performance, using inputs including land use and land cover, soil and digital elevation models (DEM) (Jantz and Goetz, 2005; Ménard and Marceau, 2005; Samat, 2006; Chaplot, 2014; Yang et al., 2014; Zhang et al., 2014; Jin et al., 2015; Tan et

al., 2015; López-Vicente and Álvarez, 2018; Fan et al., 2021). At the same time, the resolution of input data affects the accuracy of input variables, possibly leading to various degrees of uncertainty (Zhang et al., 2014; Gires et al., 2015). This issue can be explained through the concept of the modifiable areal unit problem, which discusses "the variation in results that can often be obtained when data for one set of areal units are progressively aggregated into fewer and larger units for analysis" (Openshaw, 1983). Land use classes are often small in size (such as urban and rural built-up areas) and, as such, detailed spatial data from high resolution maps is required for precise information on the physical characteristics of that land use class (Díaz-Pacheco et al., 2018). At a broader resolution, a small land use unit might be absent, leading to lower accuracy in result prediction than in its finer counterpart (Cama et al., 2016). The inaccuracies resulting from low detailed spatial data can cause the misinterpretation and incorrect analysis of terrain information included in the raster inputs. Inputs with incorrect information may, in turn, create uncertainties in model-predicted results. For example, the misclassification of land cover can lead to incorrect parameterization of the land classes, resulting in inaccurate recharge estimation (Zomlot et al., 2017). High resolution can also be advantageous since it can be modified into a lower resolution if necessary. Even though researchers have recognized the value of resolution in modeling (Ménard and Marceau, 2005; van Delden et al., 2011), specific studies inferring the influence of inputs at different spatial resolutions in groundwater recharge simulation are still lacking.

On the other hand, finer resolutions do not always lead to the best modeling performance (Ménard and Marceau, 2005; Lee et al., 2010; Ye et al., 2011; Yang et al., 2014; Arnone et al., 2016; Díaz-Pacheco et al., 2018). Increased computational load can be an issue with finer resolution data (Maleika, 2015). At a higher resolution, the number of cells to process increases, raising the amount of computational analysis needed and, thus, the time requirement, whereas lower raster resolution requires less computational power, albeit at the cost of model accuracy (Calder and Mayer, 2003). The lower resolution of rasters also improves the model execution period due to the decreased quantity of data (Munoth and Goyal, 2019). Overall, the comparison between high and low resolution of raster data creates a dilemma of prioritizing result accuracy against computational requirements. In fields such as policy planning, this is important, as results are often needed in a short time without the sufficient availability of powerful computing hardware. Hence, more research is needed to address the computational requirement and desired degree of accuracy in modeling considering the study objectives and applications.

The general aim of this study is to examine the effects of land use and land cover changes on groundwater recharge in north-western Bangladesh, comparing LULC changes between 2006 and 2016 for long-term temporal changes and between wet and dry for seasonal changes. To achieve this, the water balance model WetSpass-M was used to simulate spatially distributed groundwater recharge under different LULC conditions. In doing this, the specific objectives are to (1) identify and quantify the changes in different land cover types over the study period using remote sensing data, (2) assess the relation of groundwater recharge with rainfall, soil texture and land cover class and (3) analyze the influence of long-term temporal and seasonal LULC changes on groundwater recharge. In addition, the scaling effect of different spatial resolutions on groundwater recharge simulation will be evaluated using inputs at different resolutions. The findings of the study will be useful for strategy and policy planning regarding land and water resource management in the north-western part of Bangladesh and beyond.

Zare et al (2014) using MODFLOW predicted the extent of waterlogging in Miandaraband plain of Iran over a period of 10 years (from the start of the network operation). Due to the construction of the network of irrigation/drainage canals of the Gavoshan dam, the region experienced raised groundwater table and suffered from the problem of waterlogging, as the groundwater extraction in the region was low. Rostamian et al (2014) used SWAT to model runoff and sediments in Beheshtabad and Vanak watersheds in the northern Karun catchment in central Iran. Also, Sequential Uncertainty Fitting (SUFI2) interface within SWAT-CUP (Calibration and uncertainty Programs) package was used for calibration and uncertainty analysis of the model. Both basins were mostly agricultural, where majority of the area was rainfed. However, the region was severely affected by soil erosion, which had adversely affected the agricultural activities due to land degradation. The model was applied to both the mountainous watersheds to estimate sediment loss and runoff. The results of streamflow discharge were found to be satisfactory for the watersheds, except for a few months. However, the model was found to simulate runoff better than the sediments. The probable reason as stated may be lack of discharge data, poor characterization of snowmelt processes and groundwater-river interaction. They concluded that the model may prove useful for assessment different land management options and selection of a suitable management policy.

Albhaisi (2013) made an attempt to understand the impact of land use/land cover in the upper Berg catchment, Western Cape, South Africa. The catchment has undergone many changes in recent years, not least of all the construction of a dam on the upper reach. To reduce water loss due to evapotranspiration, non-native hill slope vegetation upstream of the Berg River Dam was cut down.

It was hypothesised that recharge has been increased due to this change in vegetation. Multi-temporal Landsat images from 1984, 1992, 2002, and 2008 were used to predict the impact land use changes on groundwater recharge. Baier et al (2013) attempted to use mathematical modelling for simulating groundwater and heat flow in complex hydrogeological structures (presence of fault zones) of the Benesov-Usti aquifer system in the Czech Republic. MODFLOW HUF package along with MT3DMS was used for this study. The study revealed that the conventional approach of using MODFLOW with BCF and LPF packages to simulate heat flow failed due to simplified discretization of the model domain. Hence, the model was discretized into 21 vertical layers in order to represent the complex and detailed hydrogeology of the region using HUF package of MODFLOW. Ehsan Shirkhani et al (2013) performed quantitative simulation of Mahidasht plain water table in Kermanshah province of Iran using Visual MODFLOW. The modelling period for this study was chosen as one day, which was the 1st of October, 2010. Since, this model was developed as a steady state model, the hydrograph data of the observation wells (Mahidasht plain) finds a constant regime in the water years 2010-2011. Further, the model was run and water budget of the study area was determined using MODFLOW. The simulated water levels were found to match with the observed values. However, the water budget suggested loss of aquifer water, which may lead to lowered groundwater table, increased water scarcity in the region as well as cause additional problems of water salinity. De Condappa et al (2012) applied SWAT and a groundwater model to assess the impact of Agriculture Water Management (AWM) in the Jaldhaka watershed, a tributary of Brahmaputra River, located in India, Bhutan and Bangladesh. The lumped groundwater model used in the study was developed by Tomer et al. (2010) and was based on a combination of groundwater budget and water table fluctuation technique. Haque et al (2012) applied the modeling technique for reliable assessment of the groundwater resource for future development in Rajshahi City Corporation area in Bangladesh. Youssef et al (2012) applied MODFLOW for planning and managing the groundwater problems and for predicting the change in the groundwater system of the El-Moghra Aquifer in Wadi El-Farigh (Egypt). The study area is considered as a water scarce region with low rainfall, high evaporation, long dry summers and short warm winters. The aim of this study was to forecast the impact of the groundwater irrigation expansion projects on the sustainability of the aquifers. The results of the simulation process reveal that the implementation of the current development policy have serious impacts on the aquifer storage. Seyed Reza Saghravani et al (2011) investigated the movement of phosphorus pollution in landfills of Seri Petalling Landfill in Selangor, Malaysia. A steady state model for 1 year and 10 years was prepared in Visual MODFLOW in order to assess the concentration of phosphorus so as to prevent future pollution. Al-Dousari et al (2010) applied SWAT model to provide continuous

simulation of overland flow, channel flow, transmission losses for the Raudatain watershed in northern Kuwait and Umm Al Aish watershed in Central Kuwait. Bejranonda et al (2010) attempted to semi-couple SWAT, a surface-soil water and MODFLOW, a groundwater model, to determine the flow behaviour and hydrological components in the Upper Great Chao Phraya Basin of Thailand. Fouépé Takounjou et al (2009) carried out a study aimed to ascertain groundwater flow and mass transport modelling in the Anga'a river watershed in Yaounde, Cameroon. Surface-groundwater interaction in the region was also studied using MODFLOW and MT3DMS. Dams et al (2008) studied the impact of land-use changes, from 2000 until 2020, on the hydrological balance and in particular on groundwater quantity, as results from a case study in the Kleine Nete basin, Belgium. Wake (2008) created a MODFLOW model in order to study the surface water-groundwater interaction in a rectangular study area in the Kleine Nete catchment of the Aa river basin. Won Kim et al (2008) suggested a new approach for integrating the quasi-distributed watershed model 'SWAT' with fully distributed groundwater model 'MODFLOW'. The method proposed for the integration included the exchange of characteristics of the hydrological response units (HRU) in SWAT model with the cells in the MODFLOW model. This HRU-Cell conversion resulted in effective simulation of the distributed groundwater recharge rate and groundwater evapotranspiration. Kilb (2005) used GIS tools and Visual MODFLOW to model the effects of groundwater mounding on the water table elevation of two flooded recharge basins situated on the northwest side of Stony Brook University's West Campus in New York, USA.

2.2 National Scenario

Vikrant Vishal et al (2014) applied MODFLOW to simulate groundwater recharge in the semi-arid region of Delhi territory in India. The NCT of Delhi is an area with political state boundaries, and no real aquifer boundaries. The boundary conditions in the model were assigned as river boundaries along the Yamuna River, Western Yamuna canal and Najafgadh drain. The study area was divided into nine zones for the estimation of groundwater recharge. The results exhibited high variation in the recharge, which the researchers concluded, would seem to reflect the diversity in the geology of the study area as well as the ongoing urbanization which influenced the overall recharge in the region. Mirudhula (2014) applied Visual MODFLOW to develop a groundwater flow model for the Lower Bhavani basin of Tamil nadu. Ground water recharge was estimated using the VISUAL MODFLOW and the amount of recharge from the lined and unlined canals was estimated by using

ZONEBUDGET package. The results of the model indicated that the seepage from the lined canals was 20% lesser than that from unlined canals. Pradeep Kumar (2014) developed a MODFLOW model to quantify groundwater in Choutuppal Mandal, Nalgonda district in Andhra Pradesh (India). The study area consists of mostly agricultural lands, where, cotton, paddy, red gram and castor are the important crops grown. The MODFLOW model was developed as a two layered weathered and fractured model having total thickness of 40 meters. Constant head, groundwater recharge and pumping wells were the boundary conditions assigned to the model. A total of 19 wells were taken into consideration. A steady state simulation was performed in MODFLOW and was calibrated using observed water levels of September 2013. The simulated water levels were found to closely match the observed water levels with correlation co-efficient of 0.993. Needhidasan (2013) highlights the usage of Visual MODFLOW and GIS techniques for groundwater assessment studies as a part of conservation of groundwater resources. The research was carried out in Thirukkazhukundram Taluk of Kanchipuram District in Tamilnadu, India. Visual MODFLOW was used for simulation of water levels in the observation wells. The model was calibrated using data from 2010 and 2011. The model results showed satisfactory correlation with the observed data after calibration. He concluded that GIS could be used very effectively for studies along with Visual MODFLOW which may give satisfactory simulation results. He also emphasized that the success of the model depends largely on the availability of more distributed data.

Rajamanickam et al (2010) applied Visual MODFLOW to simulate groundwater and solute transport in the Amravathi river basin in Karur district, Tamil Nadu (India). The model results showed reduced TDS values in the case of ZLD and artificial recharge structures. The study suggested to introduce new strategies for reduction of chemical wastes (such as ZLD) in the region and also supported the construction of percolation tanks, check dams etc. to increase groundwater recharge.

Bonell et al (2010) studied the impact of land use/land cover changes on soil hydraulic properties is one of the most important aspects in hydrology of humid tropical regions. In spite of its greater role, there is comparatively limited information in the humid tropics on the surface and sub-surface permeability of: (i) forests which have been impacted by multi-decades of human occupancy and (ii) forestation of land in various states of degradation. Even less is known about the dominant stormflow pathways for these respective scenarios. Investigations were carried out on field saturated hydraulic conductivity, K* at 23 sites at four depths (0 m, n = 166), (0.10 m, n = 139), 0.45–0.60 m, n = 117, (1.35–1.50 m, n = 117) under less disturbed forest (Forest), disturbed

production forest of various local species (Degraded Forest) and tree-plantations (Acacia auriculiformes, 7–10 years old, Tectona grandis, _25–30 years old, Casuarina equisetifolia, 12 years old) in the Uttar Kannada district, Karnataka, India (part of Western Ghats). Mondal et al (2011) applied Visual MODFLOW to develop steady state and transient simulation model for a tannery belt near Dindigul town, Tamil Nadu (India). The aim of the study was to determine the groundwater velocity and to assess aquifer response under different input stresses. Krishnaswamy et al **(2013)** carried out investigations on the hydrologic effects of forest use and reforestation of degraded lands in the humid tropics and reported its implications for local and regional hydrologic services. Ravishankar et al. (2020), assessed two decadeal land use/land cover using Remote Sensing and Geographical Information System for the year 1999 and 2019.

2.3 Effects of Reforestation on Groundwater

Mathur and Raj (1980) monitored subsurface water level fluctuations in a watershed covered with blue-gum plantation located at Nilgiris, Tamilnadu. A network of 5 piezometers was installed to measure the water level fluctuations during the period 1979-80. Initial observations indicated that the maximum water level fluctuation was 1.3 m. The existing water level was well below the root zone of bluegum trees at certain locations but was within the root zone in topographic lows. But the study did not find higher water utilization by the trees even when the water table was within the active root zone. While investigating groundwater recharge magnitudes in field plots possessing different land covers, Purandara et al. (1998) observed that there was a negligible groundwater level fluctuation in a 20 year old eucalyptus plantation. The study revealed that groundwater recharge was highest in the forested watershed followed by the teak wood plantation, eucalyptus and degraded land. The study also involved monitoring of soil moisture content (SMC) in these plots upto a depth of 2 m for a period of one year. Although a declining trend in the SMC with depth was noticed, significant differences between land covers could not be inferred because the roots of trees in the forest and the plantations extended beyond the 2 m depth. Therefore, the authors were unable to relate changes in SMC to groundwater fluctuations.

2.4 Estimating Evapotranspiration Under Reforestation

Calder et al. (1992) measured transpiration from individual trees of *eucalyptus tereticornis* plantation at Devabal, Hoskote, Puradal, and Dandupalya of Karnataka State using deuterium tracing. The transpiration measurement of individual trees was made under non-water stress period (in the month of February) for a period of 4 years (1987 to 1990). The highest transpiration rate was observed in Dandupalya site (7.35 mm day^{-1}) and the lowest transpiration rate was in Puradal (0.24 mm day^{-1}). The rate of transpiration in e*ucalyptus camaldulensis* was 6 mm day^{-1} at Puradal site in Karnataka (Roberts and Rosier, 1993).

In a similar attempt, Kallarackal and Somen (1997a) investigated transpiration rates in a 4 year old *Eucalyptus grandis* plantation located in Kerala state. Measurements carried out during 1992 involved monitoring of weather parameters above the canopy and also transpiration measurements at individual leaf level. Results indicated that the lowest transpiration of 2.49 mm day^{-1} was recorded in March 1992 and the highest of 6.94 mm day^{-1} in May 1992. In another attempt, Kallarackal and Somen (1997b) selected two sites of *Eucalyptus tereticornis*, one site located in central Kerala and the other in the southern part of the state, 250 km apart. Measured hourly transpiration rates at these sites varied between 0.4 to 1.2 and 0.2 to 0.6 mm h^{-1}, yielding daily totals of about 3.5 to 7.7 and 2.0 to 4.9 mm day^{-1} respectively.

The important role played by interception on the overall water balance and in particular transpiration processes of forested areas is now being widely recognized. Bruijnzeel (1990) noted that in natural forests interception may constitute 4.5 to 24% of the incident rainfall depending on its intensity. Measurements made in an oak forest in Garhwal hills, Uttaranchal state, indicated interception values varying between 11% of daily rainfall (<10 mm depth) to 74% for daily rainfall depth >100 mm (Sharda and Ojasvi personal communication). In contrast, Kumar and James (2007) reported interception rates 92% for daily rainfall of 2.5 mm and 4.5% for a daily rainfall amount of 135 mm in the Western Ghats.

2.5 Research Gaps

Understanding the impacts of forest and land use/land cover (LU/LC) change on the hydrologic cycle is needed for optimal management of natural resources. Impacts of LU/LC change on atmospheric components of the hydrologic cycle (regional and global climate) are increasingly recognized. The global impact of forest cover and LU/LC change on the hydrologic cycle may surpass that of recent climate change. It is also quite important to note that the impacts of forest cover change on subsurface components of the hydrologic cycle are less recognized, particularly of groundwater recharge which is potentially large as compared to surface resources. Groundwater is Earth's largest freshwater resource. Reduced reliability of surface water supplies in the world with projected climate change during the next century may result in increased reliance on groundwater. Widespread changes in LU/LC have occurred as a result of agricultural expansion. In the past 300 years, cultivated cropland has increased by factors of 70 in the US and globally. The projected global increase of agricultural lands is 20 % over the next 50 years. Most recharge studies have been conducted in natural rangeland ecosystems; however, replacing rangeland with agricultural ecosystems alters many of the parameters controlling recharge, such as climate, soils, and vegetation. Variations in recharge associated with LU/LC changes can have negative impacts on groundwater quality because, thick unsaturated zones in semiarid and arid regions contain a reservoir of salts that accumulated over thousands of years and can be flushed into underlying aquifers. Therefore, it is highly essential to conduct a systematic investigation on surface runoff and ground water recharge under varying forest cover conditions that should form a pre-requisite for the development of any water resources management project in the country. The study also attains significance with respect to on-going climate change implications which will contribute to understand, how the local changes in forest cover will influence the water availability.

3.0 STUDY AREA

The primary focus of the present research is to characterize the hydrologic regime of small catchments (here in after referred to as watersheds) located in the Sahayadri mountains of Uttara Kannada district of Karnataka through long term measurements of relevant hydrological variables. The intention was to understand the effect of different land covers on the hydrological processes at the watershed scale and to develop appropriate methodologies to up-scale this knowledge to larger watersheds (here in after referred to as catchment). Further, the study proposed to up-scale the results obtained from the watershed scale catchment to medium and major catchment and which have a heterogeneous land use and land cover. In order to achieve the objective, two more catchments namely, Barchi and Malaprabha basins were selected. In this chapter, a description of the study area, the characteristics of the selected catchment and watersheds and details of hydro-meteorological measurements and monitoring is enumerated.

3.1 Uttara Kannada District

3.1.1 Location

The Uttara Kannada district is located between north latitudes 13^0 55' 02" to 15˚31' 01" and east longitudes 74˚00′35″ to 75˚10′23″ falling in the survey of India degree sheet Nos – 48 I,48 J, 48 K, 48 M, and 48N. The district is having geographical area of 10222 km^2 (**Figure 3.1**). The study area is mainly covered by lateritic soils. Geological formation include Pre-Cambrians (Dharwar Super group) dominated by granitic gneisses, schists, greywackes and phyllites. There are basically two types of aquifers encountered in the study area, namely confined and unconfined aquifers. Ground water occurs under unconfined condition in alluvium, laterite soil cover and weathered crystalline rocks like granites, basic rocks and Deccan traps. Confined layers located at deeper depth which includes shear zones, fractured and jointed crystalline rocks, iron ore and chert, kankar, sand and gravel.

With the increase in demography and rapid industrialization water regime has been greatly perturbed along the coastal tract of Uttara Kannda district. This life sustaining commodity is under quadruple stress-consumptive, agricultural, industrial and climatic. Due to rapid urbanization and change in land use pattern recharge to groundwater is also reduced. All these factors have induced measurable changes in water dynamics equilibrium conditions and in coming years it may turn to be a major problem if corrective measures are not initiated at this stage. The quantum of water

available on earth being finite there can be no additions to it. It is humanity's ingenuity to manipulate the resource in such a way that it caters to the sustenance of life.

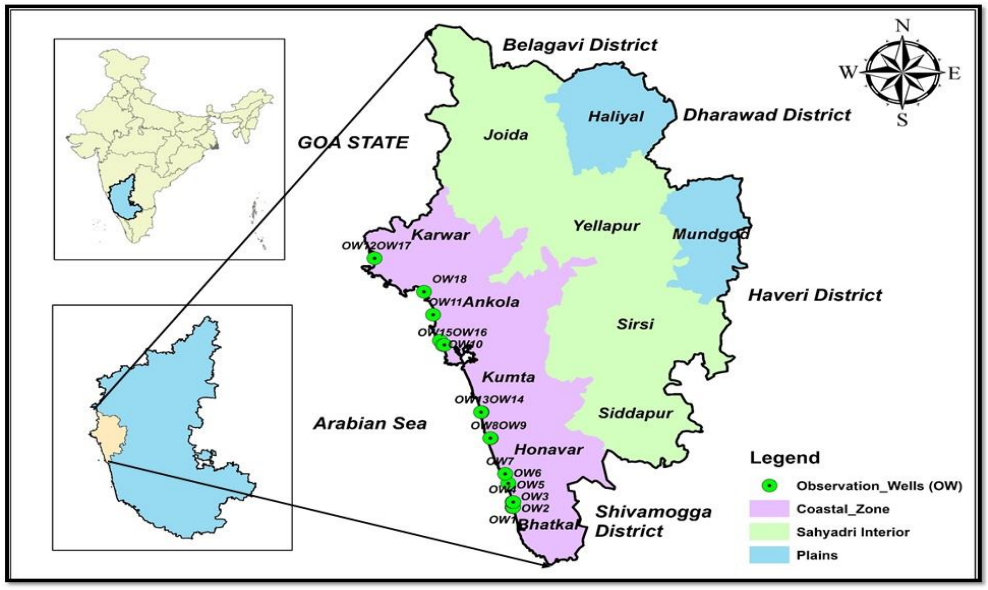

Figure 3.1: Location of the study area in Uttara Kannada district

3.1.2 Geomorphology

Based on the general topography, the Uttara Kannada district can be divided into two major units 1) Hilly areas or high lands; 2) low lands. The hilly area includes well known Western Ghats, having an average elevation of 915 m (3,000 ft), broken by valleys and very irregular hillocks. The laterites occur in the low lands and as plateau give barren appearance with wide distribution of black soils. Uttara Kannada district is endowed with large cover of forests and also involved in active afforestation activities. **Figure 3.2**, shows the land use/land cover variation found in Uttara Kannada district.

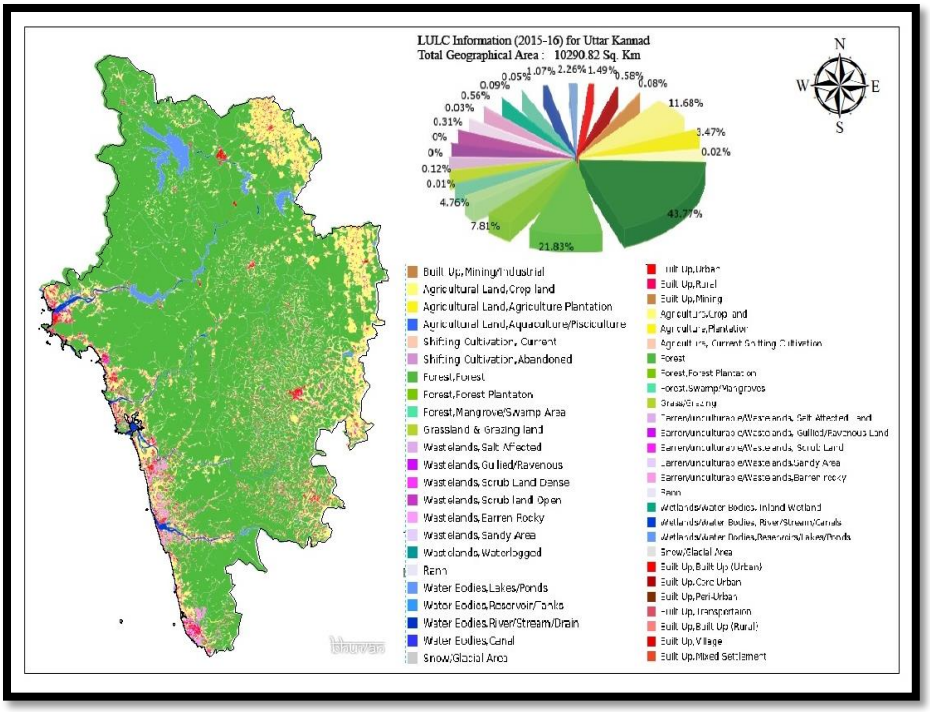

Figure3. 1: Land Use/Land Cover map of Uttara Kannada district

3.1.3 Drainage

The important rivers in the district are Sharavathi, Kali, Aghanashini and Gangavali that flows in westerly direction to Join Arabian Sea. All the rivers in the district together with their tributaries exhibit dendritic drainage pattern. Figure 3a shows the National Hydrographic stations maintained by Central Ground Water Board, Bengaluru.

3.1.4 Geology

Uttara Kannada is composed of a sequence of Precambrian geo-synclinal deposits of the Dharwar Supergroup consisting of quartzites, manganiferous cherts, argillites, banded iron formations, greywackes and phyllites with granitic gneiss as the basement (Figure 3.3). The coastal belt is characterized by Precambrian crystalline rocks (Granitic gneiss, schists and granites), basic dykes, titaniferous magnetite etc. At places these are capped by laterites. The laterites are reddish brown to yellowish in color. The granitic gneisses/granites cover a major portion of the coastal plain. These gneisses and sands constitute the part of north western coastal continuation of Peninsular gneiss (Radhakrishna, 1968), or northern continuation of South Kanara gneisses/granites (Balasubrahmanyan, 1978). The Western Ghat ranges are composed of granitic gneiss forming prominent hills along the coast and at several places enter into Arabian Sea as sea cliffs. The gneisses are moderate to well banded with an alternate dark and white colored layers enriched in

mafic and felsic minerals. The older metamorphic, which have been recognized as the oldest lithological units associated with a suite of ultrabasic rocks (Schists).

There are basically two types of aquifers encountered in the study area, namely confined and unconfined aquifers. Ground water occurs under unconfined condition in alluvium, coastal alluvium, laterite soil cover and weathered crystalline rocks like granites, basic rocks and Deccan traps. Whereas shear zones, fractured and jointed crystalline rocks, iron ore and chert, kankar, sand and gravel occurring at deeper levels covered with confining layer at top and bottom constitute confined aquifers.

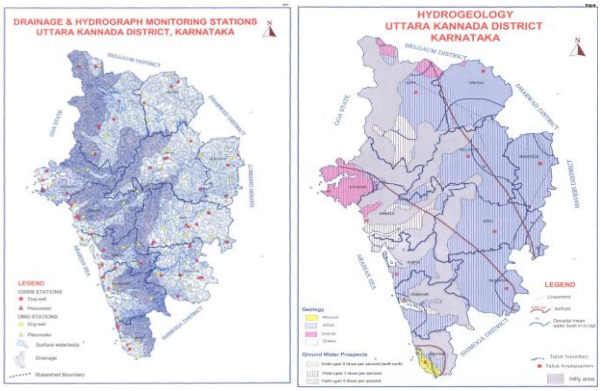

Figure 3.2: (a) Drainage & hydrograph monitoring stations (b) Hydrogeology (CGWB)

3.2 Approach to site selection

A set of 'blocks' with a range of eco-climatic and socio-hydrological conditions were identified in parts of Uttara Kannada, Kodagu and Belagavi districts. Paired catchment approach, i.e. that are proximate (and hence experiencing similar rainfall) and similar to each other in terms of shape, size and geology. In order to characterize the catchments, extensive field investigations were carried out and inventory of existing hydrological conditions that includes soil characteristics, geology, geomorphology etc. were noted. An analysis of the LU/LC showed that the region is highly heterogeneous and fragmented. It was particularly difficult to find catchments fully or predominantly covered with plantations, since the plantation boundaries always followed a different logic. Plantation species also varied from region to region. Eventually, we dropped the search for plantation-covered catchments in the Kodagu region as they were sparsely distributed in this region. Second, variation in geology and soils further reduced the choice in terms of 'intrinsically similar' catchments, andinterventions in natural stream-flows in the form of water conservation works, minor irrigation systems and other flow interruptions were widely prevalent. One of the major task is to distinguish between disturbed and undisturbed forests, particularly in Malaprabha sub basin. A strong correlation between forest condition and human presence were

observed. This means that it is difficult to find a 'relatively undisturbed' forest in areasdensely inhabited by people, and conversely, it is difficult to find catchments with heavily used forest vegetation in an area that is sparsely inhabited. The remaining dense forests are mostly on steep slopes whereas the heavily used forests and the plantations are in more accessible areas.

Table 3.1. Characteristics of eco-climatic zones or 'blocks' within the Uttara Kannada-Kodagu-Belagavi region

Variables	Coastal	Upghat	Transition
Talukas	Honnavar, Bhatkal, Ankola and karwar	Sirsi, Siddapur, Kodagu	Barchi, Khanapur, Kankumbi, Belagavi
Rainfall pattern	3000-5000 mm	5000mm-2500mm	6000-1000 mm
Terrain	Narrow coastal plain quicklymerging with foothills of the Ghats	Highly undulating terrain; dense stream network	Highly undulating to Relatively flat with a fewridges
Soil type	Red lateritic with lateriticoutcrops near the coast	Deep red lateritic with variation in clay content	Partly red lateritic with veryhigh clayey loamy content
Vegetation type	Predominantly semi-evergreen, with patches ofevergreen, mangrove, andmoist-deciduous types	Semi-evergreen and moist deciduous, with some evergreen *kans*	Predominantly sub-humid to semi-arid
Forest plantation types	Widespread planting of *Acacia auriculiformis* on most of the degraded landsin the last 10 years	Eucalyptus replaced natural forest till 1980s; subsequently widespread planting of *A. auriculiformis in open lands*	Early plantations mainly ofteak Scattered *Acacia* plantations in the last fewyears
Major crops	Coconut, paddy, arecanut, cashew,	Arecanut+spice, horticulture,paddy	Sugar cane, Jowar, Paddy and pulses
Irrigation system	Rain and stream fed, butalso significant pumping	Mainly rainfed and baseflow dependent	Mainly rainfed and minor irrigation tanks
Settlement pattern	Dense, continuous settlements along the coast,scattered settlements in theinterior	Scattered hamlets, often consisting of very few households each	Concentrated settlements
Tenure regimes	Large areas under 'MinorForest' (*de facto* open access)	Soppinabetta and MinorForests, with small RF patches	Reserve Forests - predominant tenure regime

Major forest cover change since 1980	Acacia plantations on lateritic outcrops. Denseforests converted to tree savannas/ grassland/ degraded scrub in somelocations	Acacia plantations replacing grasslands. patches of dense forest converted to grassland/ degraded scrub	Dense forests converted to tree savannas/ grassland/ degraded scrub, and also tocultivation

3.3. BILIGIHOLE CATCHMENT AND WATERSHEDS

Keeping in mind the main objectives of the present research, it was decided to identify a catchment of reasonable size (<50 km^2) in the Uttara Kannada portion of the Sahayadri mountains. The intention was to carry out detailed experimental investigations on the hydrology of the catchment with specific reference to the effect of different land covers on catchment runoff. Since experimental studies at the catchment scale can be time-consuming and expensive, it was decided to identify small watersheds within the catchment, which possessed homogeneous land covers which are characteristic of the region. Such a 'nested' approach permits detailed hydrologic investigations to be carried out to characterize hydrological processes and parameters at the watershed scale. This knowledge may be subsequently upscaled to the catchment scale to model runoff and evaluate the hydrologic impacts of anthropogenic activities.

Table 3.2: Groundwater resources in Uttara Kannada district during 2004 (CGWB)

Sl. No.	Taluk	Recharge from Rainfall during monsoon season (ha- m)	Recharge from other sources during monsoon season (ha- m)	Recharge from Rainfall during non-monsoon season (ha- m)	Recharge from other sources during non-monsoon season (ha- m)	Net ground water availability (ha-m)
1	Ankola	6178	54	320	186	6406
2	Bhatkal	3103	62	154	135	3284
3	Haliyal	6105	78	294	169	6319
4	Honnavar	3635	115	299	791	4604
5	Karwar	1798	46	115	161	2016
6	Kumta	3943	103	30	295	4155
7	Mundgod	5544	364	249	192	6041
8	Siddapur	5770	214	34	479	6177
9	Sirsi	9981	531	153	458	10578
10	Joida	11136	77	12	173	10835

11	Yallapur	10446	84	158	200	10351
12	Total	67640	1727	1819	3239	70765

Accordingly, from an analysis of Survey of India toposheets, the Biligihole catchment was identified as most appropriate for the present study. The Biligihole stream originates near Vajgar village of Siddapur taluk at an elevation of 680 m (amsl). It flows westward before it joins Somahalla downstream of Biligi village, which is a tributary of river Aghinashini, one of the major west flowing rivers.

The catchment of Biligihole lies between 74º47'30" to 74º 52'30" E Longitude and 14º 20' to 14º 22'30" N Latitude. The drainage area is 28 km^2. The catchment outlet is located about 3 km southwest of Kodigibail village (Fig. 3.4). A road bridge exists at the outlet and provided a convenient location for measuring streamflows during this study.

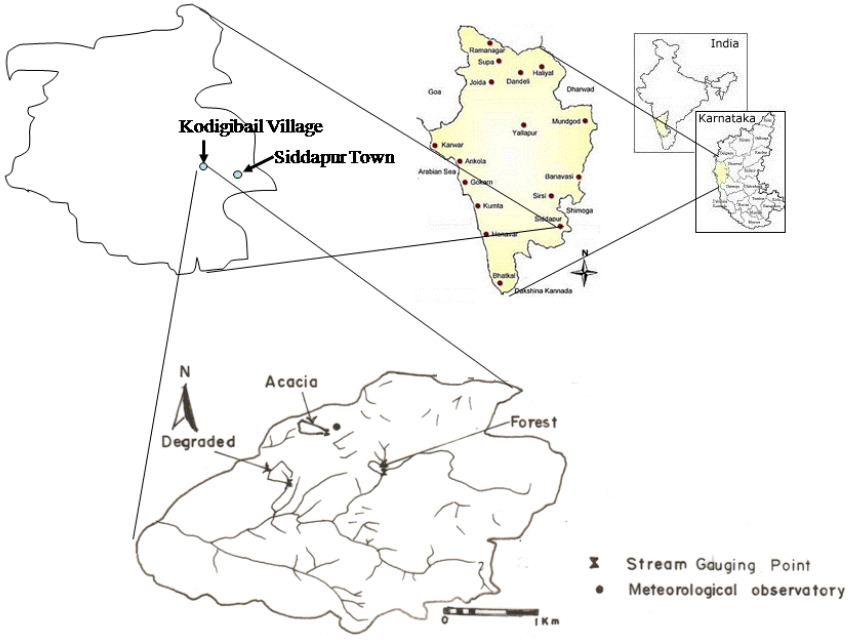

Figure 3.4: Index map of Study area showing the spatial distribution of the selected watersheds and flow measuring points

As part of a previous study (Lele et al. 2007), land use/land cover (LU/LC) mapping of the Biligihole catchment was carried out using Indian Remote Sensing (IRS) satellite data for the year 2006. Major land use/land covers were classified and verified using few ground

truth measurements. Results of the analysis showing the composition of major land covers in the catchment are tabulated in Table 3.3.

From Table 3.3 it is evident that a major portion of the Biligihole catchment is comprised of three major land covers – natural forest, degraded forest and acacia plantations. Therefore, as a next step it is decided to identify three small watersheds within the catchment possessing relatively homogeneous land covers of natural forest, degraded forest and acacia. In order to isolate the effects of only land cover on hydrological processes, it was imperative that the selected watersheds were similar with regard to other hydrogeoclimatic characteristics.

Table 3.3: Composition of major LU/LC in the Biligihole catchment in 2006

Sl. No	LU/LC	Total Area (km^2)	% Total Area
1	Natural Forest	11.00	39.29
2	Degraded Forest	10.00	35.71
3	Acacia Plantations	4.56	16.29
4	Garden Plantations	2.44	8.71
	Total	28.00	100.00

Accordingly, three watersheds were selected based on the above criteria. These are located at Kodgibail, which is a village in the Siddapura Taluk of Uttarakannada district of Karnataka State. The selected watersheds are under natural forest (considered as the control watershed), degraded forest and acacia plantation land covers. These watersheds drain first order streams and are located on the head-water of the Biligihole stream (Fig 3.3). Being located within a 1 km radius, the three watersheds possess more or less similar soils, geology and morphological conditions and differ only in type of land cover. The selected watersheds fall between 74^o 47’ 20” to 74^o 52’ 30” E Longitude and 14^o 22’ 20” to 14^o 22’ 30” N Latitude.

3.4 BARCHI NALA CATCHMENT

The Barchi nala watershed is located on the lee-ward side of the Western Ghats and is a sub basin of Kali river. It lies in the Haliyal taluk of Karwar (North Kanara) district in Karnataka. The BarchiNala stream originates from Thavargatti in Belgaum district at an altitude of about 734 m, 20 km north of Dandeli and flows through North Kanara district of Karnataka state. The catchment is relatively short in width and river flows in southerly direction and joins the main Barchi River near the gauging site. The watershed covers a total geographical area of 14 km^2. The watershed lies between 74° 36' and 74° 39' east longitudes and between 15° 18' and 15° 24' North latitudes **(Fig 3.5)**. High land region consists of dissection of high hills and ridges forming parts of the foot hills of Western Ghats. It consists of steep hills and valleys intercepted with thick vegetation. The slope of the Ghats is covered with dense deciduous forests. The forest occupies around 80% of the study area. The watershed is mainly covered in Bamboo, Teak and mixed plantations. The brownish and fine-grained soils are the principal types of soils found in the area.

Figure 3.5. Location of Barchi watershed from Google Earth

The stream gauging site is located at an elevation of 480 m, where the Nala crosses the Dandeli- Thavargatti road, about 5 km from Dandeli. The stream is a 4^{th} order stream and joins the main Barchi River downstream of the gauging site.

The Barchi raingauge station is located at 15° 18' N and 74° 37' E. Average annual rainfall for the watershed is about 1500 mm, majority of which occurs during the south-west monsoon period.

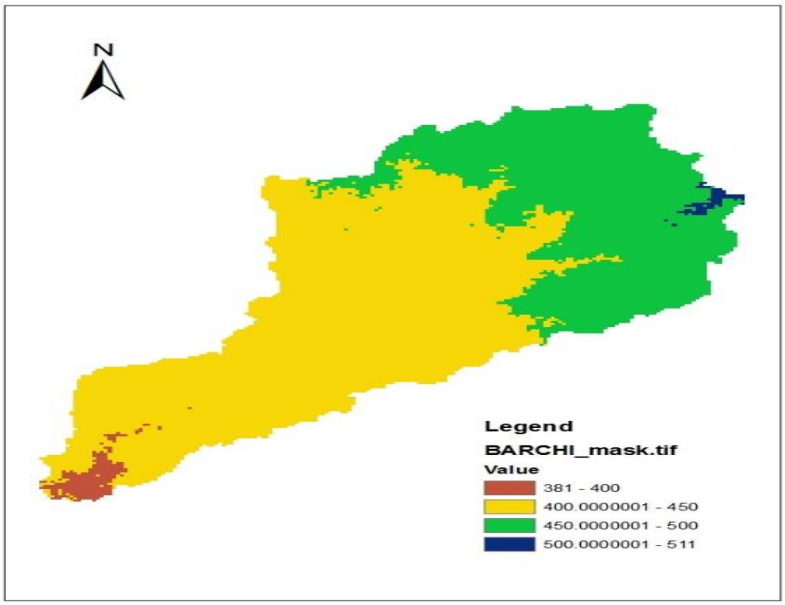

Figure 3.6. Color-coded elevation map of Barchi watershed

The ground surface elevation in the study area varies from 381 m to 511 m above msl. The summary of the topography and slope of the region as obtained from the DEM is shown in the Figure 3.16. Table 3.4 and Table 3.5 show the % area under different elevation and slope distribution in the Barchi Nala catchment, while Table 3.6 discusses the area covered under various land use/ land cover in the region.

Table 3.4 Elevation distribution in Barchi Nala catchment

ELEVATION	% AREA UNDER ELEVATION
Below 400 m	1.33%
400 - 450 m	60.91%

450 - 500 m	37.16%
Above 500 m	0.60%

Table 3.5 Slope distribution in Barchi Nala catchment

SLOPE	% AREA UNDER SLOPE
0 to 5	27.85%
5 to 10	46.94%
10 to 15	20.75%
15 to 20	3.85%
Above 20	0.61%

Table 3.6 Land use pattern in Barchi Nala catchment

LAND USE	AREA
Savannah	**47.46%**
Deciduous broad-leaf forests	**24.29%**
Evergreen broad-leaf forests	**28.25%**

3.5 MALAPRABHA SUB-BASIN UPTO KHANAPUR

The Malaprabha sub-basin lies in the extreme western part of the Krishna basin. It extends between 74° 20’ and 74° 30’ longitudes and 15° 20’ and 15° 40’ latitudes and encompasses an area of 540 sq. km. of the Belgaum district in Karnataka state. Digital elevation map Malaprabha catchment up to Khanapur is shown in Figure 3.7.

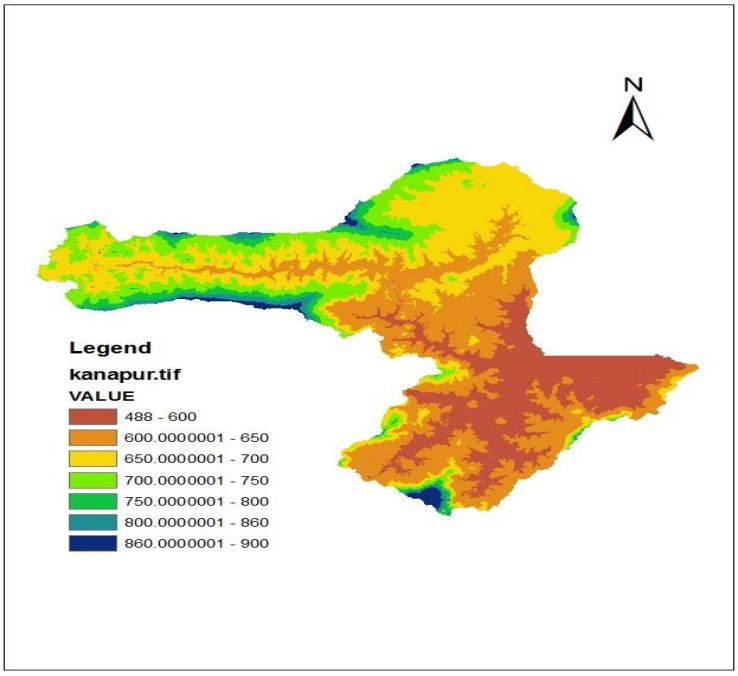

Figure 3.7 Location of the Malaprabha sub-basin

This sub-basin is the major source of water yield for the Naviluteerth dam constructed at 35-45 km downstream of its mouth. This dam impounds about 1377 MCM water and provides water for irrigation approximately for 2.17 lakh hectare lands. Elevation classification and slope variation in the catchment up to Khanapur (Gauging site) is given in Table 3.7 and table 3.8 respectively.

Table 3.7 Topography of the Malaprabha up to Khanapur

ELEVATION	% AREA UNDER ELEVATION
Below 600 m	15.61
600-650 m	30.94
650-700 m	30.07
700-750 m	15.48
750-800 m	4.58
800-850 m	1.88
850-900 m	1.13
Above 900 m	0.31

Table 3.8. Slope distribution in the Malaprabha (up to Khanapur)

SLOPE	% AREA UNDER SLOPE
0 to 5	30.29
5 to 10	32.84
10 to 15	18.68
15 to 20	9.83
Above 20	8.36

3.5.1 Hydrometeorological Network

There are five raingauge stations and two hydro-meteorological stations consisting of Stevenson screens (to record temperature and humidity), pan evaporimeter, anemometer, windvane, self-recording and ordinary rain-gauges at different places in the Malaprabha basin.

3.5.2 Basin characteristics:

A brief description of the Malaprabha sub-basin characteristics, i.e. geology, soils, land use pattern and geomorphological parameters are given below:

3.5.3 Geology:

Geologically, the malaprabha sub-basin comprises of two main geological formations (i) tertiary basalts (ii) sedimentary formations of the Pre Cambrian age

(i) ***Tertiary basalts-*** A major portion (96 %) of the sub-basin is covered in tertiary basalts. The hydrology of basalts is different from that other types of hard rocks. One of the main differences is that the various basalt flow units can form multi-aquifer system somewhat similar to a sedimentary rock sequence, having alternate pervious and impervious horizons.

(ii) ***Sedimentary rocks-*** The sedimentary rock formation is of pre-Cambrian age. This types of rocks are confined in the south eastern part of the study area.

Sedimentary rocks generally act as good aquifer if it is not interrupted by intertrappean clays and other impermeable rocks.

Soils- Pedologically speaking, the basin rocks are covered by thin (0.5 m) to thick (10 m) layer of soils, which are divisible into two major groups. These are red loamy soils and medium black soils.

(i) ***Red loamy soils-*** the upper reaches of the basin, i.e. on crest and gently sloping mid-crest regions, viz., pediplains are characterized by red loamy soils. The top soil texture varies between sandy loam to clayey loam underlain by gravel and sandy loam, sub-soil horizon. About 80% area of the Malaprabha sub-basin is covered by red loamy soils.

(ii) ***Medium black soils-*** this type of soil occurs extensively in parts of Khanapur taluk. Soils are moderately deep to very dark greyish brown, dark reddish brown or black in colour, usually calcerous cracking and clayey. These are moderately well drained with low permeability.

3.5.4 Land use pattern

Land use pattern of the Malaprabha sub-basin is very complex comprising of forest, agriculture, shrubs and barren land (Table 3.9). A brief description of the different land use is given below:

Forests- About 62.65% of the Malaprabha sub-basin, that includes Kanakumbi, Jamboti and Gunji areas are covered by dry tropical forests. The major species are covered by teakwood, rosewood, jackwood, bamboo etc. The ground of these forests are covered by shrubs (2-4 m high) and grasses.

Shrubs- the eastern facing watershed of the area having steep slope (20-30) are covered by shrubs and small trees and bushes (3-5 m high). The most important feature of this class is that these are relatively shallow soil areas. About 19.3% area of the basin is covered by shrubs.

Agricultural land- the gentle slopes and level valley bottom areas, where the most fertile soil is confined, have been occupied by man for the cultivation of various cereals (paddy, ragi etc) and cash crops (cotton, sugarcane). About 16.85 % of the total basin falls under agricultural land.

Barren land- About 1.15% of the area is in form of small patches, on steep slopes and on gentle slopes having very thin film of soil, is in form of barren land. This land is used for the grazing purpose of cattles.

Table 3.9 Land use pattern in the Malaprabha up to Khanapur

LANDUSE	% AREA UNDER LAND USE
DRYLAND CROPLAND AND PASTURE	8.9
IRRIGATED CROPLAND AND PASTURE	2.85
CROPLAND/GRASSLAND MOSAIC	11.27
CROPLAND/WOODLAND MOSAIC	9.05
SHRUBLAND	2.68
SAVANNA	53.92
DECIDUOUS BROADLEAF FOREST	2.46
EVERGREEN BROADLEAF FOREST	8.77
MIXED FOREST	0.1

4.0 Introduction

The present project is initiated to understand the impact of land cover and land use changes on runoff and groundwater processes. In order to understand these dynamics, it is require to do field measurements such as discharge, soil moisture, measurement of in-situ saturated hydraulic conductivity, evapotranspiration and other required parameters. Therefore, this chapter describes methods which were adopted for achieve the set objectives;

4.1 Measurement of Infiltration and Saturated Hydraulic Conductivity of Soil Infiltration

Infiltration, the process of water entry through the soil surface, plays an important role in the soil water cycle as it controls how much, and at what rate, water will enter soil. In turn, this can affect soil water storage, crop yields, irrigation efficiency and solute entry into the soil profile. The two main factors affecting infiltration are hydraulic conductivity and infiltration rate. Hydraulic conductivity refers to the ease of water movement through soil, both horizontally and vertically, and it decreases with a decrease in pore size and water content. Infiltration rate, the speed at which water enters the soil, is related to the soil's infiltration capacity; meaning its ability to absorb water. If water is applied at a rate less than the soil's infiltration capacity, all the water will move through the soil and the infiltration rate will be equal to the rate of delivery. Soil acts as a sponge to take up and retain water. Movement of water into soil is called *infiltration*, and the downward movement of water within the soil is called *percolation*, *permeability* or *hydraulic conductivity*. Pore space in soil is the conduit that allows water to infiltrate and percolate. It also serves as the storage compartment for water.

4.2 Determination of Infiltration/Hydraulic Conductivity using Disc Permeameter

The **disc permeameter** is a field instrument used for measuring water infiltration in the soil, which is characterized by in-situ saturated and unsaturated soil hydraulic properties. It is mainly used to provide estimates of the hydraulic conductivity of the soil near saturation. Single and double ring infiltrometer only measures flow under ponded (saturated) conditions, and when used in soil with distinct macro-pores, preferential flow will dominate the flow. This does not reflect infiltration under rainfall or sprinkler irrigation. Therefore, many authors attempted to create a negative potential (tension) on the water flow. This is to exclude macropores in the flow process, hence only

measuring the soil matrix flow. The disc permeameter was designed by Perroux and White (1988) from CSIRO. Figure 4a and 4b shows the experimental set up of double ring infiltrometer and disc permeameter. The double ring infiltrometer was used for estimating field determined infiltration parameter under different land use land covers, so that errors in the recharge estimate may be reduced. Further, disc permeameter was also used for the estimation of hydraulic conductivity and to understand the preferential flow paths occurring in the study area.

Double Ring Infiltrometers:

Double ring infiltrometers are usually metal rings with 30 cm diameter and a height of about 60 cm in length. The metal tube is so driven into the ground that it protrudes about 10 cm above the soil. Water is poured into this ring to a depth of 25-50 cm depending upon the presence of vegetation and humus on the soil surface. A constant water depth is maintained by adding measured volume of water. The volume of water added is noted at each interval of time and the average infiltration rate for the time interval can be computed. Usually, it takes about two to three hours for the infiltration rate to become constant.

Disc Permeameter

The disc Permeameter has become a popular apparatus for measuring in situ sorptivity (S), and hydraulic conductivity, (K), of the soil at some prescribed potential. Measurements of sorptivity (S), and hydraulic conductivity (K), are important for predicting how water will enter, redistribute within, and drain from soils. Methods that can rapidly and accurately measure S and K are valuable. The disc Permeameter (Per roux and White 1988) is a relatively new method that has gained popularity because of its simplicity, the speed at which measurements can be made, and because it does not greatly disturb the soil surface being measured (White and Sully 1987; White and Perroux 1987 and 1989; Smettem and Clothier 1989; Ankeny et al 1991). Different methods have been devised for calculating S and K are compared using same set of data. These methods are all based on the approximate, but usefully accurate, solution of flow from a disc source found by Wooding (1968). This linearized solution uses a hydraulic conductivity (K) function of the exponential form (Gardner 1958):

$$K = Ks\, e^{\varphi/\lambda c} \qquad \textbf{(Eq 1)}$$

Where Ks is the saturated hydraulic conductivity (m s-1), λc is the macroscopic capillary length

scale (m) and φ is the matric potential (m).

Principles of Operation

When a source of water, such as a wet circular disc or shallow pond, is placed on the soil surface, the initial stages of flow into the soil are dominated by the soil's capillary properties. As time progresses, both the size and geometry of the water source and the force of gravity influence the water flow rate. For uniform soils a time is eventually reached where the flow rate from the source becomes steady. This steady state flow rate is governed by capillarity, gravity, the size of the disc and the pressure at which water is supplied to the soil surface.

In this technique we make use of both the initial and steady-state flow rates to separate the capillarity and gravity contributions to soil water flow. In addition, by selecting the water supply pressure we can dictate the sizes of pore sequences or fissures which participate in the flow process.

4.3 Hydraulic conductivity and Sorptivity

The method for determining soil hydraulic properties from disc Permeameter measurements in the field is based on an analysis of the three-dimensional flow from a shallow circular pond or surface disc. For a pond or disc of radius r_0, on a homogeneous soil, when water is supplied at a potential of ψ_0, the steady state volumetric flow rate q (Wooding) is

$$q = \pi r_0^2 (K_0 - K_n) + 4 r_0 \psi \qquad \textbf{(Eq. 2)}$$

The first term on the right essentially represents the contribution of gravity to the total flow from the surface disc and the second term contains the contribution due to capillarity. In the gravity term K_0 is the hydraulic conductivity at the supply potential $\square_0$, and K_n is the hydraulic conductivity at the initial soil water potential $\square_n$. For relatively dry materials K_n is much smaller than K_0 and we can safely ignore its effect. The capillarity term contains the matric flux potential, which is related to the conductivity by

$$\boldsymbol{\psi = K_0 \lambda_c} \text{ ---------- } \textbf{(Eq. 3)}$$

The macroscopic capillary length (λc), is related to the sorptivity, S_0, and the hydraulic conductivity (White and Sully, 1987),

$$\lambda c = bSo^2 / (\Theta o - \Theta n) \qquad \textbf{(Eq. 4)}$$

is the initial moisture content at Θn is the moisture content at ψ_n, Θo is the moisture content at the supply potential, Θ_0, So is the sorptivity at Θ_n with supply potential ψ_0 and `b' is a dimensionless constant whose value lies between 1/2 and π/4. For field soils a good mean value for b is 0.55. With simplification and, dividing by the area of the disc, we find the steady-state flow rate per unit area

$$q = Ko + \frac{4bS2}{\Theta s - \Theta r} \quad \textbf{(Eq. 5)}$$

Rearranging (Eq.6) to find the conductivity, we have

$$Ko = q - \frac{4bS2}{\Theta s - \Theta r} \quad \text{----------(Eq. 6)}$$

During the early stages of flow from the disc, capillarity dominates flows irrespective of the disc. At short infiltration times the system behaves as if it were one-dimensional. In this case the cumulative infiltration is given by (Philip, 1969). Where Q is the total volume of water infiltrated and t is time from the commencement of infiltration. Sorptivity, is the Slope of the cumulative infiltration vs. $t^{1/2}$ plot to calculate the hydraulic conductivity from (Eq 6). The measurements required are the sorptivity, the steady state flow rate, the initial volumetric moisture content at the supply potential.

4.3.1 Guelph Permeameter

The instrument was used to characterize the saturated hydraulic conductivity of the soil at various depths in a borehole of depth up to 1.2 m. This data is helped to understand the hydrologic processes occurring along the soil profile and how much it contributes to shallow aquifer recharge. Though this is not a direct method for the estimation, the parameters are useful to characterize the soils regionally and in parameterization of SWAT model.

The Guelph Permeameter method (Reynolds et al. 1985) measure the steady state liquid recharge Q, necessary to maintain a constant depth of liquid (H), in an uncased cylindrical well of radius `a' finished above the water table. Constant head level in the well hole is established and maintained by regulating the level of the bottom of the air tube which is located in the center of the Permeameter. As the water level in the reservoir falls a vacuum is created in the air space above water. When the Permeameter is operating, equilibrium is established.

When a constant well height of water is established in a cored hole in a soil, a bulb of saturated soil with specific dimension is rather quickly established as shown in above figure. The bulb is very

stable and its shape depends on the type of soil, the radius of the well and the head of water in the well. The shape of the bulb is numerically described by the C factor used in the calculations. Once the bulb shape is established, the outflow of water from the well reaches a steady state flow rate which can be measured. The rate of this constant outflow of water, together with the diameter of the well and height of water in the well can be used to determine the field saturated hydraulic conductivity of the soil.

The Richard analysis of steady state discharge from a cylindrical well in unsaturated soil, as measured by the Guelph Permeameter technique accounts for all the forces that contribute to three dimensional flow of water into soils, the hydraulic push of water into soil, the gravitational pull of liquid out through bottom of the well and the capillary pull o water out of the well into the surrounding soil. The Richard analysis is the basis for the calculation of field saturated hydraulic conductivity. The C factor is a numerically derived shape factor which is dependent on the well radius `a' and head `H' of water in the well.

4.4 Soil Moisture Variables

The overall methodology adopted in this study focused on analyzing the temporal and spatial characteristics of observed soil matric potentials and equivalent soil moisture contents. Given a dataset of soil moisture measurements made at several depths at multiple locations on different occasions, Qiu et al. (2001) proposed computation of the several variables to characterize temporal and spatial variabilities in a quantitative manner. Let soil moisture content of site i, layer j and sampling occasion k be expressed as $M_{i,j,k}$ and let N_p be the number of sites, N_l the number of sampling layers or depths and N_t the number of sampling occasions. Then, the following variables may be defined:

1. Mean soil moisture content of site i. (M_i)

$$M_i = \frac{1}{N_l N_t} \sum_{j=1}^{N_l} \sum_{k=1}^{N_t} M_{i,j,k} \tag{5.2}$$

2. Mean soil moisture content at soil layer j (M_j)

$$M_j = \frac{1}{N_p N_t} \sum_{i=1}^{N_p} \sum_{t=1}^{N_t} M_{i,j,k} \tag{5.3}$$

3. Time averaged soil moisture content on plot i, and at layer j ($M_{i,j}$)

$$M_{i,j} = \frac{1}{N_t} \sum_{k=1}^{N_t} M_{i,j,k} \tag{5.4}$$

4. Profile Variability of time averaged soil moisture content on plot, i, (VP_i)

$$VP_{i,k} = \sqrt{\frac{N_l \sum_{j=1}^{N_l} (M_{i,j})^2 - \left(\sum_{j=1}^{N_l} M_{i,j} \right)^2}{N_l (N_l - 1)}} \tag{5.5}$$

5. Temporal Variability of layer averaged soil moisture content on plot, i, (VT_i)

$$VT_i = \sqrt{\frac{N_t \sum_{k=1}^{N_t} M_{i,k} - \left(\sum_{k=1}^{N_t} M_{i,k} \right)}{N_t (N_t - 1)}} \tag{5.6}$$

6. Spatial variability of layered averaged soil moisture at soil layer j (VS_j)

$$VS_j = \sqrt{\frac{N_p \sum_{i=1}^{N_t} (M_{i,j})^2 - \left(\sum_{i=1}^{N_p} M_{i,j} \right)^2}{N_p (N_p - 1)}} \tag{5.7}$$

7. Profile gradient of time-averaged soil moisture on plot i, (G_i)

$$G_i = \frac{M_{i,3} - M_{i,1}}{1.5} \tag{5.8}$$

In the present study, the seven variables defined by Eqs. 5.2-5.8 were computed for 4 sites (N_p) in each of the watersheds at 3 depths (N_i) at 7 day time steps (N_t) during the period October 2019 to December 2022.

4.5 DESCRIPTION OF SWAT MODEL:

SWAT is a physically based, semi distributed river basin or watershed scale model developed by Arnold et al (1998) in order to predict impacts of land management practices on water, sediments, and agricultural chemicals yields in large complex watersheds with varying soil, land use and management conditions over long

period of time. SWAT operates on a daily time step and is designed to predict the impact of land use and management on water, sediment, and agricultural chemical yields in ungauged watersheds. The model is process based, computationally efficient, and capable of continuous simulation over long time periods. Major model components include weather, hydrology, soil temperature and properties, plant growth, nutrients, pesticides, bacteria and pathogens, and land management. In SWAT, a watershed is divided into multiple sub-watersheds, which are then further subdivided into hydrologic response units (HRUs) that consist of homogeneous land use, management, topographical, and soil characteristics. The HRUs are represented as a percentage of the sub-watershed area and may not be contiguous or spatially identified within a SWAT simulation. Alternatively, a watershed can be subdivided into only sub-watersheds that are characterized by dominant land use, soil type, and management.

4.5.1 Description of SWAT model

SWAT requires many sets of spatial and temporal input data. As semi-distributed model, SWAT has to process, combine and analyze spatially these data using GIS tools. Therefore, to facilitate the use of the model, it was coupled with GIS software as free additional extension ArcSWAT for ArcGIS.

The model is based on the water balance equation

$$\mathbf{SW_t = SW + \sum_{t=1}^{t}(Ri - Qi - ETi - Pi - QRi)} \quad \text{----------(10)}$$

where SW is the soil water content minus the 15-bar water content, t is time in days, and R, Q, ET, P, and QR are the daily amounts of precipitation, runoff, evapotranspiration, percolation, and return flow; all units are in mm.

Ground water flow contribution to total streamflow is simulated by creating a shallow aquifer storage. The water balance for the shallow aquifer is

$$Vsa_i = Vsa_{i-1} + Rc - revap - rf - perc_{gw} - WU_{SA} \quad \text{----------(11)}$$

Where, Vsa is the shallow aquifer storage (mm), Re is recharge (percolate from the bottom of the soil profile) (mm), revap is root uptake from the shallow aquifer (mm), rf is the return flow (mm), $perc_{gw}$ is the percolate to the deep aquifer (mm), WU_{SA} is the water use (withdrawal) from the shallow aquifer (mm), and i is the day.

4.6 Morphometric Analysis

Drainage morphology analysis is essential to any hydrological study. Hence, the determination of stream networks behavior and their interrelation with each other is of great importance in many water resources studies. Digital Elevation Map was extracted from CARTOSAT image by using SAGA system. GIS tools for drainage analysis has been employed to evaluate several drainage parameters. The morphometric analysis of the sub-watersheds in the upstream region revealed a predominantly dendritic drainage pattern which is formed by interlinking of the streams.

The drainage density map obtained from the SAGA is compared with the Topo sheet map. The SAGA extracted map was devoid of majority of the first order streams particularly in downstream areas of the sub-basin. This could be attributed to change in land use/land cover changes where the area is encroached by agriculture crops. Table 4.1 shows the various methods involved in the estimation of morphometric parameters.

Table 4.1 Methods involved in Morphometric Analysis

Parameters	Formulae	References
Stream Order(U)	The smallest permanent streams are called "first order". Two first order streams join to form a larger, second order stream; two second order streams join to form a third order, and so on. Smaller streams entering a higher-ordered stream do not change its order number.	Strahler (1964)
Stream Length (Lu)	The average length of streams of each of the different orders in a drainage basin tends closely to approximate a direct geometric ratio.	Horton (1945)
Stream Length Ratio (RL)	$RL = Lu/Lu-1$	Sreedevi et al
Bifurcation Ratio (Rb)	$Rb = Nu/Nu+1$	Horton (1932)
Areal Aspects		

Drainage density	$Dd = Lu/A$	Horton (1945) (Dd)
Drainage texture T	$T = Dd \times Fs$	Smith (1950)
Stream Frequency (Fs)	$Fs = \Sigma Nu/A$	Horton (1945)
Elongation ratio (Re)	$Re = \frac{D}{L} = 1.12\sqrt{\frac{A}{L}}$	Schumm (1956)
Form factor (Ff)	$Ff = A/L^2$	Horton (1945)
Relief Aspects		
Relief R	$R = H - h$	Hadley and Schumm (1961)
Relief Ratio Rr	$Rr = R/L$	Schumm (1963)
Slope	$Sb = H - h/L'$	Mesa (2006)
Gradient Ratio	$Gr = H - h/\quad L$	Sreedevi et al (2005)

Accordingly, the above parameters were estimated in the ArcGIS environment. GIS based maps were prepared to exhibit the morphological parameters of hydrological importance such as Slope, L S Factor, Aspect, Topographic Wetness Index, Convergence Index, Drainage Density etc.

4.7 Estimation of Ground water Availability using GEC Norms

The basic objective of estimation of groundwater availability is to know the hydrogeological characteristics such as lithology, groundwater level fluctuations and distribution of groundwater, groundwater use etc. Detailed household survey to know the groundwater usage and also input from local farmers were collected and the specific data used to calculate the groundwater balance which is essential for the primary assessment of the groundwater occurrence in different parts of the catchment.

The dynamic groundwater resources of Malaprabha river basin was computed based on Groundwater Estimation Methodology 2015. In the present study, the entire catchment was divided based on litho-stratigraphic units rather than the usual practice of watershed criteria. The assessment made for each unit was transferred to sub-basin scale (as a whole Malaprabha sub basin) for future

planning and development purposes. As the study area comprises of hard rock areas, the specific yield was estimated by applying the water level fluctuation method for the dry season data, and then used the specific yield value in the water level fluctuation method for the monsoon season to get recharge.

4.7.1 Estimation of Ground Water Draft

Ground water draft is estimated for all the ground water uses viz. Domestic, Irrigation and Industrial. Domestic draft is estimated based on well census method or requirement method. Irrigation draft is estimated using well census method, cropping pattern method or power consumption method. Industrial draft is estimated using well census method, power consumption method or requirement method. Sum of all these drafts is the Gross ground water draft.

Estimation of Ground Water Recharge

4.7.2 Ground water recharge due to rainfall is to be estimated using ground water level fluctuation method and rainfall infiltration factor method.

The water level fluctuation method is applied for the monsoon season to estimate the recharge using groundwater balance equation. The groundwater balance equation for the monsoon season is expressed as,

$$RG - DG - B + IS + I = \Delta S \text{ ----------(Eq. 7)}$$

Where,

RG = gross recharge due to rainfall and other sources including recycled water

DG = gross groundwater draft

B = base flow into streams from the area

IS = recharge from streams into groundwater body

I = net ground water inflow into the area across the boundary (inflow - outflow)

ΔS = increase in ground water storage.

In the present investigation, it is considered that inflow, base flow and stream aquifer interactions are negligible and therefore, the above equation is re written as

$$R = \Delta S + DG = h \times Sy \times A + DG\ S \text{ ----------(Eq. 8)}$$

Where,

R= Possible recharge, which is gross recharge minus the natural discharges in the area during monsoon season (RG - B + I +IS)

h = rise in water level in the monsoon season

A = area for computation of recharge

Sy = specific yield, ΔS = change in ground water storage

DG = gross ground water draft

The recharge calculated from the above equation gives the available recharge from rainfall and other sources for the particular monsoon season. For non-command areas, the recharge from other sources such as recharge from water conservation structures including tanks and ponds and also from irrigation return flow were also considered, The recharge from rainfall is given by,

$$Rrf = R - Rgw - Rwc - Rt = hxSy \times A + DG - Rgw - Rt - Rwc \quad \textbf{----------(Eq. 9)}$$

Where Rrf = recharge from rainfall

Rgw = recharge from groundwater irrigation in the area

Rwc = recharge from water conservation structures

Rt = Recharge from tanks and ponds

4.8 Description of Visual MODFLOW

Visual MODFLOW is the most complete and easy-to-use modeling environment for practical applications in three – dimensional groundwater flow and contaminant transport simulations. This fully- integrated package combines MODFLOW, MODPATH, zone budget, MT3Dxx/RT3D, and WinPEST with graphical interface. Visual MODFLOW is designed with a modular structure each dealing with a specified feature of the hydrologic system. Visual MODFLOW provides professional 3D groundwater flow and contaminant transport modeling using MODFLOW-2000, MODPATH, MT3DMS and RT3D. Visual MODFLOW Pro seamlessly combines the standard Visual MODFLOW package with WinPEST and the Visual MODFLOW 3D-Explorer to give the most complete and powerful graphical modeling environment available. This fully-integrated groundwater modeling environment allows to:

- Graphically design the model grid, properties and boundary conditions,
- Visualize the model input parameters in two or three dimensions,
- Run the groundwater flow, path line and contaminant transport simulations,
- Automatically calibrate the model using WinPEST or manual methods, and Display and interpret the modeling results in three-dimensional space using the Visual MODFLOW 3D-Explorer.

The three-dimensional movement of ground water of constant density through porous earth material may be described by the partial-differential equation

$$\frac{\partial}{\partial x}\left(K_{xx}\frac{\partial h}{\partial x}\right)+\frac{\partial}{\partial y}\left(K_{yy}\frac{\partial h}{\partial y}\right)+\frac{\partial}{\partial z}\left(K_{zz}\frac{\partial h}{\partial z}\right)+W=S_s\frac{\partial h}{\partial t} \quad \text{..... (12)}$$

Where,

K_{xx}, K_{yy}, and K_{zz} are values of hydraulic conductivity along the x, y, and z coordinate axes, which are assumed to be parallel to the major axes of hydraulic conductivity (L/T); h is the potentiometric head (L); W is a volumetric flux per unit volume representing sources and/or sinks of water, with W<0.0 for flow out of the ground-water system, and W>0.0 for flow into the system (T-1); S_s is the specific storage of the porous material (L-1); and t is time (T).

In general, Ss, Kxx, Kyy, and Kzz may be functions of space (Ss = Ss(x,y,z), Kxx = Kxx(x,y,z), and so forth) and W may be a function of space and time (W = W(x,y,z,t)). Equation (1) describes ground-water flow under non-equilibrium conditions in a heterogeneous and anisotropic medium, provided the principal axes of hydraulic conductivity are aligned with the coordinate directions. Equation (1), together with specification of flow and/or head conditions at the boundaries of an aquifer system and specification of initial-head conditions, constitutes a mathematical representation of a ground-water flow system. A solution of equation (1), in an analytical sense, is an algebraic expression giving h(x,y,z,t) such that, when the derivatives of h with respect to space and time are substituted into equation (1), the equation and its initial and boundary conditions are satisfied. A time-varying head distribution of this nature characterizes the flow system in that it measures both the energy of flow and the

volume of water in storage, and can be used to calculate directions and rates of movement.

Figure 8 shows a spatial discretization of an aquifer system with a grid of blocks called cells, the locations of which are described in terms of rows, columns, and layers. An i,j,k indexing system is used. Within each cell there is a point called a "node" at which head is to be calculated. Many schemes for locating nodes in cells could be used; however, the finite-difference equation developed in the following section uses the block-centered formulation in which the nodes are at the center of the cells.

Calibration is an effort to better parameterize a model to a given set of local conditions, thereby reducing the prediction uncertainty. Model calibration is performed by carefully selecting values for model input parameters (within their respective uncertainty ranges) by comparing model predictions (output) for a given set of assumed conditions with observed data for the same conditions. Model validation is the process of demonstrating that a given site-specific model is capable of making sufficiently accurate simulations, although “sufficiently accurate” can vary based on project goals (Refsgaard, 1997). Validation involves running a model using parameters that were determined during the calibration process, and comparing the predictions to observed data not used in the calibration. SWAT-CUP was developed for the calibration and validation process and provided a decision-making framework that incorporates a semi-automated approach (SUFI2) using both manual and automated calibration and incorporating sensitivity and uncertainty analysis. In SWAT-CUP, parameters and ranges can be manually adjusted iteratively between auto-calibration runs.

In SUFI-2, parameter uncertainty accounts for all sources of uncertainties such as uncertainty in driving variables (e.g., rainfall), conceptual model, parameters, and measured data. The degree to which all uncertainties are accounted for is quantified by a measure referred to as the *P-factor*, which is the percentage of measured data bracketed by the 95% prediction uncertainty. As all the processes and model inputs such as rainfall and temperature distributions are correctly manifested in the model output (which is measured with some error) - the degree to which we cannot account for the measurements - the model is in error; hence

uncertain in its prediction. Therefore, the percentage of data captured (bracketed) by the prediction uncertainty is a good measure to assess the strength of our uncertainty analysis. The 95PPU is calculated at the 2.5% and 97.5% levels of the cumulative distribution of an output variable obtained through Latin hypercube sampling, disallowing 5% of the very bad simulations. As all forms of uncertainties are reflected in the measured variables (e.g., discharge), the parameter uncertainties generating the 95PPU account for all uncertainties.

Another measure quantifying the strength of a calibration/uncertainty analysis is the *R-factor*, which is the average thickness of the 95PPU band divided by the standard deviation of the measured data. SUFI-2, hence seeks to bracket most of the measured data with the smallest possible uncertainty band. As parameter uncertainty increases, the output uncertainty also increases. Hence, SUFI-2 starts by assuming a large parameter uncertainty (within a physically meaningful range), so that the measured data initially falls within and then decreases this uncertainty in steps while monitoring the *P-factor* and the *R-factor*. In each step, previous parameter ranges are updated by calculating the sensitivity matrix (equivalent to Jacobian), and equivalent of a Hessian matrix, followed by the calculation of covariance matrix, 95% confidence intervals of the parameters, and correlation matrix. Parameters are then updated in such a way that the new ranges are always smaller than the previous ranges, and are centered around best simulation.

The goodness of fit and the degree to which the calibrated model accounts for the uncertainties are assessed by the above two measures. Theoretically, the value for *P-factor* ranges between 0 and 100%, while that of *R-factor* ranges between 0 and infinity. A *P-factor* of 1 and *R-factor* of zero is a simulation that exactly corresponds to measured data. The degree to which we are away from these numbers can be used to judge the strength of our calibration. A larger *P-factor* can be achieved at the expense of a larger *R-factor*.

Hence, often a balance must be reached between the two. When acceptable values of *R-factor* and *P-factor* are reached, then the parameter uncertainties are the desired parameter ranges. Further goodness of fit can be quantified by the $R2$ and/or Nash-Sutcliff (*NS*) coefficient between the observations and the final "best" simulation. It should be noted that we do not seek the "best simulation"

as in such a stochastic procedure the "best solution" is actually the final parameter ranges.

Input Data:

Kumar (2013) explains that a large amount of information and a complete description of the flow system are required to make the most efficient use of the models. In situations where only rough estimates of the flow system are needed, the input requirements of models may not justify the use. The credibility of any model depends on the availability of wide range of data and proper incorporation of this data into the model. Higher the extent of detailed input data, higher will be the accuracy of the model. The model inputs required for the SWAT and MODFLOW models are discussed briefly below:

1. *Digital Elevation Model (DEM)*: The DEM for the study areas were obtained from BHUVAN portal of the Indian Space Research Organization (ISRO). The DEM available for the areas were CARTOSAT-1 DEMs with a spatial resolution of 30 meters. The ground surface elevations for the areas were taken from the obtained DEM. Also, these were pre-processed using ArcGIS before being used in ArcSWAT for watershed delineation process.
2. *Land use maps*: The land use maps used in the present study were extracted from the global land use/ land cover maps prepared by WATERBASE. These maps are available in the public domain and can be downloaded without charge from www.waterbase.org. The resolution of the land use maps was quite coarse.
3. *Soil maps*: The global soil map prepared by the Food and Agricultural Organization (FAO) called as 'Harmonized World Soil Database (HWSD)' was used in this study. The HWSD can be freely downloaded from the official FAO website. Additionally, the database is also available at the website www.waterbase.org and www.swat.tamu.edu. Apart from the FAO soil map, the detailed soil and lithology map for the study area were obtained from the Karnataka State Water Resource Department.
4. *Meteorological data*: The gridded dataset of the meteorological data for the entire India for a period of 30 years from 1975 to 2005 is available as the

'Indian Meteorological Department (IMD) weather generator database'. It was presented at the 2012 International SWAT conference held at New Delhi and was developed specifically for the SWAT users to incorporate the weather parameters conveniently in the model database. The IMD database consists rainfall data for a mesh of raingauges located for every 0.5 degree and temperature gauges located at every 1 degree throughout the entire country. The IMD weather generator database is available in the public domain and can be obtained from official SWAT website www.swat.tamu.edu. Apart from the IMD gridded data, observed weather data such as rain and temperature values for the study areas were collected from the concerned state and central government departments.

5. *Hydrogeological data*: In order to accurately represent the real-world condition in the mathematical model, it is very essential to have sound knowledge and adequate dataset regarding the hydrogeological system of the study area. The data regarding the basic hydrogeology of the study areas was obtained from previous reports based on the field studies conducted by NIH, Belgaum. The 2012 report titled 'Aquifer systems of Karnataka' published by Central Groundwater Board, Bangalore imparted sufficient idea regarding the formations and geology of the study areas as well as value ranges for the basic soil parameters.

CHAPTER V: HYDROLOGICAL ANALYSIS

5.0 INTRODUCTION

The present study was focused on field experimentation aimed at characterizing hydrological processes as influenced by land cover at the watershed scale. As part of

the research, equipment/instruments were installed to monitor/measure rainfall, climatic variables, soil matric head/soil moisture content, soil physical and hydraulic properties, soil water fluxes and runoff. The present chapter provides a detailed description of the manner in which measured data was analyzed with the objective of gaining an improved understanding of the effect of land cover on hydrological processes and parameters. As an effort in this direction, the present chapter addresses the following aspects: i) analysis of rainfall in the study area; ii) detailed analysis of measured runoff; iii) Characterization of soil physical and hydraulic properties and detailed analysis of spatio-temporal variability of observed soil matric potentials and soil moisture contents is addressed in the next chapter.

5.1 RAINFALL CHARACTERISTICS OF THE STUDY AREA

Rainfall is the major driving force in determining the overall climatic conditions and the disposition of the hydrological cycle in a given region. Variations of rainfall in time and space exert a significant influence on the magnitude and characteristics of various hydrological processes. Therefore, there is a need to characterize, as accurately as possible, the water input from rainfall in studies aimed at understanding hydrological processes and water resources availability at the scale of a region/catchment.

Several studies on the hydrological aspects of rainfall have been reported in the literature. Excellent reviews of world-wide research on the temporal and spatial variability of rainfall are presented by Ward and Robinson (1990) and Jackson (1977). However, as Jackson (1986) notes, very little quantitative analysis of rainfall variability has been undertaken in tropical regions, in comparison to temperate regions of the world. Large parts of the Asian tropical region come under the influence of the unique monsoon phenomenon, which is the large scale annual wind regime that is set up due to differences in temperature of the Asian sub-continent and the surrounding seas. In India, which can be considered to be a typical example of a monsoon environment, studies have revealed that the climate of the country is determined almost

exclusively by the characteristics of the monsoon. Also, it has been noted that the evolution of the moisture regimes of various climatic regions in India is mainly due to the interactions between monsoonal circulation and topographical features.

The Sahayadri mountains present a good example of the manner in which orographic effects influence the monsoon circulation in producing a unique pattern of rainfall variability characterized by heavy rainfall on the windward slopes and a rain shadow region on the leeward side. The presence of the mountain barrier results in one of the steepest environmental gradient reported in the tropics (Gunnell 1997). Few of the studies carried out to understand rainfall variability in the Sahayadri mountains are by Sarkar (1967); Patwardhan and Asnani (2000); Gadgil et al. (1988); Kulkarni and Reddy (1994) and Simon and Mohan Kumar (2004). However, none of these studies have reported the intra-annual and inter-annual variations of rainfall events of different sizes and neither have rainfall events of short duration analyzed.

5.1.1 Rainfall Analysis

Rainfall data have been downloaded from various digital data sources. Measurements were also taken for the specified sites (Kodagibail and Vajgar) during the study period (event based) in order to account for rainfall intensity. Monthly rainfall totals are shown in tables. Yearly rainfalls were divided into three classes based on the long term rainfall data of Siddapur taluk. The selected group of rainfall data falls under three categories Below Normal (< 3000 mm), Normal (3000 – 3500 mm) and Above Normal (3500 and above). Results of this analysis are shown in Table 5.1.

Table 5.1: Rainfall Analysis of Siddapura Raingauge station

1901							1940					
Rainfall Class by depth (mm)	**No. of Rainy Days**	**Rainfall Amount (mm)**	**% of Total Rainy Days**	**% of Annual Rainfall**	**Cumulative % Annual Rainfall**		**Rainfall Class by depth (mm)**	**No. of Rainy Days**	**Rainfall Amount (mm)**	**% of Total Rainy Days**	**% of Annual Rainfall**	**Cumulative % Annual Rainfall**
>80	5	675.02	3.55	26.15	26.15		>80	3	263.3	1.9	8.7	8.7
40.1 to 80	10	516.6	14.10	20.01	46.16		40.1 to 80	23	1376.3	36.8	45.2	53.9
20.1 to 40	28	807.6	19.86	31.28	77.44		20.1 to 40	29	827.6	18.1	27.2	81.1

10.1 to 20	23	330.18	16.31	12.79	90.23		10.1 to 20	26	377.6	16.3	12.4	93.5
5.1 to 10	21	150.24	14.89	5.82	96.05		5.1 to 10	18	138.6	11.3	4.6	98.0
<5	54	101.94	38.30	3.95	100.00		<5	61	59.5	38.1	2.0	100.0
Annual Total	141	2581.58					Annual Total	160	3042.8			
1980							**2020**					
Rainfall Class by depth (mm)	**No. of Rainy Days**	**Rainfall Amount (mm)**	**% of Total Rainy Days**	**% of Annual Rainfall**	**Cumulative % Annual Rainfall**		**Rainfall Class by depth (mm)**	**No. of Rainy Days**	**Rainfall Amount (mm)**	**% of Total Rainy Days**	**% of Annual Rainfall**	**Cumulative % Annual Rainfall**
>80	13	1902.0	9.0	34.6	34.6		>80	5.0	574.8	3.3	19.5	19.5
40.1 to 80	39	2148.0	56.6	39.0	73.6		40.1 to 80	21.0	1150.6	31.9	39.0	58.5
20.1 to 40	35	964.2	24.1	17.5	91.1		20.1 to 40	22.0	619.3	14.5	21.0	79.6
10.1 to 20	20	337.3	13.8	6.1	97.3		10.1 to 20	21.0	301.5	13.8	10.2	89.8
5.1 to 10	17	126.8	11.7	2.3	99.6		5.1 to 10	26.0	193.3	17.1	6.6	96.3
<5	21	23.5	14.5	0.4	100.0		<5	57.0	108.0	37.5	3.7	100.0
Annual Total	145	5501.7					Annual Total	152.0	2947.5			

5.1.2 Hourly Rainfall Intensity

Rainfall intensity analysis was also carried out with reference to normal rainfall, i.e. above, normal and below. Sahayadri region is characterised by long duartion low intensity rainfall. It is reported that the 15 minute intensities often exceed 40mm/hr contributing about 15 % of total annual rainfall. Venkatesh et al (2007) analysed hourly rainfall data of 12 recording stations covering Uttara Kannada district of Karanataka. The study was carried out by dividing the district into three gographical units namely costal, up - ghats and the plains. In the present analysis, hourly rainfall data recorded at Kodigibail using a recording type of raingauge was analysed to understand inter - annual and intra - annual variabilities. Rainfall intensities of hourly rainfall were extracted from the rainguage charts and categorised under 6 classes depending on the magnitude of intensities. Results of this analysis are presented in Table 5.2, Table 5.3 and Table 5.4.

Table 5.2. Rainfall intensity characteristics for Below Normal Rainfall

Rainfall Class by depth (mm)	Duration of rainfall events(hrs)	Amount of rainfall (mm)	% of total duration	% of Annual Rainfall	Cumulative % Rainfall	Equivalent days
>25	3	102.20	0.46	3.46	3.46	<1
20-25	5	108.80	0.77	3.69	7.16	<1
15-20	10	250.80	1.54	8.51	15.65	<1
10-15	33	410.80	5.10	13.94	29.61	1.38
5-10	116	936.50	17.95	31.78	61.40	4.83
<5	479	1137.00	74.14	38.59	100	19.96
Annual Total	646	2946.10				

Table 5.3 Rainfall intensity characteristics during Normal Rainfall

Rainfall Class by depth (mm)	Duration of rainfall events(hrs)	Amount of rainfall (mm)	% of total duration	% of annual rainfall	Cumulative % Rainfall	Equivalent days
>25	1.00	25.60	0.09	0.77	0.77	<1
20-25	3	62.10	0.26	1.88	2.65	<1
15-20	7	111.50	0.61	3.37	6.01	<1
10-15	53	603.50	4.65	18.21	24.22	2.21
5-10	138	989.00	12.11	29.86	54.09	5.75
<5	938	1520.53	82.28	45.91	100	39.08
Annual Total	1140	3311.73				

Table 5.4 Rainfall intensity characteristics for Above Normal Rainfall

Rainfall Class by depth (mm)	Duration of rainfall events(hrs)	Amount of rainfall (mm)	% of total duration	% of Annual Rainfall	Cumulative % Rainfall	Equivalent days
>25	6	323.20	0.88	8.05	8.05	<1
20-25	15	441.90	2.20	11.01	19.06	<1
15-20	15	260.00	2.20	6.48	25.54	<1
10-15	72	972.00	10.56	24.29	49.54	3.00
5-10	145	1122.50	21.26	27.97	77.79	6.04
<5	429	891.30	62.90	22.21	100	17.88
Annual Total	682	4013.70				

From the analysis of the hourly rainfall intensities during below normal rainfall, normal rainfall and above normal rainfall, it was noted that the recorded maximum hourly intensity was of the order 50.5 mm/hour during above normal rainfall years. The total number of rainfall hours varied from 1140 hr (47.5 equivalent days) for normal rainfall category to a minimun of 646 hr (27 equivalent days) for below normal rainfall category showing large inter annual variation. The corresponding percentage of days (in comparision to the total number of rainy days) for normal rainfall and below normal rainfall were 47 % and 30 % respectively. During above normal rainfall, high rainfall occurred within 682 hrs. This suggest that the intensity of rainfall was very high with an average hourly intensity of 5.88 mm/hr in comparision with other two years (2.90 mm/hr for 2011 and 4.56 mm/hr for below normal rainfall).

Table 5.2 to Table 5.4 show that the major contribution to total annual rainfall comes from intensities less than 10 mm/hr. All it was observed that intensities less than 5mm/hr were recorded for maximum duration during the period of analysis. In above normal rainfall category, the rainfall intensity >10mm/hr contributed about 42% towards annual rainfall total. The contribution in the same intensity class during other two categories of rainfall i.e normal rainfall and below normal rainfall are comparitively lower the major portion of rainfall in the Sahayadri regoin is contributed by 4 to 5 spells each lasting 8 to 10 days but with relatively moderate rainfall intensities. Figure 5.1, shows the average rainfall intensity of the study area.

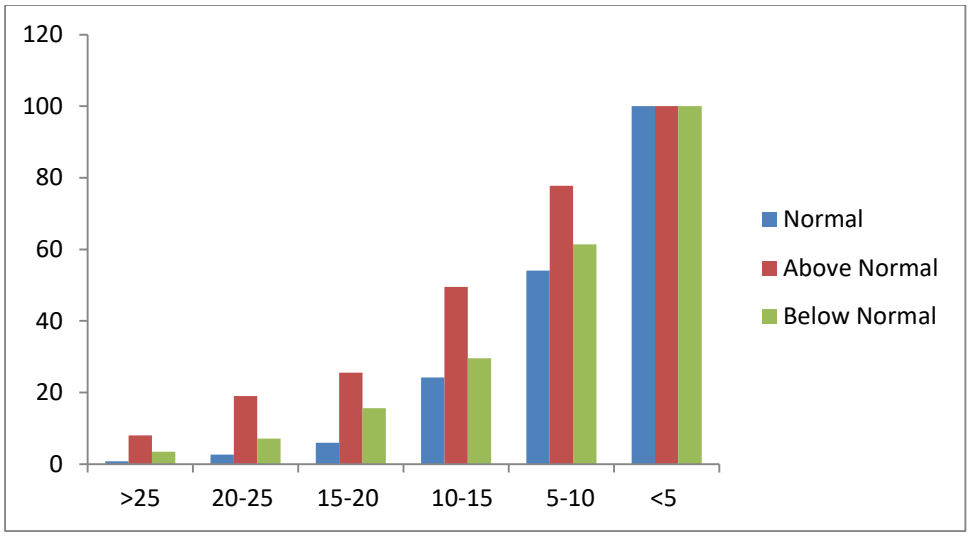

Figure 5.1. Hourly rainfall intensity for the study area

Further, the results showed that the study area received high intensity rain (>25mm/hr) only on few occasions and their contributions were also lower (1 %, 8 % and 4 % respectively in all three categories of rainfall). Low intensity rainfalls contributed more than 70 % for normal rainfall category and below normal rainfall category lasting for 94 % of the time and above 50 % for above normal rainfall category lasted for 80 % duration. Contributions from rainfall of moderate intensity between 10 to 25 mm/hr were 24 %, 42 % and 26 % approximately for all the three category of rainfall which lasted for 6, 15, and 7% of the times. Results showed evidences of rainfall at Kodigibail being contributed mostly by the spells of low intensity rainfall rather than higher intensity rains though there were large year to year variations in the intensities.

5.2 Runoff Analysis

Runoff analysis of three selected three watersheds possessing distinctly different land covers were done. The stream flows were also measured on event basis from the experimental watersheds during the study period using calibrated broad crested notches. These observed mean daily discharge values were converted to equivalent runoff depth units (mm) so as to facilitate the comparison with the rainfall. Also the observed flows were used to derive the following parameters:

1. Specific discharge: discharge per unit area of watershed.
2. Specific peak discharge: peak discharge per unit area of watershed.

As a first step, daily rainfall values recorded at- site and the associated daily runoff measured at the outlets of the three watersheds were used to obtain plots of cumulative rainfall versus cumulative runoff for all three categorized types of rainfall.

5.2.1 Annual Rainfall-Runoff

The salient feature of the observed flow from these three land-use types are shown in Table 5.5 for the year 2019. Observed data depict the overall runoff characteristics of the selected watersheds. In order to understand the influence of land cover on runoff generation, parameters such as specific discharge and specific peak discharge were computed for selected watersheds.

Table 5.5. Annual rainfall-runoff and peak discharges in monitored first-order catchments, 2019

Sl No	Land use type	Area (ha)	Rainfall (mm)	Runoff (mm)	Specific Discharge (cumec/ha)	Specific Peak Disch. (cumec/ha)	% Runoff
1	Acacia1	8.728	2846.30	696.90	0.081	0.005	24.48
2	Acacia2	4.481		1096.02	0.247	0.008	38.51
4	Degraded1	10.083		916.56	0.092	0.009	32.20
5	NF1	6.545		410.50	0.063	0.002	14.42
6	Degraded Vajgar	8.655	2726.82	1232.53	0.144	0.007	45.20
7	NF Vajgar	9.131		729.10	0.081	0.004	26.74
1	Acacia1	8.728	3662.44	1287.91	0.1491	0.0078	35.17
2	Acacia2	4.481		1587.57	0.3576	0.0141	43.35
4	Degraded1	10.083		1743.77	0.1745	0.0099	47.61
5	NF 1	6.545		725.70	0.1119	0.0116	19.81
6	Degraded Vajgar	8.655	3602.95	1732.74	0.2021	0.0159	48.09
7	NF Vajgar	9.131		1029.99	0.1138	0.0107	28.59

It can also be seen from the above tables that the % of runoff is lowest in forest and followed by the acacia and degraded yielded the highest. Similar observations are reported for some of the New Zealand catchment Rowe (2003) and for Coweeta watersheds in USA (Hewlett. et. al., 1979). Also, it can be seen from the table that the specific peak discharge is also quite high for the degraded watersheds than other two watersheds with Acacia and Forest. This implies that, the acacia

watersheds over a period of time may restore the land to behave as that of the forested watersheds.

5.2.2 Peak flow analysis

The peak discharges of 0.00382 m^3/sec, 0.00624 m^3/sec and 0.00209 m^3/sec or greater (assuming these values as threshold) respectively for Acacia, degraded and forested watersheds are compared during the study period. The so obtained values were than divided by the respective areas of these watersheds to get the specific peak discharges. The results indicate that there is a significant increase in the peak flow observed in degraded watersheds as compared to Acacia and forest (Table 5.6).

Table 5.6. Peak flow (cumec/ha) for selected rainfall events under different land-uses for (a) year 2019, (b) year 2020; (c) Kodgibail 2020.

Date	Rainfall (mm)	Acacia 1	Degraded 1	Natural forest 1
3rd -Jun-2019	149.80	0.38	0.82	0.26
4th week-Jun-2019	113.40	0.33	0.71	0.23
1st -Jul-2019	92.60	0.24	0.50	0.33
2nd week -Jul-2019	77.10	0.12	0.32	0.25
28-Jul-2019	65.00	0.33	0.36	0.20
Aug'2019	56.20	0.08	0.29	0.15
21-Aug-2019	66.00	0.28	0.18	0.17
Sept'2019	55.70	0.14	0.28	0.13
4-Sept'2019	68.90	0.13	0.19	0.07
1st week-Oct'2019	56.20	0.08	0.29	0.15
Last week-Oct'2019	55.70	0.14	0.28	0.13
	81.58	**0.21**	**0.40**	**0.20**

(b)Year 2019 (Vajgar area)

Date	Rainfall (mm)	Acacia 2	Degraded 2	Natural forest 2
3rd week June 2019	86.39	0.177	0.331	0.168
4th week -Jun-2019	79.87	0.338	0.865	0.191
15-July-19	96.99	0.439	0.826	0.210
1 week Aug-19	154.20	0.462	0.679	0.233
2nd week Aug-19	108.40	0.596	0.988	0.254
3rd week -Aug'19	96.33	0.295	0.554	0.150
4th week -Aug-19	94.54	0.280	0.496	0.113
1st Sept 2019	79.06	0.257	0.411	0.190
2nd Sept 2019	75.80	0.241	0.357	0.165
4th Sept. 2019	73.35	0.240	0.641	0.134
	94.49	**0.33**	**0.61**	**0.18**

(a) Year 2020 (Kodagibail)

Date	Rainfall (mm)	Acacia 1	Degraded 1	Natural forest 1
30-Jun-20	118.34	0.64	1.04	0.48
29-Jun-20	113.45	0.66	0.36	0.15
28-Jun-20	103.99	0.58	0.10	0.09
5-Jul-20	105.46	0.29	1.11	0.45
25-Jul-20	160.07	1.05	1.15	1.27
26-Jul-20	108.88	0.67	0.84	0.87
28-Jul-20	115.73	0.52	0.37	0.66
2-Aug-20	135.45	0.80	0.77	0.39
3-Aug-20	117.69	0.78	0.92	0.41
24-Aug-20	125.67	0.53	0.93	0.51
	120.47	**0.65**	**0.76**	**0.53**

5.2.3 Soil Moisture Variation and Runoff Process

Soil moisture is an important variable for understanding and predicting a range of hydrological processes including flooding, erosion, solute transport and land-atmosphere interactions. Soil moisture exhibits a high degree of spatial and temporal variability. Both surface soil moisture and subsoil moisture have profound effects on the above processes. While, many researchers have studied the horizontal variation and temporal changes of soil moisture, but little attention has been paid to the profile features of the soil moisture. There have been a number of recent papers indicating that land use (Fu et al., 2000), slope gradient (Moore et al., 1988), aspect and curvature (Western et al., 1999), slope position and relative elevation (Crave and Gascuel -odux, 1997), precipitation (Famiglietti et al., 1998) and mean soil moisture (Bell et al., 1980) have influence of the distribution of soil moisture. However, in the present study, in order to gain a better understanding of soil moisture variations in relations to land use is analysed. The results are presented below;

The temporal variation of soil moisture for three land-uses is shown in Table 5.7. The results indicate that standard deviation of soil moisture within upper layers is more variable than in the lower soil layers. This is nature of variation in the upper layer has been observed in some of the watersheds under different land covers in China (Fu, et al., 2003; Wang et al., 2001). The deeper layer in the forest soil shows a stable variation. But the soil moisture under degraded watershed shows a higher variation below150 cm depth. However, a greater variation of soil moisture is observed below 120cm depth in watershed covered with Acacia plantation. These variations indicate that the moisture is influenced by the land-use and land cover of the watersheds and also the texture of the soil at different depth with increase in the clay content with the depth It is also

observed from the table.8, is that, the gradient of moisture under degraded and forest have a negative value compared to that of the acacia watershed. A higher moisture variability is observed in the Acacia watershed followed by the forested watershed.

Table 5.7. Statistics of profile features from time averaged soil moisture content (gravimetric content, in %) at different soil layer on different plots

Sl. no	Layers (m)	Land use / Land cover type			Standard Deviation		
		Acacia	Degraded	Forest	Acacia	Degraded	Forest
1	0.75	15.95	16.54	21.50	7.26	10.64	11.40
2	0.225	16.92	15.05	18.36	6.43	9.74	6.82
3	0.375	17.60	18.70	17.70	8.45	7.93	3.98
4	0.525	13.59	17.86	17.96	5.37	7.46	3.92
5	0.675	15.20	15.67	16.30	4.38	5.83	3.55
6	0.825	15.24	14.92	17.29	2.58	4.73	5.68
7	0.975	18.16	12.72	16.39	4.54	7.23	3.57
8	1.125	19.34	12.72	15.26	4.81	6.68	3.17
9	1.275	22.94	12.60	14.64	5.05	5.18	3.93
10	1.425	23.94	11.91	14.98	6.76	6.28	3.69
11	1.575	15.15	10.34	14.86	6.90	7.31	3.20

This is quite obvious as the plants use more moisture in their root zone in these watersheds. The table also depicts that the moisture content increases below the depth of 150cm. This sudden increase may be attributed to change in the soil type (may be the composition of soil with respect to percentage of sand, clay and silt). However, these watersheds show a higher temporal variability in the moisture.

In the acacia plantation, the soil moisture fluctuation with depth is observed. This could be due to the fact that the major portion of the watershed covers with the 12 year old acacia plantation and the height of the plants vary between 12-15 m, while some regenerated younger plants are also present in the watershed. The roots of the older trees may have a reached at a greater depth for extracting the moisture. The younger trees may be extracting water at the surface layer. But below 150 cm, the moisture content is increasing; this indicates that, the roots have mostly concentrated within 100 to 150 cm depth from ground surface. In the case of degraded forests, relatively high moisture content was observed up to a depth of 75cm, however, at further depth it showed a steady decline. The observations clearly indicated the impact of LU/LC and geomorphological features on the hydrological behavior of any catchment/watershed or landscape.

The available soil moisture in the forested watershed is being used by the trees for transpiration. This is quite evident from the soil moisture pattern observed, wherein the soil moisture decreased

till the root depth and thereafter remained uniformly across the profile. The variation of soil moisture could also be due to change in root density. It is noticed that, the roots in acacia plantation have penetrated down to 1m and above. The density of these roots does vary at different depth with the soil moisture. It is also observed that, the soil moisture is quite high even at 2 m depth in acacia in comparison to that of the forested watershed. The higher root density is observed in the forested watershed alter the soil moisture content. The horizontal and profile variation of soil moisture (both spatially and vertically), have been identified due to the effect of topography on the soil moisture and its distribution (Famiglietti, et al., 1998; Western et al., 1998). The previous studies carried out elsewhere, e.g., Fu et al., 2001; Fu and Chen, 2000; have identified parameters such as slope, relative elevation and aspect that are the main factors controlling the soil moisture. The study area is of undulating type that plays an important role in distribution of soil moisture.

5.3 Soil Hydarulic Properties

The nature of the soil surface is the key factor in deciding how rainfall will infiltrate and move through the soil, i.e., whether water will move downwards or sideways. Surface soil hydraulic properties control the entry of water (i.e., infiltration) but, if unimpeded vertically, incoming water will move through the regolith as percolation to reach the water table. More commonly, however, there is a reduction in the permeability in the upper soil horizons at various points because of the presence of more impervious oil layers. These deflect water laterally, either at the surface as infiltration excess, the Hortonian Overland Flow (HOF), or Subsurface Storm Flow (SSF). The SSF can emerge at the surface as return flow and combine with precipitation falling on saturated soils to produce saturation (or saturation excess) overland flow- SOF, which is known as the Dunne mechanism (Dunne and Black, 1970). As highlighted by Bonell and Williams (1986), the soil hydraulic properties of the 'undisturbed' forested landscapes tend to be in equilibrium with the prevailing rainfall characteristics. Thus in closed tropical forest, HOF is not generally favored because of the dense root mat and the incorporation of soil organic matter in the topmost soil layers, which encourage high infiltration rates. Due to the population explosion in the recent decades, there is a dramatic land use changes taking place in the tropical region (Drigo, 2006). These changes may influence the properties within the soil mantle and may cause a shift towards disequilibrium state. The surface soil hydraulic

properties sensitive to any of these perturbation which may cause a dramatic shift in the amount of rainfall portioned between lateral and vertical pathways of storm water transfer.

Elsenbeer and Vertessy (2000) presented the first attempt at providing a conceptual framework for comparing the preferred storm flow pathways across the humid tropics. The authors have observed that it is the soilscape properties and their interaction with the prevailing rainfall intensities which control hydrological response patterns. Bonell (2006) provided a comprehensive overview of the existing work on identifying the runoff generation mechanism elsewhere in the humid tropics.

In the Western Ghats region, there are not much research carried out to understand the runoff generation mechanisms. Putty and Prasad (2000a,b) made an attempted to identify the runoff generation mechanism of the watersheds located in the Western Ghats. The results obtained through their experiments suggested that the pipe flow and return flow are the dominant pathways in the evergreen forests. No detailed soil description were provided by these authors except that the soil thickness extended upto 20 m on well vegetated slopes which originated from a Precambrian formations with gneiss and intrusive granites being the principal rock types. Surface soil layer was observed to be mostly sandy loams (Putty and Prasad, 2000b)

In another study by Bonell et al., (2010) have measured the soil hydraulic properties using the disc and Guelph permeameters across different land covers in the Uttarakannada district of Karnataka. Their measurements showed that within an evergreen forest of light textured soil, log mean K* (field saturated hydraulic conductivity) at surface was 62mm h^{-1}., at 0.1m depth was 38mm h^{-1} and 0.45-0.6 m depth was 76.6 mm h^{-1} confirming high transmissivities of the upper evergreen forest soils in this region. However, at 1.5m depth K* declined to 7.5 mm h^{-1}, confirming the occurrence of SSF. This study was carried out basically at plot scale as reported by the authors. When these values were superimposed by the regional rainfall intensities to identify the runoff generation mechanism under these plots results indicated infiltration-excess overland flow (Hortonian flow) as the dominant mechanism of runoff generation.

The present analysis aims at testing the hypotheses on suggested flow pathways emerging from previous soil hydraulic conductivity work in the region on (1) enhanced

Hortononian overland and quickflow in degraded catchments, and (2) low to moderate hydrologic restoration under *Acacia* plantations at degraded sites. In order to evaluate these hypotheses, a number of field measurements on field saturated hydraulic conductivity were done using the Disc and Gulphe permeameter upto a depth of 1.5m in the selected watersheds. Each of these watersheds were divided into number of grids of size 100mX100m. Two to three measurements were taken at the surface and 0.1m depth and 2 measurements at other depths in each of the grids. The measured values were then used to compute the mean values at each of these layers. Some of the statistics for the observed K* values could be seen in the Table. 5.8.

Table 5.8 Field saturated hydraulic conductivity values under different land covers

Soil Type / *Land use*	Layer	No of Samples	K* mmh^{-1}			Antilog S_l
			Arith. Mean	Log Mean	Range	
Natural Forest	0.00 m	18	180.62	149.66	51.15 - 384.18	0.647
	0.10 m	18	76.98	57.45	11.89 - 171.56	0.870
	0.45 m	13	17.35	16.07	11.44 - 36.00	0.384
	0.60 m	13	16.44	15.23	11.8 - 42	0.359
	0.90 m	13	16.20	15.19	10.08 - 36	0.346
	1.20 m	13	16.20	14.50	4.35 - 37.11	0.518
	1.50 m	13	18.39	17.36	9.61 - 37.55	0.347
Degraded	0.00 m	18	42.30	39.31	14.41 - 75.95	0.409
	0.10 m	18	40.19	29.47	2.26 - 106.52	0.910
	0.45 m	13	25.83	25.40	17.56 - 36.00	0.190
	0.60 m	13	8.16	5.63	1.8 - 21.6	0.909
	0.90 m	13	3.84	2.85	0.72 -21.6	0.846
	1.20 m	13	2.51	2.15	0.91 - 6.7	0.564
	1.50 m	13	2.73	2.19	1.05 -6.9	0.683
Acacia	0.00 m	18	61.80	57.32	31.59 109.88	0.406
	0.10 m	18	38.23	35.64	19.93 - 74.11	0.371
	0.45 m	13	19.93	16.16	8.55 - 68.40	0.613
	0.60 m	13	16.88	15.88	9.12 - 36.00	0.352
	0.90 m	13	21.22	19.17	10.6 - 43.20	0.455
	1.20 m	13	13.47	12.18	7.03 - 31.80	0.442
	1.50 m	13	7.06	5.35	2.18 -19.45	0.639

The Table.5.8, showed the descriptive statistics of K* for the specific layers under each of the land covers. Some of the earlier studies (e.g. Talsma, 1969; Rogowski, 1972; Nielsen et al, 1973; Baker, 1978) reported that the K* values often fitted a logarithmic statistical distribution. In this study also the pooled K* data when transformed with a log10- transformation produced a symmetrical B-W plot, indicating that the underlying distribution was log-normally distributed. Other researchers (e.g. Elsenbeer *et al*, 1992; Zimmerman *et al*, 2006) have found a less skewed K* statistical distributions for selected soil layers. Zimmerman and others (2006) thus used root transformations of K* data such as the fourth – root transformation as better descriptor of this variable for the upper soil 0.1m layer whilst reverting to the log transformation below 0.1m depth. The present study emphasized on the geometric means and their equivalent log means (expressed in original standard units of mm h^{-1} following taking the antilog) rather than the arithmetic means, to compare across the sites and soil layers.

To check for intra-site variability of soil hydraulic properties linked with the small number of samples taken, the antilog of the standard deviation of the log transformed K* data (antilog S_l) were used as an index of variability (Baker, 1978). A value of 2 for this index was suggested by Rogowski (1972) as the upper limit of uniformity of K in soil series. Despite the small sample sizes (Table. 5.8), most of the antilog S_l indices were below the value of 2 which prompts to use the existing log means of K* (which are the same as the geometric mean) in subsequent discussion which concerns the spatial variability (inter-soil layer comparison between sites as well as vertically within sites) of K*.

5.3.1 Comparison of K* across land covers with selected rain intensity-duration – frequencies (IDF)and possible dominant stormflow pathways

To evaluate the dominant runoff pathways, K* data were measured for selected watersheds, namely the Forest, Degraded Forest and Acacia Plantation and these data were presented Table. 5.8 and summarized as B-W plots for different depths super imposed by the 15 minutes rainfall intensity for different recurring period in Figure 5.2.

As with most tropical forests (Elsenbeer, 2001, Bonell, 2006), the K* data in Table. 5.8. show the highest K* values in the surface horizons (≤0.10m depth) under the Forest. The subsoil K* (below 0.10m depth) also remain relatively permeable (≥ 16 mmh^{-1}). Thus the value suggested significant recharge to deep groundwater could be expected. The B-W plots however also indicated the possible occurrence of deeper SSF during higher rainfalls.

Table 5.9: Comparisons of log-mean hydraulic conductivities, K* between land covers at different depths. The means, and corresponding standard errors are shown.

Depth (m)	Forest	Degraded	Acacia plantation
0	180.62±25.92	42.30±3.76	61.74±5.67
0.10	76.98±11.95	40.18±7.81	38.23±3.76
0.30	17.79±21.22	25.09±1.45	19.93±4.61
0.60	17.45±2.45	8.91±1.95	16.88±1.89
0.90	16.93±1.91	4.27±0.821	21.22±2.96
1.20	15.82±2.06	2.38±0.423	13.40±1.96
1.50	18.90±1.86	2.84±0.519	7.06±1.29

The surface log mean K* of the degraded forest watershed in contrast were of an order of magnitude lower than the forested watershed (Table.5.9), but the subsoil K* between the 0.10 - 0.45 m depths remained similar to the forest. Thereafter there was further decline in the order of magnitude of K* below 0.45m depth under the degraded forest, the forested K* values are comparable with K* at 1.20-1.50m depth under the nearby acacia watershed. Therefore one could expect a slower percolation to deep groundwater under both these land covers than the forested cover because of the reduction in K* at depth.

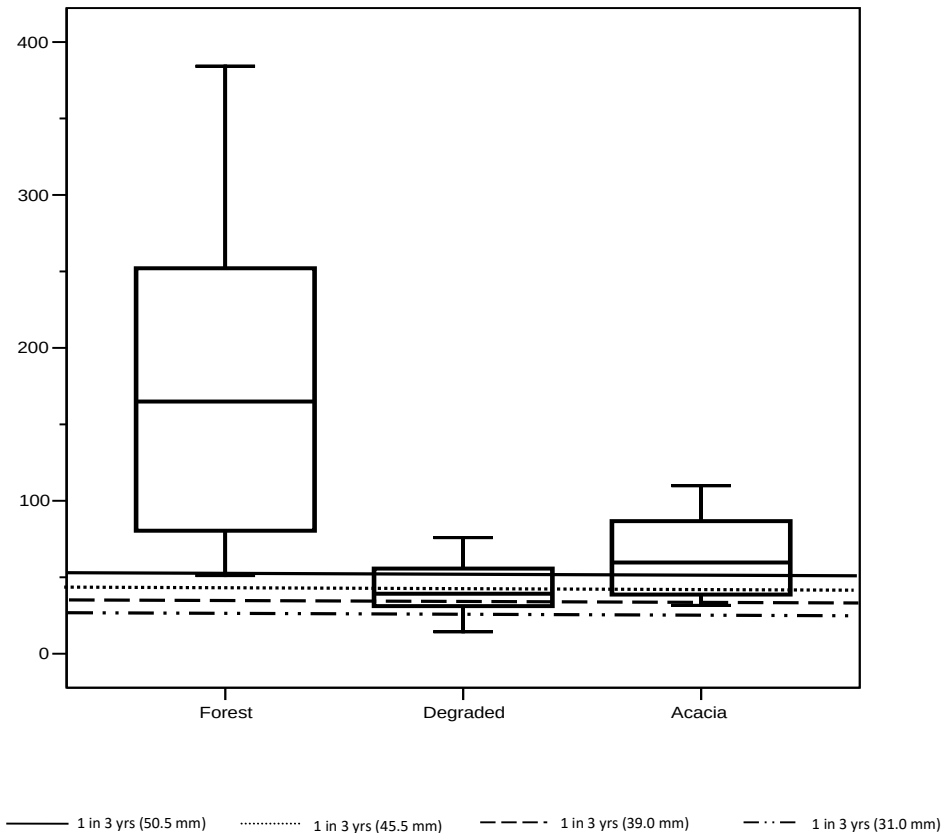
400
300
200
100
0
Forest
Degraded
Acacia
1 in 3 yrs (50.5 mm)
1 in 3 yrs (45.5 mm)
1 in 3 yrs (39.0 mm)
1 in 3 yrs (31.0 mm)

Figure 5.2(a)

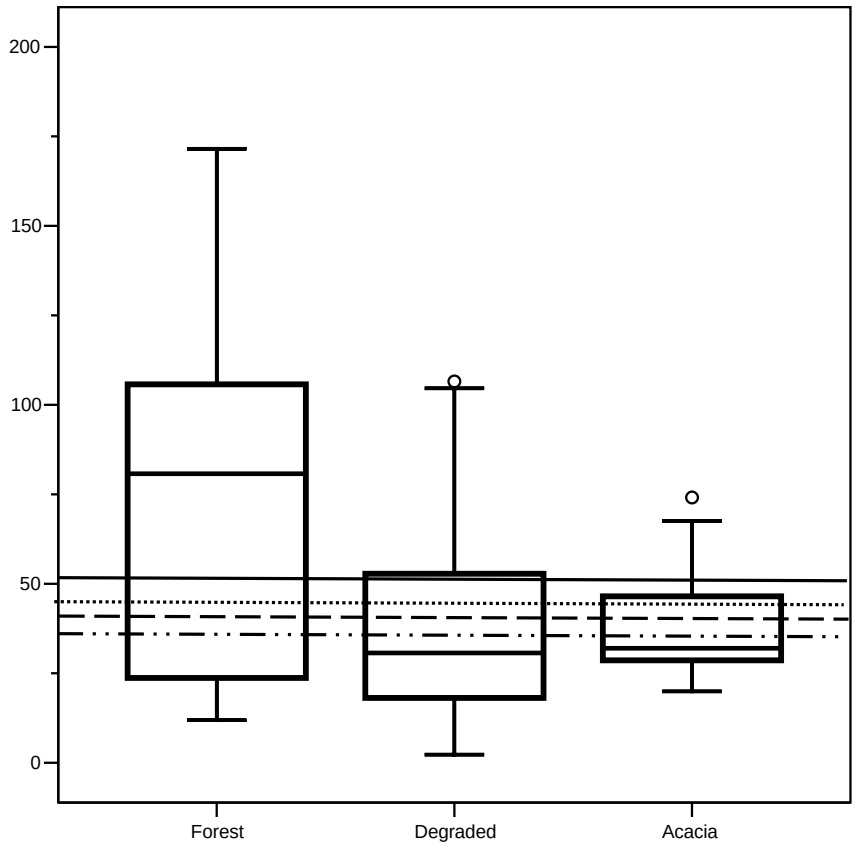

Figure. 5.2(b)

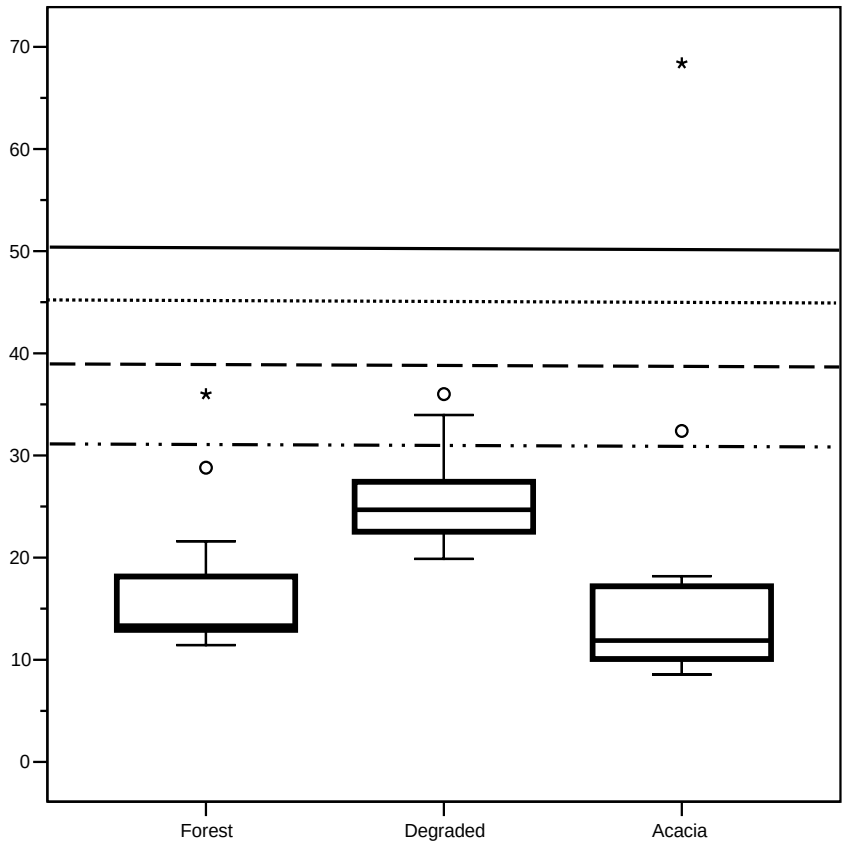

Figure. 5.2(c)

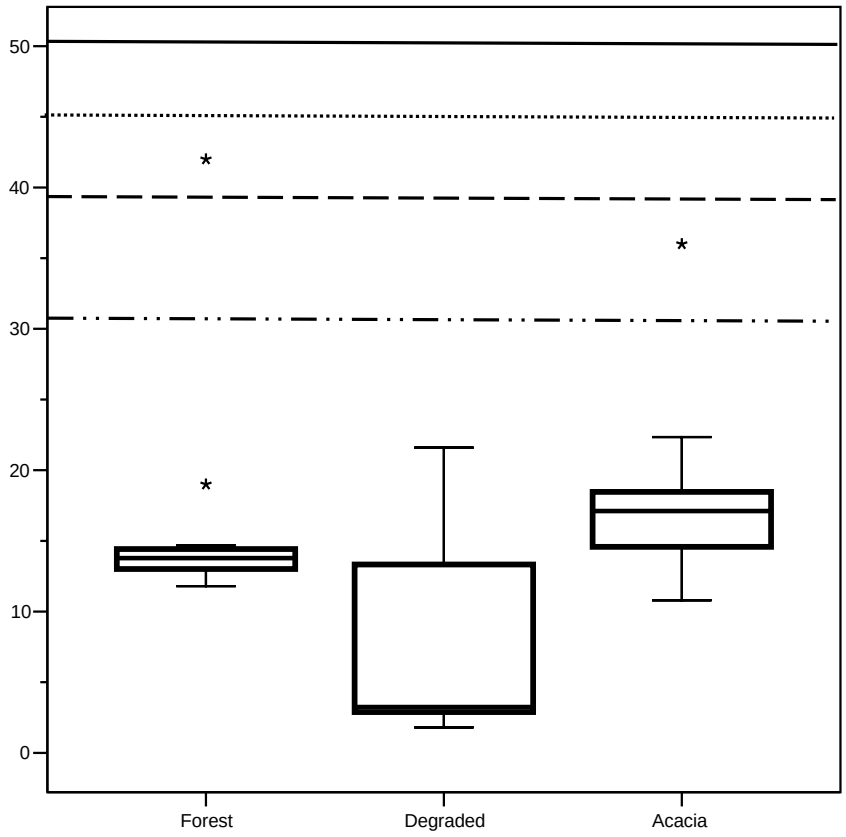

Figure. 5.2 (d)

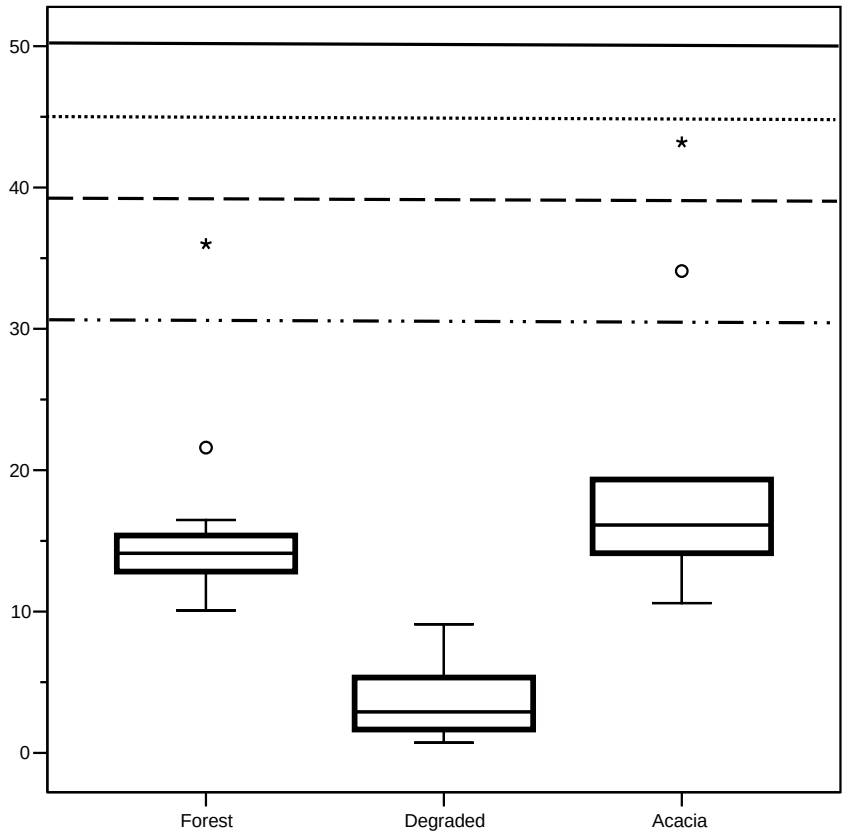

Figure. 5.2(e)

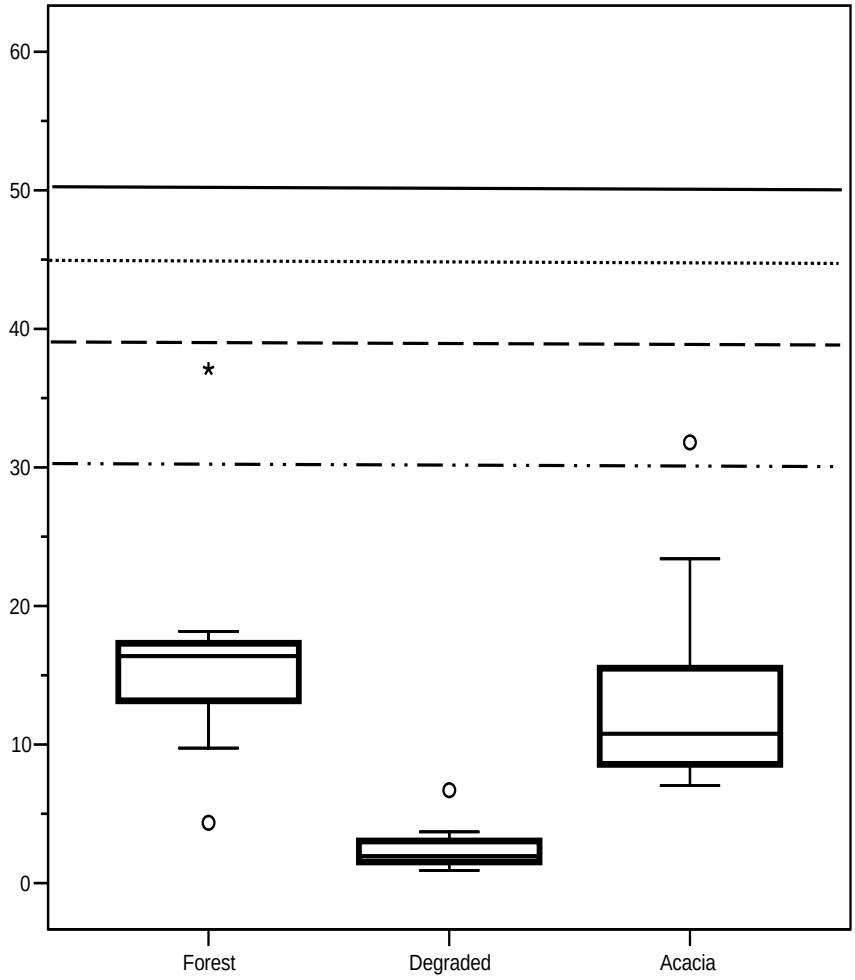

Figure. 5.2(f).

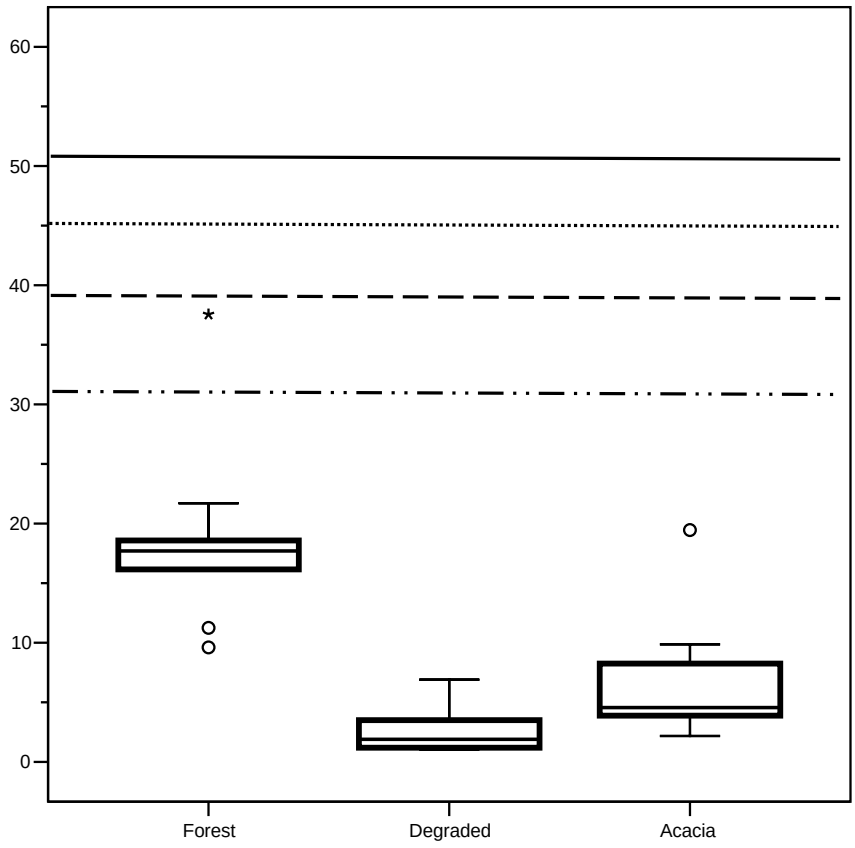

Figure. 5.2(g)

Figure. 5.2. The box plot of saturated hydraulic conductivity (K*) by land cover for (a) at surface, (b) at 0.1m, (c) at 0.3 m, (d) at 0.6m, (e) at 0.9 m, (f) at 1.2 m and (g) at 1.5 m depth

In comparison of surface mean K* values of degraded forest watershed, mean K* values under the acacia plantations (i.e. an increase of ~ 20mmh^{-1}), were increasing at constant magnitudes. Except these, the vertical changes in K* under the acacia were similar to those of the forest (except below 1.20m depth). Thus the impacts of degradation-forestation were seen to be concentrated in the top 0.1m of these soil profiles. The order of magnitude of the vertical changes of K* were similar to those reported by Bonell *et al* (2010) for other similar land cover sites in the Uttara Kannada region. Moreover it was found that this particular soil type remained resilient to any disruption of the surface soil fabric in the summer monsoon from factors such as the raindrop compaction and others and thus no change noted in magnitude of surface K* between dry and wet season measurements. Consequently, the B-W plots linked with the selected IDFs as showed in

figures 4.18 provid a reasonable basis for inferring dominant storm flow pathways assuming optimal conditions of soil wetness during the summer monsoon and a prevailing unit hydraulic gradient in the vertical plane.

Evidences showed that HOF was not possible in the forest (Figure. 5.2) and impedance to percolation was only possible for the lowest return periods (i.e.1 or 2 in 2 years) where deep SSF might occur at depths 0.6m and below. For the more frequent rainfalls, vertical percolation was shown as they favoured pathway and thus significant groundwater recharge could be expected. Above 0.6m depth in the degraded forest (Figure.5.2), vertical percolation is also indicated despite a lowering of K*. However the lowest return period lines intersect the B-W plots at 0.1m depth in the lower quartile so impedance were possible at such times to produce more shallow SSF and possibly some SOF. The main difference is below 0.6m depth where the same IDFs exceed the medians of all the B-W plots. At such times deeper SSF is indicated which could result in less recharge to groundwater, c.f. the Forest. On the other hand for the higher frequency rains, a substantial part can continue as deep percolation to groundwater. Thus the principal differences between the Degraded Forest and the Forest concerns a potential deflection laterally of percolation during the heavier, less frequent rains at ~ 0.6m depth and a reduction in groundwater recharge. Plus, the occurrence of shallow SSF and SOF during the less frequent but higher rainfalls is possible.

Using the degraded forest as the benchmark, acacia plantations are increasing the saturated hydraulic conductivity in the surficial horizons (≤0.1m depth). These shallow depths are more directly affected by the incorporation of soil organic matter and a reduction in human use and disturbance. Nonetheless the degraded forest and acacia plantations have the same order of magnitude in surface K*, the forest (Table. 5.9), and is linked with the land cover history. It is also noticed that, the rank order of median K* is Forest > Acacia Plantation > Degraded Forest for the upper layers (≤0.1m depth). At 0.6m and below, the above trends in the median K* for each of the land cover surprisingly remains the same (Table.5.9). The causes for the persistence of higher permeability beneath the acacia when compared to the degraded forest however are inconclusive.

Overall, the acacia plantation (Figure. 5.2) indicated a greater prospect of overland flow (HOF and /or SOF in combination with SSF) occurrence because the more extreme rainfalls of higher return periods are close to the surface median. Further even the more frequent rains (12 in 3 years) exceed the median K* at 0.1m depth. Below 0.3m depth all rain frequencies far exceed the medians and the quartiles of the B-W plots overall thus indicating a reduction in ground water recharge.

CHAPTER VI SOIL MOISTURE MODELING

6.0 Soil Moisture Modeling

Soil moisture is an important component of the hydrological cycle and a key mediator between land surface and atmospheric interactions. Also it is an important component while assessing the hydrological response of a catchment in particularly, the runoff formation processes in a catchment. Near absence of high density soil moisture observation network is an obstacle for weather and climate prediction. Unavailability of long-term homogeneous soil moisture data for various depths of the root zone also prevents from better understanding how this quantity varies over different time-scales under different land uses within heterogeneous hydroclimatic domains. Modeling of soil moisture and creating a long term data set can be used to answer some of the issues viz., (1) variability of soil moisture at different time-scales under different hydroclimatic regimes, (2) impact of land use on the variation of soil moisture. This chapter tries to address issues that are related to the above themes. In particular it is concerned with the following issues; can we evaluate the model parameters and their association with changes in land cover? What are the adaptation strategies of the plants to the varying climate of the area? Can we identify an appropriate statistical distribution for the observed soil moisture and Can derive a time series model to predict the soil moisture under changing climate and land covers.

6.1 HYDRUS - 1D

General

HYDRUS – 1D is a public domain computer software package that simulates the one dimensional movement of water, heat and multiple solutes in variably saturated media. It numerically solves the Richards equation for variably-saturated water flow and advection-dispersion type equations for heat and solute transport. The flow equation incorporates a sink term to account for water uptake by plant roots. The flow equation may also consider dual-porosity type flow in which one fraction of the water content is mobile and another fraction immobile, or dual-permeability type flow involving two mobile regions, one representing the matrix and one the macropores. The heat transport equation considers transport due to conduction and convection with flowing water. Coupled water, vapor, and energy transport can be considered as well. The solute transport equations consider advective-dispersive transport in the liquid phase, as well as diffusion in the

gaseous phase. The transport equations also include provisions for nonlinear nonequilibrium reactions between the solid and liquid phases, linear equilibrium reactions between the liquid and gaseous phases, zero-order production, and two first-order degradation reactions: one which is independent of other solutes, and one which provides the coupling between solutes involved in sequential first-order decay reactions. Physical nonequilibrium solute transport can be accounted for by assuming a two-region, dual-porosity type formulation which partitions the liquid phase into separate mobile and immobile regions. Additionally, the transport equations may include provisions for kinetic attachment/detachment of solutes to the solid phase, thus permitting simulations of the transport of viruses, colloids, or bacteria.

The program may be used to analyze water and solute movement in unsaturated, partially saturated, or fully saturated porous media. The flow region may be composed of non-uniform soils. Flow and transport can occur in the vertical, horizontal, or a generally inclined direction. The water flow part of the model can deal with prescribed head and flux boundaries, boundaries controlled by atmospheric conditions, as well as free drainage boundary conditions. The governing flow and transport equations are solved numerically using Galerkin - type linear finite element schemes. HYDRUS-1D also includes a Marquardt-Levenberg type parameter optimization algorithm for inverse estimation of soil hydraulic and/or solute transport and reaction parameters from measured transient or steady-state flow and/or transport data.

HYDRUS-1D further incorporates modules simulating carbon dioxide production and major ion solute movement. The CO_2 transport processes include diffusion in both the liquid and gas phases and advection in the liquid phase. The CO_2 production model is described in detail.

6.1.1 Governing Water Flow Equation

Uniform water flow

One-dimensional uniform (equilibrium) water movement in a partially saturated rigid porous medium is described by a modified form of the Richards equation using the assumptions that the air phase plays an insignificant role in the liquid flow process and that water flow due to thermal gradients can be neglected.

$$\frac{\partial \theta}{\partial t} = \frac{\partial}{\partial x}\left[K\left(\frac{\partial h}{\partial x} + \cos \alpha \right) \right] - S$$

Eqn 13

where h is the water pressure head [L], θ is the volumetric water content [L^3L^{-3}], t is time [T], x is the spatial coordinate [L] (positive upward), S is the sink term [L^3L^{-3}], α is the angle between the flow direction and the vertical axis (i.e., α = 00 for vertical flow, 900 for horizontal flow, and 00 < α < 900 for inclined flow), and K is the unsaturated hydraulic conductivity function [LT^{-1}].

Uniform Water Flow and Vapor Transport

The Richards equation considers only water flow in the liquid phase and ignores the effects of the vapor phase on the overall water mass balance. While this assumption is justified for the majority of applications, a number of problems exist in which the effect of vapor flow cannot be neglected. Vapor movement is often an important part of the total water flux when the soil is relatively dry.

Root Water Uptake

Root water uptake without compensation

The sink term, S, is defined as the volume of water removed from a unit volume of soil per unit time due to plant water uptake. Feddes et al. [1978] defined S as

$$S(h) = \alpha (h)\, S_p \qquad \text{Eqn 14}$$

where the root-water uptake water stress response function α(h) is a prescribed dimensionless function of the soil water pressure head ($0 \leq \alpha \leq 1$), and Sp the potential water uptake rate [T^{-1}].

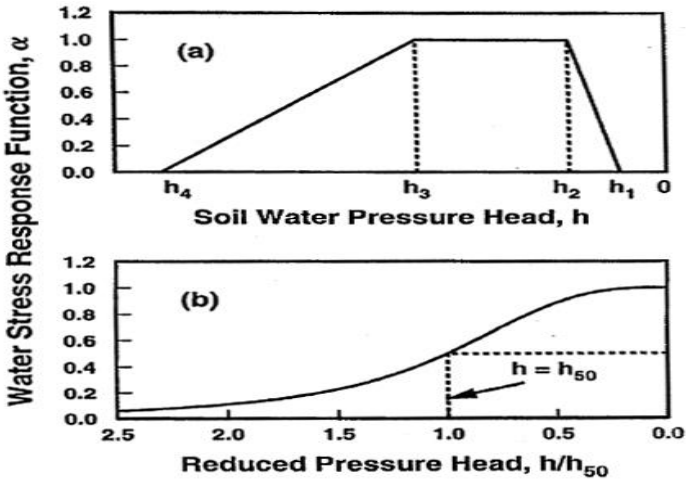

Figure 6.1. Schematic of the plant water stress response function, α(h),as used by a) Feddes et al. [1978] and b) van Genuchten [1987].

6.1.2 Unsaturated Soil Hydraulic Properties

Uniform Water Flow System

The unsaturated soil hydraulic properties, θ(h) and K(h), are in general highly nonlinear functions of the pressure head. HYDRUS permits the use of five different analytical models for the hydraulic properties [Brooks and Corey, 1964; van Genuchten, 1980; Vogel and Císlerová, 1988; Kosugi, 1996; and Durner, 1994]. The soil water retention, θ(h), and hydraulic conductivity, K(h), functions according to Brooks and Corey [1964] are given by

$$S_e = \begin{cases} |\alpha h|^{-n} & h < -1/\alpha \\ 1 & h \geq -1/\alpha \end{cases}$$

$$K = K_s \, S_e^{2/n+l+2}$$

Eqn 15

respectively, where Se is effective saturation:

$$S_e = \frac{\theta - \theta_r}{\theta_s - \theta_r}$$

Eqn 16

in which θr and θs denote the residual and saturated water contents, respectively; Ks is the saturated hydraulic conductivity, α is the inverse of the air-entry value (or bubbling pressure), n is a pore-size distribution index, and l is a pore-connectivity parameter assumed to be 2.0 in the original study of Brooks and Corey [1964]. The parameters α, n and l in HYDRUS are considered to be empirical coefficients affecting the shape of the hydraulic functions.

HYDRUS also implements the soil-hydraulic functions of van Genuchten [1980] who used the statistical pore-size distribution model of Mualem [1976] to obtain a predictive equationfor the unsaturated hydraulic conductivity function in terms of soil water retention parameters. The expressions of van Genuchten [1980] are given by

$$\theta(h) = \begin{cases} \theta_r + \dfrac{\theta_s - \theta_r}{[1 + |\alpha h|^n]^m} & h < 0 \\ \theta_s & h \geq 0 \end{cases}$$

Eqn (17)

Where θs and θr are the saturated and residual moisture and α and n are the van-Genutchen parameters, and

m =1- 1/n ----------(Eqn 18)

INPUT DATA

Based upon the available information, two distinct soil layers were identified. The following input data was used for simulation of soil moisture movement through Hydrus.

Rainfall : Daily rainfall data for the period of 2011 – 2013, were collected from the statistical department (Karnataka State) for raingauges located within the catchment of Kodgibail basin.

Soil Hydraulic Parameters

The unsaturated soil hydraulic properties in the HYDRUS code are shown in Table 6.1 (a, b & c). Soil samples were collected during the experimental studies and analysed for hydraulic parameters. θs and θr are the saturated and residual moisture and α and n are the van-Genutchen parameters, and

$m = 1 - 1/n$ ---------- (19)

The averaged van-Genuchten parameters for the soil layer were obtained by non-linear regression analysis.

Table 6.1 (a) Soil Hydraulic Parameters for Forest

θ_r	θ_s	α	n	K_s
0.09	0.35	0.0058	1.82	191.04
0.09	0.25	0.0058	1.77	41.6

Table 6.1(b) Soil Hydraulic Parameters for Degraded

θ_r	θ_s	α	n	K_s
0.021	0.29	0.00043	2.12	38.56
0.04	0.1	0.00043	2	41.66

Table 6.1(c). Soil Hydraulic Parameters for Acacia

θ_r	θ_s	α	n	K_s
0.109	0.23	0.0233	1.6782	148.32
0.16	0.51	0.0016	1.739	91.752

6.1.3 Output of HYDRUS – 1D

Potential Surface Flux

The potential flux in three land covers viz. forest, degraded land and acacia auriculiformis showed considerable variations during the study period. In all three watersheds, it varied between 0 and 25 cm/days. The gaining and recession limbs showed a rapid movement indicating the variation of soil moisture variation at the top of the soil layer due to climatic conditions. In the case of bottom flux, gain and recession limbs show a lag time which could be attributed to the changes in the hydraulic properties. It is also important to note that this gradual increase and decrease depends on the root length and root density, apart from soil physical and chemical characteristics. The variation of potential flux predicted by model is shown in fig 23.

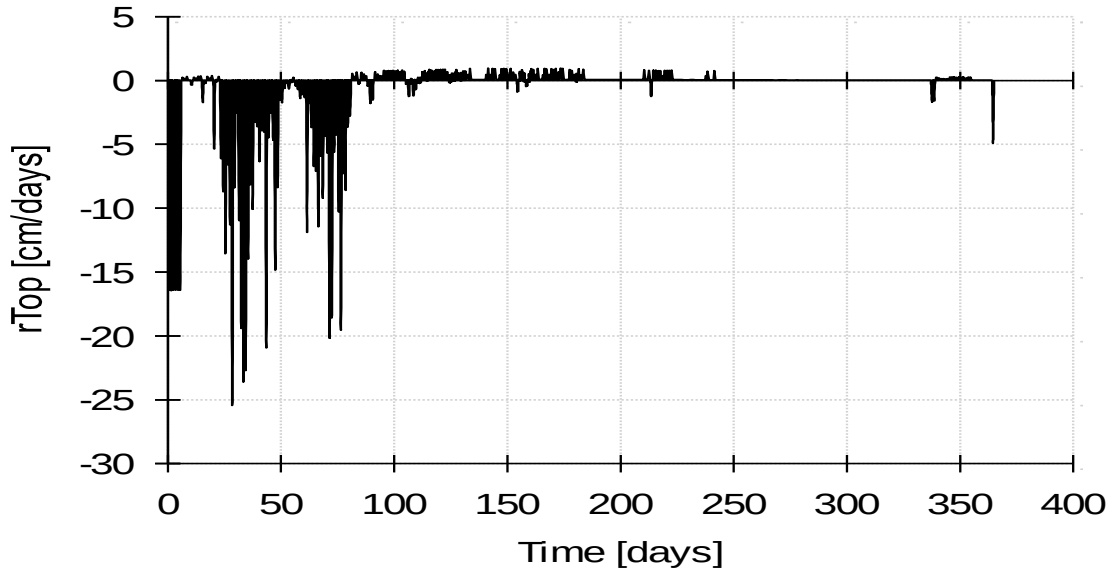

Figure 6.2. Potential surface flux for Selected watersheds

Root Zone Pressure Head

Root zone pressure head obtained from the HYDRUS model shows that, it is maximum in the degraded lands as compared to forests and acacia auriculiformis. In the degraded lands the root zone pressure goes up to -4000cm (figure 6.3) and in acacia auriculiformis, -200cm (figure 6.4) and in the forest watershed, it is -600cm (figure 6.5). The higher root zone pressure head in the forested watersheds could be due to excessive evapotranspiration through forest plants and hydro-climatic conditions existing in the forested watersheds. The variation of root zone pressure head predicted by model are shown in figures 6.3, 6.4 and 6.5.

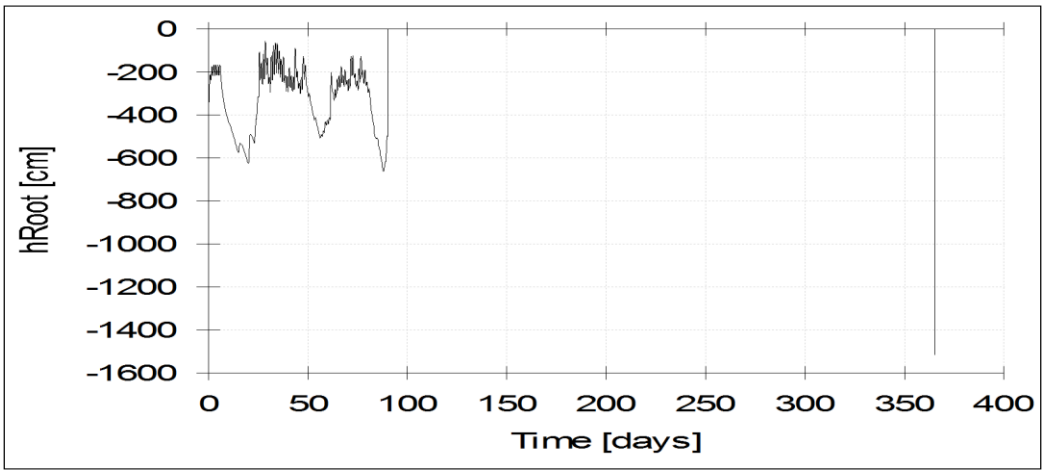

Figure 6.3 Root zone pressure head for forested watersheds

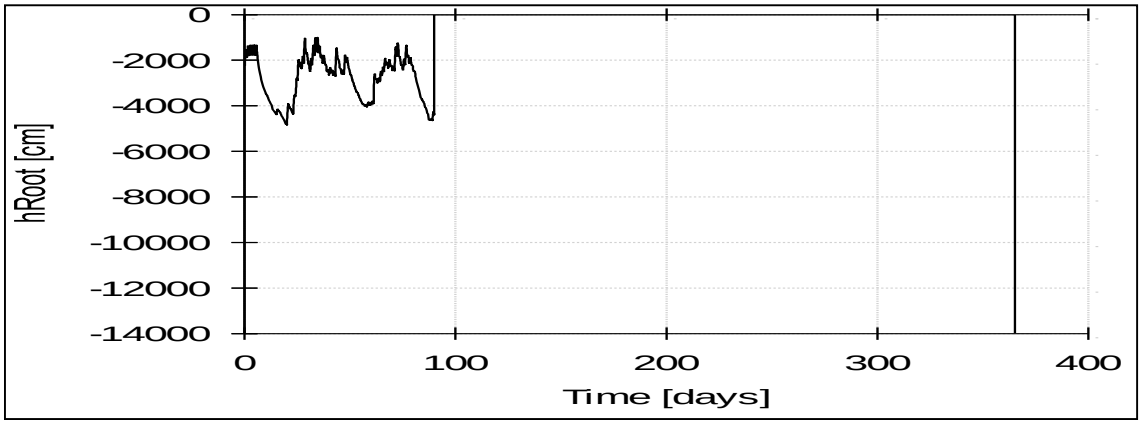

Figure 6.4. Root zone pressure head for Degraded watersheds

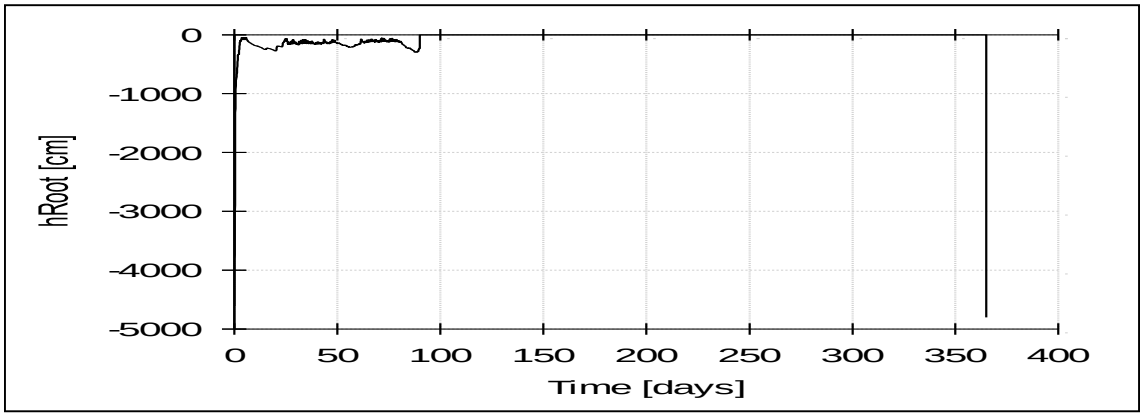

Figure 6.5. Root zone pressure head for acacia watersheds

Soil Hydraulics Properties

θ - h relationship observed under three land covers, the forest soils exhibit a sharp decline in the water content with pressure head initially and it smoothens and move parallel to the x-axis as the theta value approaches 0.1. The same trend is seen in the case of bottom soils also. In the case of degraded lands, the movement of soil moisture is gradual and becomes parallel when h is 5000 cm. The variation in the θ – h relationship is very low in the case of bottom soil. In Acacia one of the interesting result is that unlike forests and degraded lands, there is a larger variation in theta- h relationship of top and bottom soils. The variation of soil hydraulic properties predicted by model are shown in figures 6.6, 6.7 & 6.8.

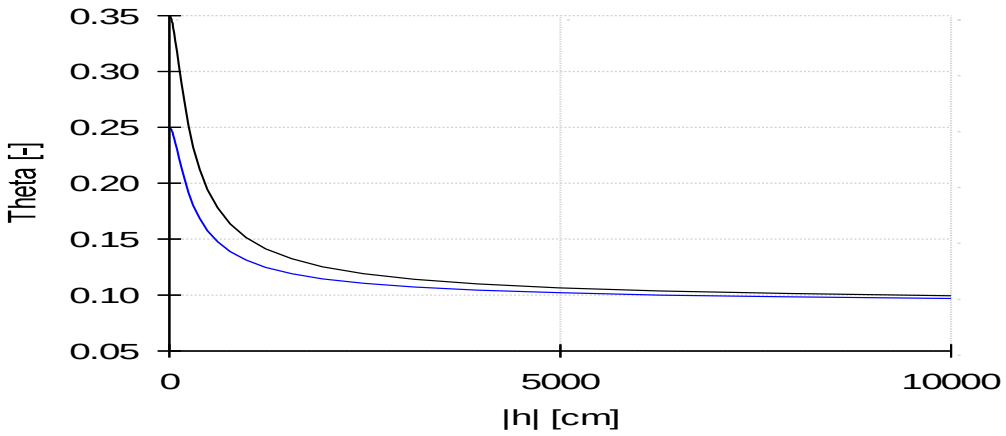

Figure 6.6. Soil hydraulic properties for forested watersheds

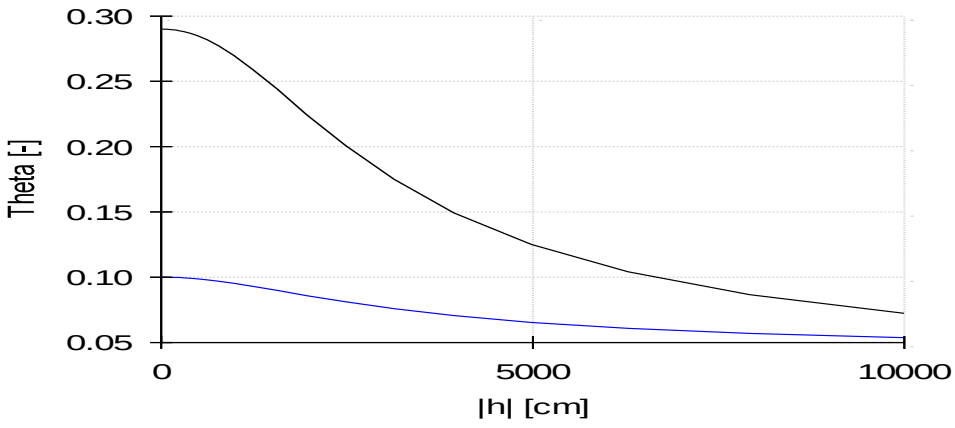

Figure 6.7. Soil hydraulic properties for degraded watersheds

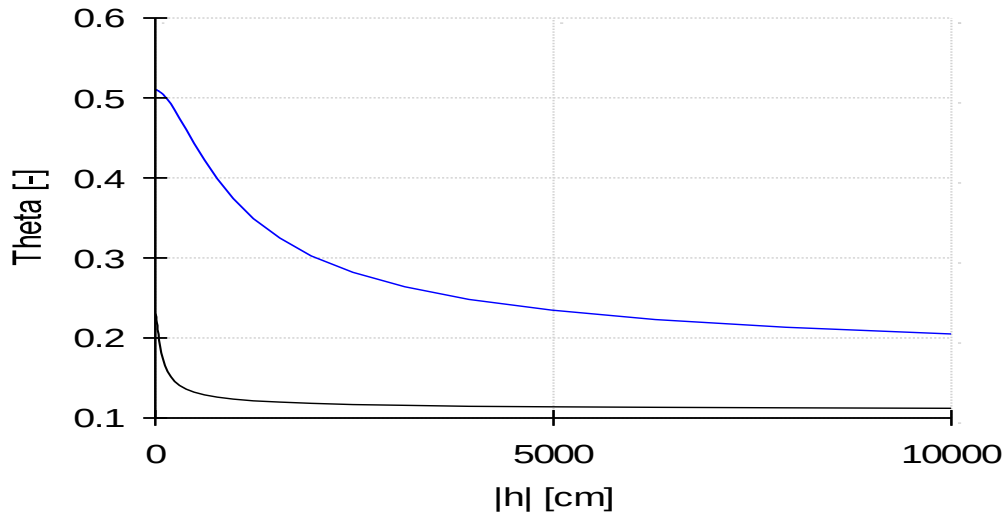

Figure 6.8. Soil hydraulic properties for acacia watersheds

Soil Water Storage

The soil water storage is one of the major components which contribute to the groundwater recharge. In the present investigation it is noticed that Acacia auriculiformis transmits more water to the groundwater storage. The variations of soil water storage predicted by model are shown in figures 6.9, 6.10 and 6.11. The HYDRUS model results indicate that the maximum recharge in the forested water is 16.5% which declines to 7.8 % during non-monsoon seasons. In Acacia, the recharge is slightly higher than the forests and the maximum recharge estimated is 19.5 % with an annual recharge of 9.5 %. As expected, in the degraded lands, it is found that 9.5 % is the maximum recharge and 3.2 % is the minimum recharge.

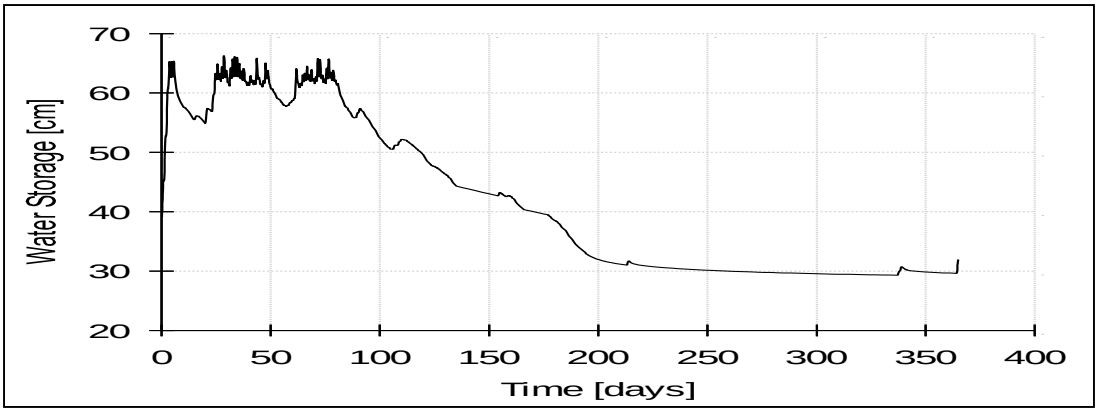

Figure 6.9. Soil water storage for forested watersheds

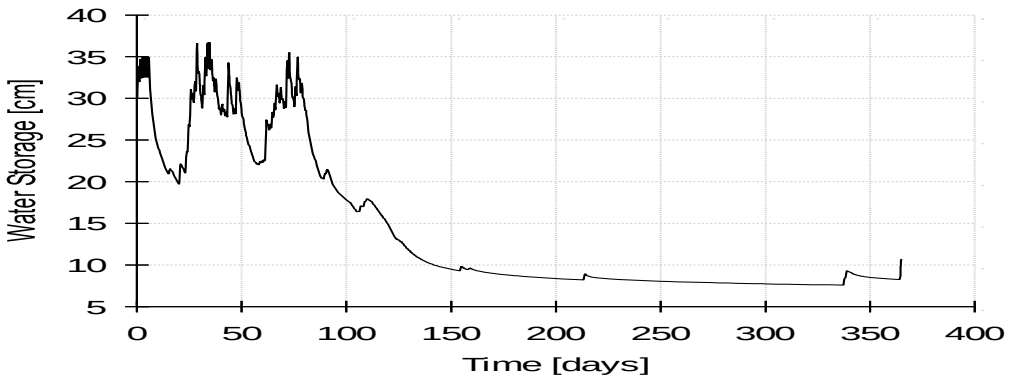

Figure 6.10. Soil water storage foe degraded watersheds

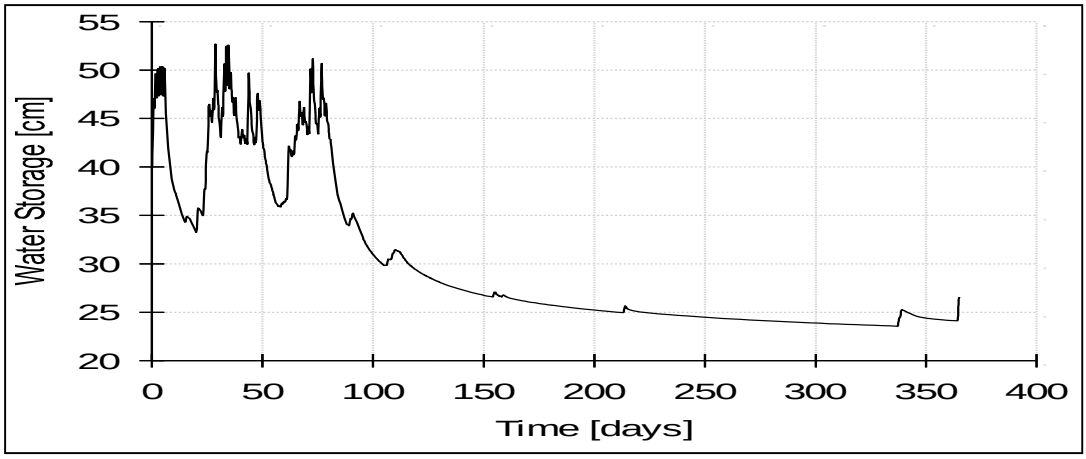

Figure 6.11. Soil water storage for acacia watersheds

Summary

In the current study an attempt is made to quantify the hydrologic response of different landscapes covering forest, degraded and acacia plantation in sub watersheds of Biligihole catchment, a sub-catchments of Aghanashini River basin. Our observations are insights to the plausible hydrological scenarios in future at a landscape scale which is a crucial step forward for a developing country like India in the context of today's increasing focus on integrated water resources management (IWRM) in River basins. As a part of the study, hydrological data monitoring, analysis and interpretation have been carried out. It is revealed that, the conversion of forest land to crop lands in the head water catchments leads to to an increase in the extreme flows and mean annual flows. Analysis of other hydrological components have shown that the increase in flows is caused by the increase in runoff and decrease in ET. The uncertainties due to model parameterization in land use

change impacts, varies from one landscape to another. The uncertainties did not alter the trend of changes when compared to the baseline; however, a considerable variation is observed especially in the magnitudes of extreme flows simulated for the different land cover scenarios. This result suggests a significant constraint on the usage of hydrological models for the variations of extreme flows due to land use change. Modeling studies also showed that the groundwater recharge is significantly high in the forests and acacia plantation as compared to degraded lands. It is found that the excessive deforestation activities my result in the occurrence of extreme events of flows causing floods in the basin. Therefore, the uncertainties from model parameters should be considered in land use change impact assessment for more robust and reliable analysis, which shall make the land cover change mitigation strategies and water resources management plans more effective. It is also observed there are likely chances of occurrence of extreme flows during the monsoon which if combined with the impacts resulting from land cover changes might result in adverse flooding in the basin. Therefore, Future studies shall focus on modelling the combined impacts of climate and land cover changes on hydrology of Aghanshini river basin, considering the uncertainties from model parameterization, which is currently lacking in many studies.

6.2 Geophysical survey analysis

Quantitative interpretation allows getting the real numbers of layers, their resistivity and thicknesses. The selected resistivity data obtained through field investigations were plotted (**Figure 6.12a, b & c**) for three different sections of the study area (i.e. Q, H and K type curves).

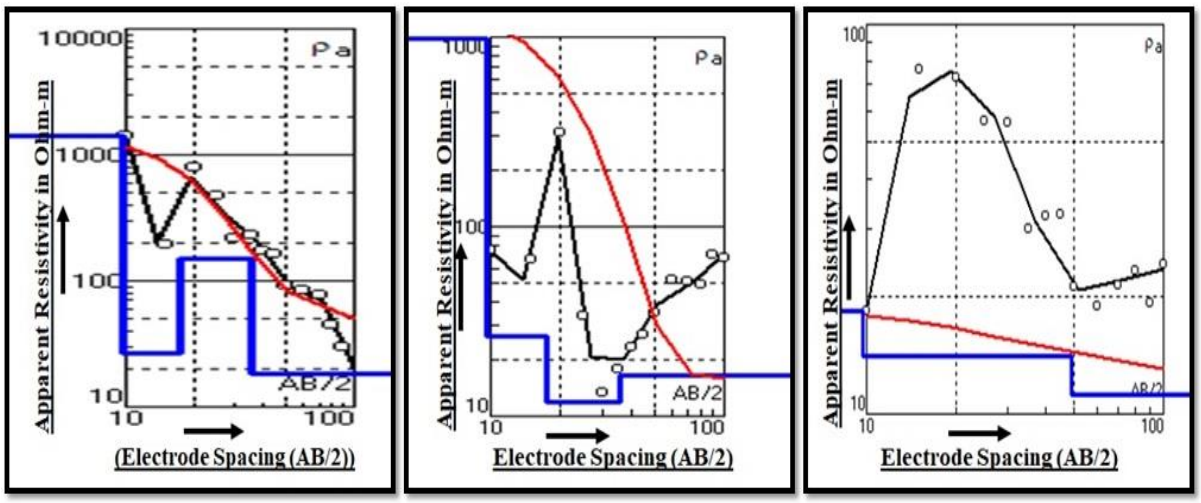

(a) (b) (c)

Figure 6.12: Typical Resistivity curves of the study area

Q Type: (p1> p2> p3): A resistivity curve with a continuously decreasing resistivity is called 'Q' type curves. Figure 42a shows the cross-section of the coastal zone with varying apparent resistivity. This is the most common section found in hard lateritic terrain occupying the top layer.
H Type: (p1> p2 <p3): Seen generally in hard rock terrains consisting of top soil of high resistivity followed by either a water saturated or weathered layer of low resistivity and then a compact hard rock of very high resistivity at the bottom. Figure 42b indicate the H-type curve with initial fluctuation with relatively high resistivity at the top which is followed by a water saturated and weathered layers of low resistivity and then a compact hard rock of high resistivity at the bottom.
K type (p1< p2> p3): Seen usually in basaltic areas such the 'K' type curves show a peak with values lowering towards the sides. Also present in coastal areas where freshwater aquifer occurs between clayey layer at the top and a saline zone in the bottom. Though this type of curves (Figure 42c) common in basaltic area, in the present case, it indicates the fresh water zone between clay layer and saline zone.
The resistivity data was converted to 2D images and presented in Figure 6.13 (a to c). Comparison of the Electrical resistivity ERT image and field observations indicated reasonably good agreement. The profile up to 5m depth with a very low resistivity in range of 0.2 to more than 4000 Ωm has been observed which indicate the presence of the top soil and sand within the clay formation. The high resistivity values could be attributed to the extension of lateritic plateau in the deeper layer.

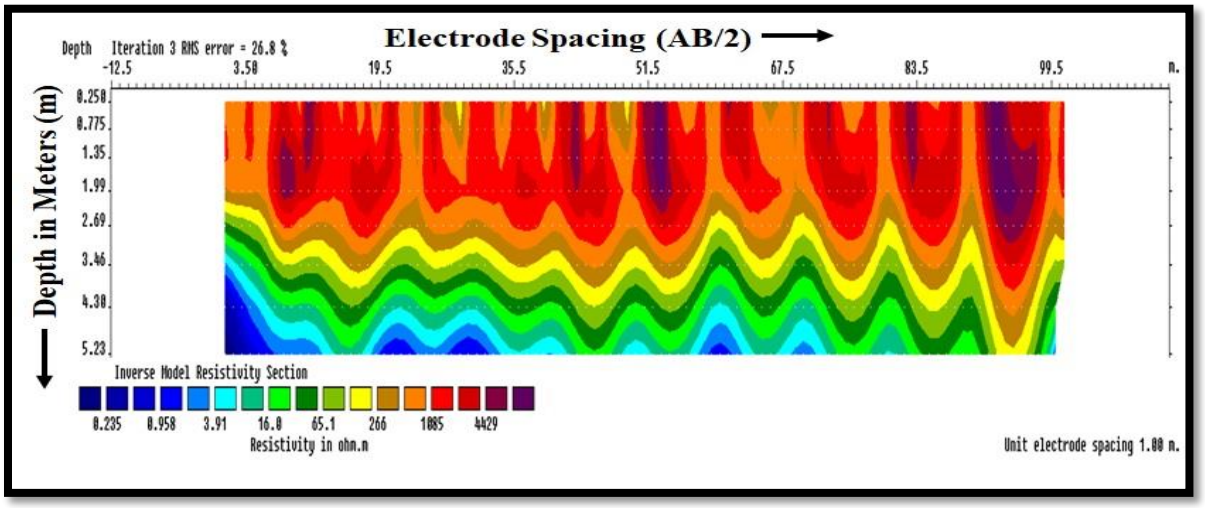

(a) ERT profile of Q –type curve

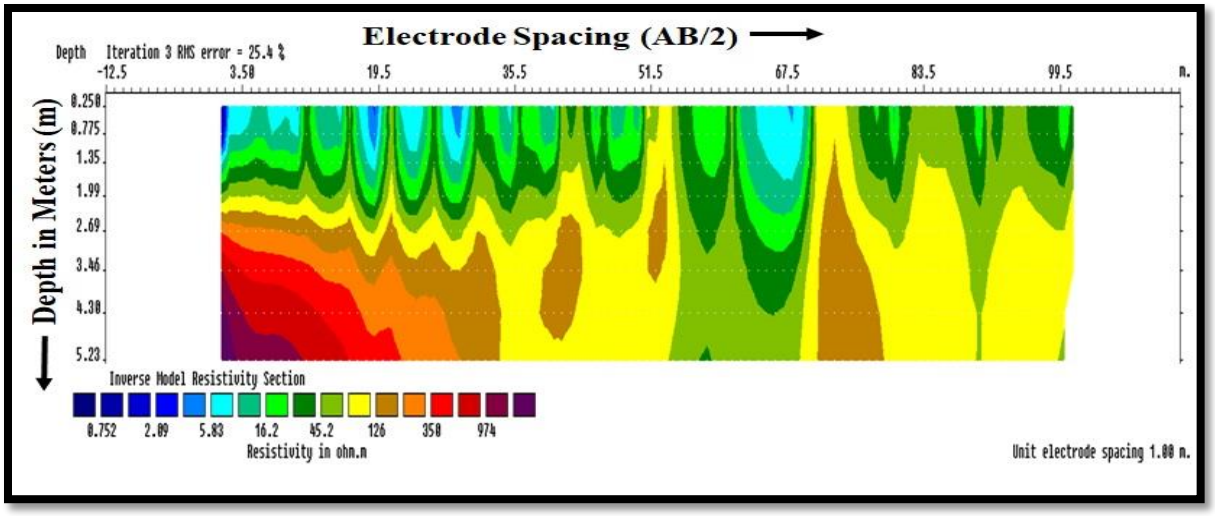

(b) ERT profile of H –type curve

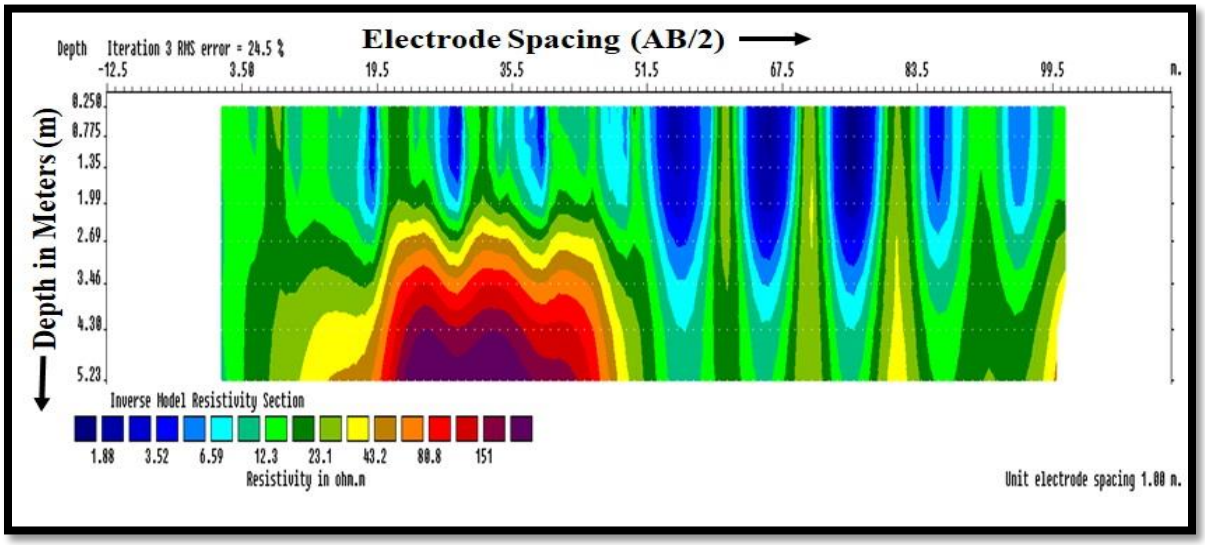

(c) ERT profile of K type curves

Figure 6.13: Electrical Resistivity survey results

The maximum current electrode spread and potential electrode separation were 100 and 10m, respectively. Data acquired were interpreted using the manual partial curve matching method and a fast computer iteration technique to generate the geo-electric layer of various resistivity values and thicknesses. The geo-electric sections revealed the lithological sequence as: topsoil, weathered layer and fresh bedrock. The overburden coefficient of anisotropy also revealed that, the underlying basement rock is suspected to be granite gneiss/granite. At locations where current terminated at the fresh bedrock region, the thicknesses were undetermined. Groundwater potential is presumed to be very low except in few isolated patches within the study area as outcrops of gneissic rocks dominate the area. Locations where the regolith is of appreciable thickness, the resistivity of the

layer suggests a material medium likely composed of clay/sandy clay or clayey sand which are not good aquifer media from which groundwater could be extracted.

Most of the sounding curves are of H, QH and KH types, which are considered as the most suitable types of resistivity curves to estimate the hydraulic parameters where current flow is approximately horizontal. The occurrence of a significant typical H type curve indicates the presence of a highly resistive top lateritic soil followed by a saturated zone and then the basement topography (Anoop et al., 2021). In the present study also the prevalence of 'H' type and its combinations can be taken as indicator of the top lateritic layer followed by saturated zone and then the basement. Additionally, inspection of the field curves reveals that, the H curve type is dominant all over the entire area indicating that, most of the sounding curves have the same number of layers. However, the thicknesses of those layers may differ from one locality to another.

Weathering is not a uniform phenomenon in any environment and results in heterogeneity in hydrological characteristics of the rock formations. The conceptual structure of hard rocks is that of a fresh basement overlain by materials which have undergone different stages of weathering. Groundwater availability is therefore attributed to weathering in the overburden and basement surface. Basement weathering presents themselves as zones of disintegration. These zones appear as low electrical resistivity anomalies compared to the massive basement rocks that surround them. Consequently, basement troughs with deep weathering are points of disintegration which are hydro-geologically viable as far as groundwater aquifers are concerned (K'Orowe et al., 2008). A fence diagram based on hydrogeological characteristics is presented below (**Figure 6.14**).

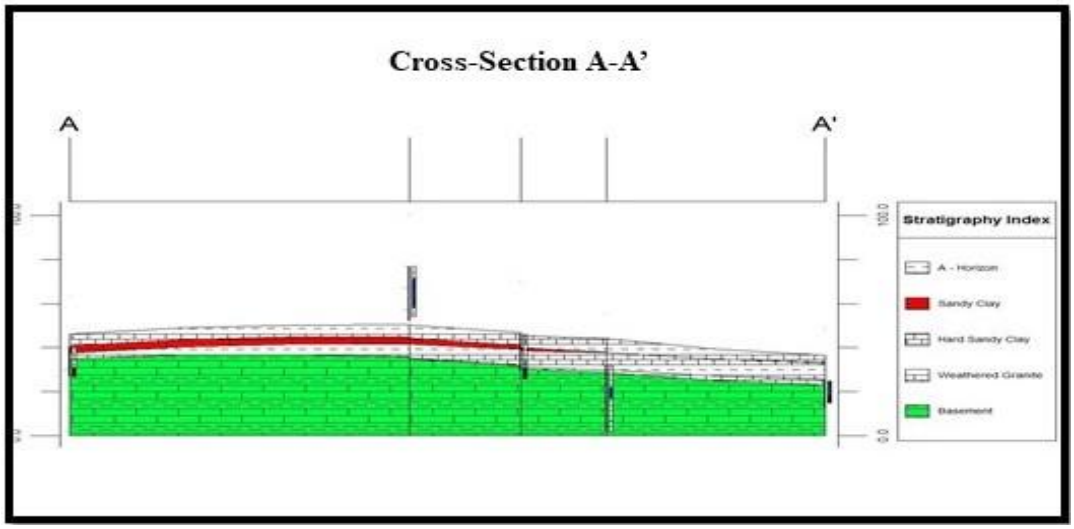

Figure 6.14: Stratigraphy of coastal tract of Uttara Kannada district

6.3 Groundwater level fluctuations

The frequency of water-level measurements is one of the most important aspects of a water quality monitoring system. While this may be influenced by economic factors frequency measurements should be considered as far as possible in relation to the expected variability of water level fluctuations in viewing sources and data resolution or the amount of data required to fully reflect the hydrologic performance of the aquifer. Groundwater level, either aquifer water of an unconfined aquifer or a piezometric surface of a closed aquifer, indicates the height of the atmospheric pressure. Differences between the supply and supply of groundwater create volatile levels.

The method of water level fluctuations is based on the acknowledgment that water level rise is due to recharge reaching groundwater. Estimation of the specific yield of the region of fluctuation for applying the method, the ground water level is required. Groundwater level data (2002 to 2012) of fourteen wells observed by CGWB during pre-monsoon and post-monsoon in different parts of the coastal taluka are plotted and shown in figures 6.15 and 6.16.

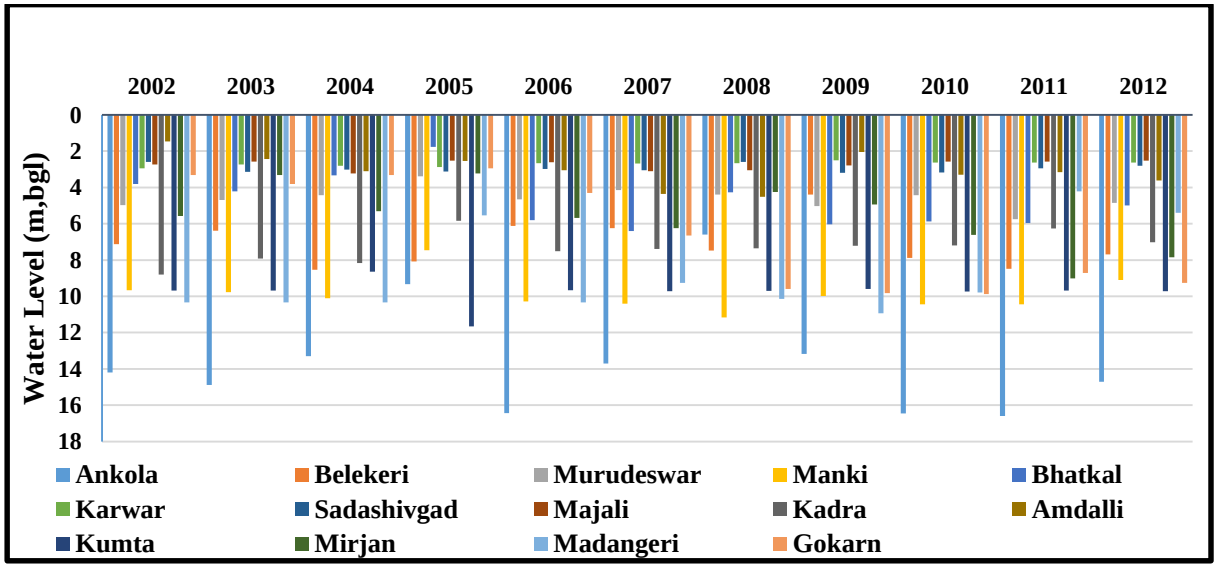

Figure 6.15: Groundwater levels (Pre-Monsoon)

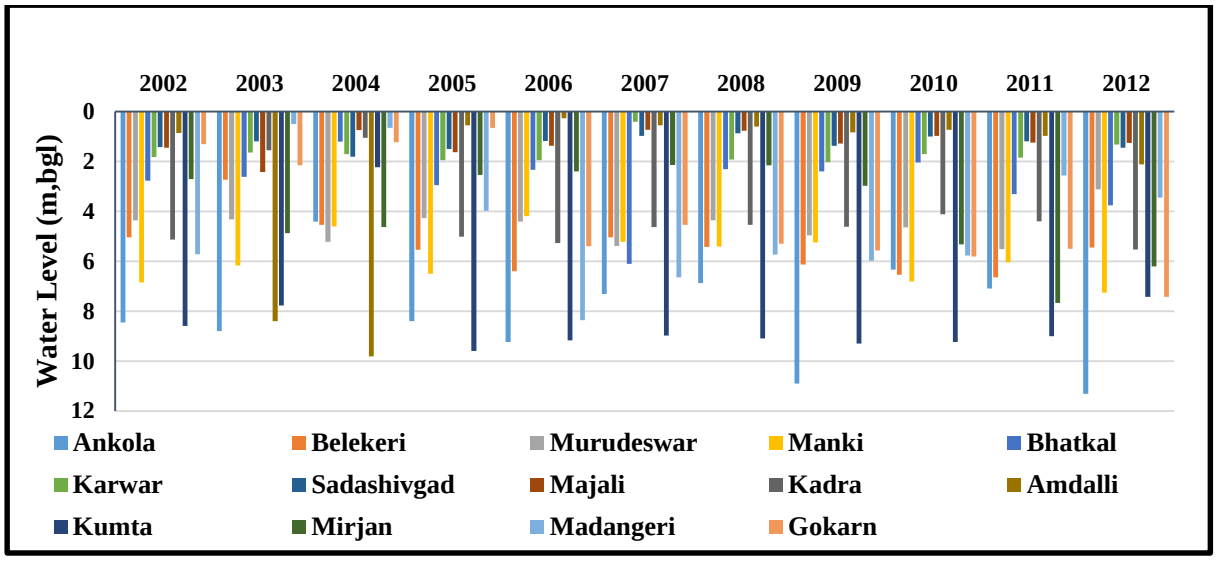

Figure 6.16: Ground water levels (post-monsoon)

Groundwater level monitoring was also carried out by NIH during 2017, 20018 and 2019 in selected wells of coastal zones covering Honnavara, Kumta, Ankola and Karwar taluka are presented in Figures 6.17, Figure 6.18 and Figure 6.19.

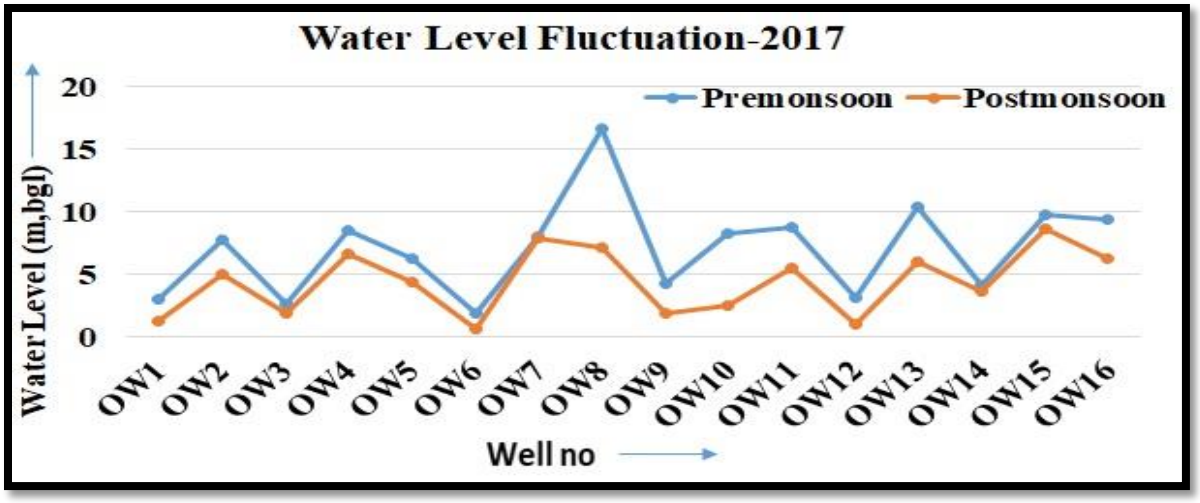

Figure 6.17: Ground water levels (2017)

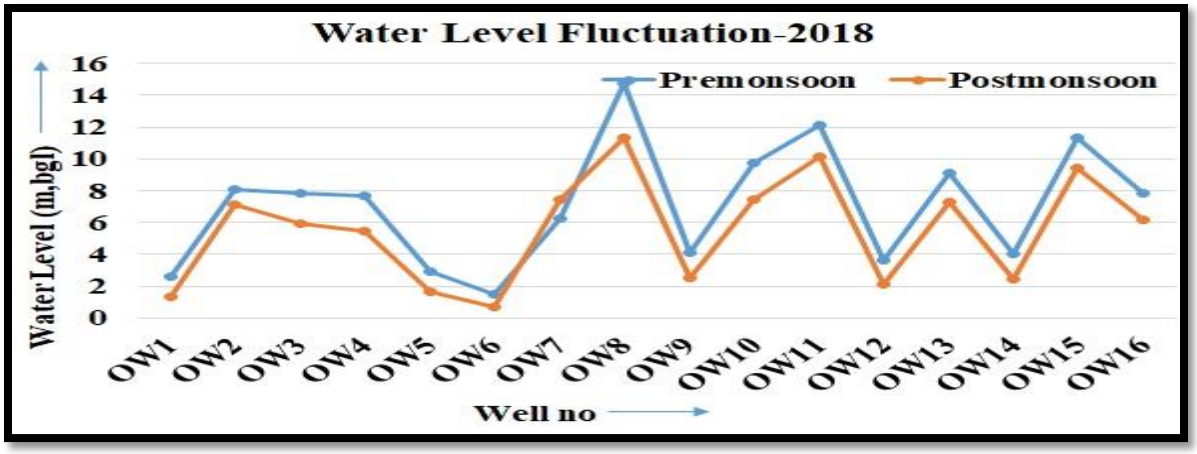

Figure 6.18: Ground water levels (2017)

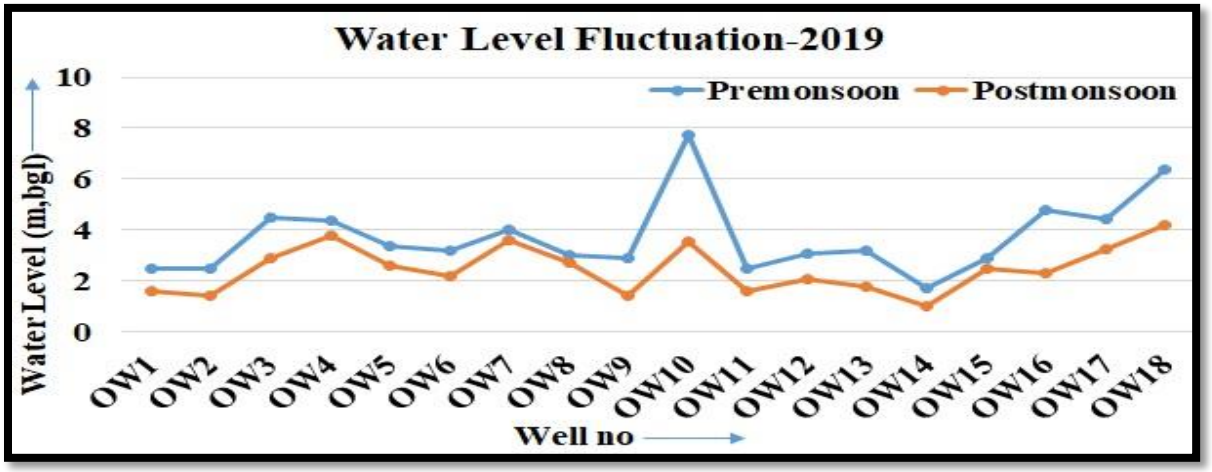

(l)

Figure 6.19: Annual groundwater level fluctuation graph

6.4 Soil Hydrology and Hydrogeological Analysis of Uttara kannada Groundwater Level Contours

A pre-monsoon water level observation of CGWB taken during May 2006 for the 30 national hydrograph network monitoring stations (Figure 9). The major part of the Uttara Kannada district is having the pre monsoon water levels between 5 to 10 mbgl during 2006. The area having water levels less than 2 mbgl is observed around Karwar town. Water levels between 2-5 m bgl were observed around Karwar town, along the coast between Kumta and Ankola, also on southern parts of Ankola. The major part of the Uttara Kannada district is having the post monsoon water levels between 2 to 5 mbgl during 2006. The perusal of the table shows is in the range of -0.19 – 13.03 m. The maximum water level fluctuation recorded is 13.03 m in Honnavar station and negative

fluctuation of –0.19 m is recorded at Murudeshwara station. The seasonal water level fluctuation, available for 10 piezometer hydrograph network stations in the range between –0.14 – 6.07m. The maximum water level fluctuation of 6.07 m recorded at Bandel piezometer national hydrograph station in Halyal taluk and minimum water level fluctuation of –0.14 m was recorded at Karwar piezometer national hydrograph station. Groundwater level contours for a period from 2017 to 2018 are shown in **Figures 6.20** (a to d) (Data Source: CGWB, Bengaluru).

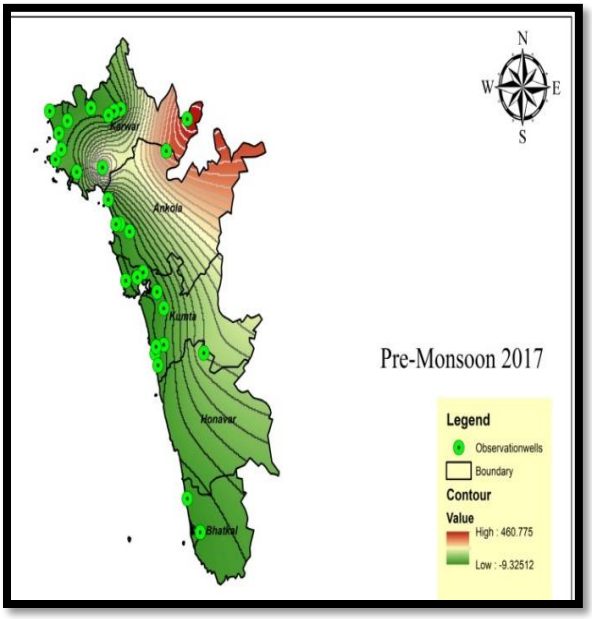

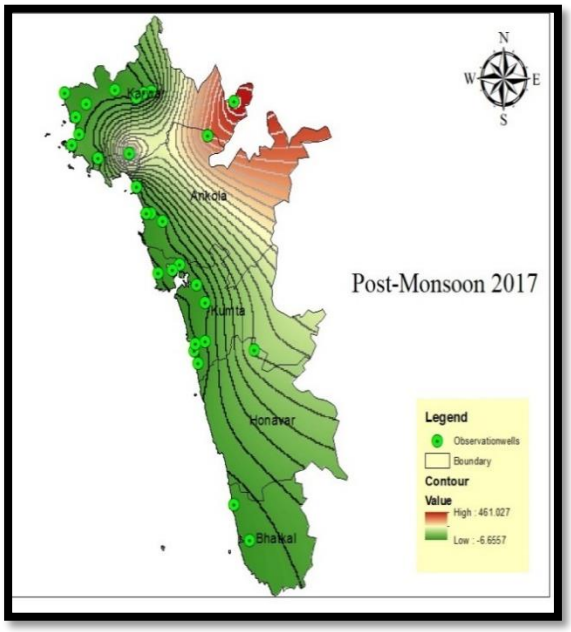

(a) (b)

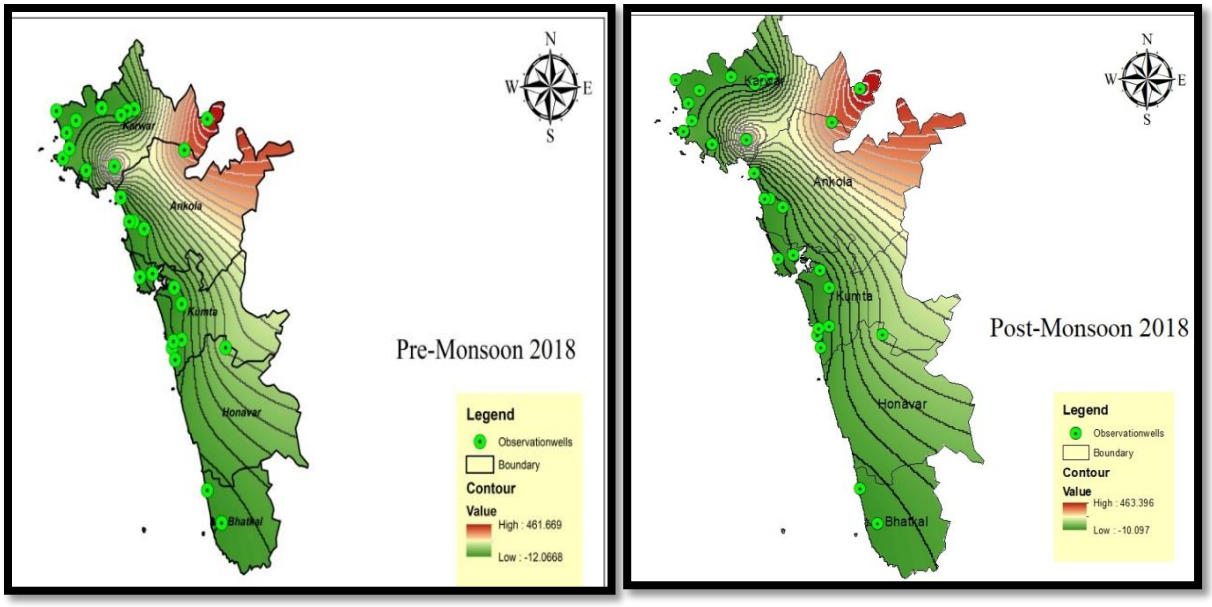

(c) (d)

Figure 6.20: Groundwater levels of Uttara Kannada district

6.5 Summary

Groundwater recharge is complex, influenced by both land use/land cover changes, aquifer lithology, and topography. Climate and LULC have significant effect on the recharge process due to their direct impact on soil infiltration. In the present investigations, three types of landscapes, viz. forest, degraded and afforested land covers have been monitored along the coastal tract of Uttara kannada district (Karnataka) for flow, infiltration and groundwater levels during the study period (2018-2020). The study was accomplished in two parts, with the first part based on direct observations from the study area aided by satellite datasets and secondary datasets. The second part is on forecasting future scenarios, based on modelling. A series of LANDSAT satellite data sets were used to analyse the historical LULC dynamics of Uttara kannada district of Karnataka. The analysis indicates that the rapid urbanisation and other anthropogenic activities have adversely affected all major natural land cover classes for the past three decades. From the observations, it is understood that the urbanisation-induced LULC changes lead to the rise in impervious surface coverage, causing a decrease in infiltration and a significant decline in groundwater recharge rates.

- The average annual rainfall of Uttara Kannada district is 3427.80 mm obtained from period 2002-2020 out of which maximum was 4668.80 and minimum 2361 mm. Mean is 3427.79. Standard deviation is 703.66.

- The soil profile observed up to a depth of 5m showed resistivity variation between 0.2 and 4000 Ωm which indicate the presence of a thin layer of top soil followed by hard rocks. However, in the present case, the high resistivity values could be attributed to the extension of lateritic plateau in the deeper layer.
- The groundwater recharge estimated showed that the recharge is maximum in 2008 that is about 20.02% and minimum in 2007 (13.55%). According to the SWAT analysis, the surface runoff is found to be 1754.25 mm, Lateral flow is 136.78 mm, Recharge to deep aquifer is 55.53 mm, precipitation and evapotranspiration is 3492.3 mm and 490.8 mm, respectively.
- Hydrogeological investigations have shown that the coastal aquifers of Uttara Kannada do not show any signature of seawater intrusion as it is evident from the present investigations. This is further established from the high groundwater recharge value (15-20% of annual rainfall). High recharge of groundwater may keep the groundwater level always above the mean sea level due to which, the possibility of seawater intrusion become rare. However, there are chances of temporary phenomena which occur mainly due to advancement of sea towards the land during heavy monsoon causing enormous losses due to coastal erosion and fishery resources.
- River flow characteristics of some of the rivers have been analysed based on the discharge data. Base-flow estimated indicate that, submarine groundwater discharge occurs during dry seasons mainly due to high rainfall and high groundwater recharge. The estimated saturated hydraulic conductivity showed that the soils are highly permeable in lateritic areas, particularly below the top soil due to which the infiltrated water flows to sea continuously. From the present study, a rough estimate of about 0.15% to 0.18% of rainfall enter the sea as submarine ground discharge from March to May. This is mainly based on monthly moisture trend which were observed at three sites and found a reasonably high moisture content in three locations namely, Murudeshwar, Kumta and north of Karwar taluks. Groundwater quality investigations carried out in more than thirty wells all along the coast also demonstrated that, the coastal aquifers are safe for drinking, irrigation and domestic purposes.

CHAPTER – VII : CATCHMENT MODELING

7.0. INTRODUCTION

As the population has been growing rapidly and more stress is put on the land to support the increased population, one question that arises is how hydrologic resources will be affected. It is generally recognized that, across all climatic regions this has resulted in land degradation in terms of soil erosion, reduced productivity and deterioration of fragile natural ecosystem (Lorup, et al., 1998). Furthermore, land mismanagement may have inadvertent negative effects on the hydrological regime, such as increasing occurrence of floods and decreasing dry season flows. Thus, the thrusts in the hydrologic modeling are the assessment of the effects of land-use and land cover changes on water resources. These changes are the results of natural processes as well as anthropogenic influences.

Water availability is a critical issue facing humanity in the decades ahead. Land cover changes play an important role in water quality and quantity. Therefore there is a greater need to integrate land cover change science and hydrology to predict such an impact. In such situations, the mathematical model can be used in making the policy of water management of a region. Up to now, there have been great efforts to examine potential impact of climatic change upon water resources (IPCC, 1996). At the same time, very less focus has been paid in assessing the potential effects of land use changes on spatial and temporal availability of water. Therefore, in the recent times, thrust has been on the assessment of the effects of land-use and land-cover changes on water resources using the hydrologic modeling.

The relationship between land use changes and hydrology is complex, with the linkages existing at a wide variety of spatial and temporal scales; however, land cover change unquestionably has a strong influence on water yield. Land cover and land use directly impact the amount of evaporation, groundwater, infiltration and overland runoff that occurs during and after precipitation events. These factors control the water yield of surface streams and groundwater aquifers and thus amount of water available for both

ecosystem function and human use (Musterd and Fiesher, 2004; Sahin & Hall, 1996; DeFries & Eshleman, 2004; Farely, et al., 2005).

The hydrologic impacts of deforestation have been studied in detail for many decades. In their classic analysis of 94 previous paired watershed studies, Bosch & Hewlett (1982) found a consistent relationship between forest cover and water yield; reduction in forest cover led to increased stream flow while an increase in forest cover decreased stream flow. The amount of stream yield increases as a result of deforestation within a given watershed varies depending upon the local climate, geology and type of use to which the land is converted. Some studies suggest that stream discharge may increase as much as 50% as a result of deforestation (Musterd & Fisher, 2004).

In contrast to the effects of deforestation, reforestation and afforestation (the planting of trees in areas that are naturally non-forested) can be expected to result in reduced water yields. Case studies from variety of climate zones support this hypothesis, though it should be noted that deforestation/afforestation processes are not 'opposite and reversible' and changes in water yield resulting from each may differ (Farely, et.al., 2005). The findings of Bosch and Hewlett (1982) suggested that the impact of afforestation on stream flow is less severe in arid areas than in more humid areas. These findings are mostly originated from a smaller watersheds consisting of variety of tree species. Nonetheless, couple of studies of meso-scale watershed in Amazon was consistent with the findings reported by Bosch and Hewlett. But in recent past, the monoclutural species have been finding place in afforestation strategies in most of the country. Already there are world wide concern about increased establishment of plantation of exotic forest species and their detrimental effect on hydrology.

As reported by Rai (1999) that more than half of the Indian forestation has undertaken within the farm forestry sector notably in the Western Ghats. Most of these activities are being done using the monoculture species such as Acacia ariculiformis. The portion of the western ghat falls within the Karnataka state is locally called as Sahayadri Mountains. In the recent years, there is an increased anthropogenic activities in the in these areas. In view of reported land cover changes and increased plantation forest in Sahayadri Mountains, one question arises how hydrologic resources will be affected by these changes.

As this is very essential for better management of water resources of the peninsular India, since, most of the major river originates from these mountain range. Therefore, the purpose of this work will be to examine the potential impact of changes in land cover and land use on the hydrologic regime of the selected watersheds in Sahayadri Mountains using a mathematical model. The model is initially calibrated and validated using the measurements made at the experimental watersheds located in Sahayadri Mountain range. Further, the calibrated model is then used for simulating the impact of expected land cover changes to take place in the region.

7.1 WHY MODELING APPROACH IN THIS STUDY

Very few of the experimental catchment studies were carried out in the Western Ghat region. Majority of these studies have been carried out in a small and often head water catchments. Many of the catchments were often unhabitated or sparsely populated and with a controlled and often uniform land use (James, et.al., 2000; Sikka, et.al., 1998). On the other hand, most of the land use changes occurred in catchment heavily populated by farmers and their livestock and often with a mixed land use and a variety of contrasting topographical features, which experimental catchments seldom contain.

In this study, whatever hydrological understanding so far gained is through the experimental watersheds of uniform land cover type having mostly the identical topographical characteristics with catchment area varying from 6ha to 9ha. However, in the vicinity of these experimental watersheds, there have been tremendous land cover changes are being experienced. The results from these small experimental watersheds can not be assumed valid when they are extrapolated to larger catchments. Therefore there is a clear lack of studies focusing on larger catchments that are experiencing the land use changes.

The larger catchment, namely Biligi hole catchment, which is considered here for modeling approach is undergoing a dynamic change with respect the land cover. A scrutiny of land cover changes shows that, there was an unidirectional land cover change from natural forest to the agricultural activity over last 2-3 decades. Also, there have been large

open lands which were earlier used for the cattle grazing, have been brought under the afforestation activities. In the present situation, it is more of a complex land cover within a 1km grid. Understanding the impact of these activities on the hydrological regime has been a tough task. The key problem constraining the understanding is the lack of adequate data sets. The farmers in the study area are dependent on the base flow for their summer crops as the economy of the area is depending on the crops. Therefore, there is a need for use of a mathematic model which can predict the impact of these changes on hydrologic regime of the area and more importantly the baseflow in the stream. The identified model, initially calibrated using the observations made from the experimental watersheds. This calibrated model is assumed to describe the hydrological processes of the selected experimental watersheds. The calibrated model will then used to predict the impact of land cover changes on flow at a larger scale watershed.

In this study, a conceptual model namely, ARNO rainfall-runoff model, which is classified as Explicit Soil Moisture Accounting model (ESMA) has been used. The model uses the average soil moisture at each time step to compute all the hydrologic processes. The model is lumped conceptual type operating by continuously accounting for the moisture contents in 4 mutually interrelated storages. The parameters of the model represent different processes such as infiltration, percolation and deep percolation. The runoff is represented as the excess of rainfall over the storage capacity of the soil which is considered as variable within the watershed. The evapotranspiration process is defined as function of average soil moisture available to that of the maximum capacity of the soil in the ARNO model. The principle of this model well suits the study area, as Purandara, et.al., (2009) observed the infiltration excess overland flow (HOF) and saturated excess overland flow (SOF) are the dominant runoff generation mechanisms in most part of uttara kannada district covering the western ghats.

7.1.1. Model calibration and validation

Model calibration involved the automatic and/or manual adjustment of model parameters to minimize the difference between observed and predicted values, which is called the objective function. The conceptual models require a large number of parameter

values to be calibrated in applications to real catchments. Sensitivity analysis, however, suggests that the simulations are relatively more sensitive to some parameters than to others. This also allows limiting excessive over-parameterization of model (Beven, 1996).

Model validation involves testing the ability of a model to simulate the hydrologic response of a basin for conditions different from that used during the calibration period (Klemes, 1986; Lorup et al., 1998; Refsgaard and Kjudsen, 1996). In this study the model simulation period was divided into two (calibration and validation) an the simple split sample test proposed by Klemes (1986) was adopted at daily time step.

7.1.2. Model performance criteria

Uncertain inputs, uncertain structures, uncertain initial conditions and randomness of natural system are inherent ingredients in modeling hydrologic systems (Leavesley, 1994; Troutman, 1985). Similarly, data available for any specific system are incomplete and often uncertain. It is therefore a common practice to develop a model performance or validation criteria in order test the integrity of the modeling exercise.

In this study, model performance was evaluated using different technique (1) joint plots of the daily simulated and observed hydrographs, (2) index of agreement (d-index), (3) computing the RMSE (both systematic and un-systematic RMSE) and (4) the Nash-Sutcliffe coefficient of efficiency (r^2), based on the sequence of observed and simulated flows over the calibration and validation periods. The visual inspection of the joint plots helped to subjectively judge the ability of the model to simulate the inter-annual and seasonal variability and extreme conditions. They are subjective in nature and thus cannot be used as formal criteria in a rigorous model validation test. The other indices help in assessing the ability of the model to compute the water balance components. Therefore, only three numerical criteria were used for calibration and validation tests.

7.2. RESULTS and DISCUSSION

7.2.1. Calibration of SWAT model to three watersheds with varying

land covers.

Since its derivation, the SWAT model, given its simplicity and robustness, was used in various parts of the world as the basic tool for the development of several real-time operational flood forecasting system, to assess the impact of global climate change on the water resources, and also been used as the tool to analyse the effect of land cover change on the runoff regime (Todoni 1986; Todini 1996; Adams, et.al., 1995).

The watersheds selected for the SWAT application are the part of a meso-scale watershed namely, Biligihole with a catchment area of 28 km^2 . The major land covers in the watershed are Acacia plantation, Natural forest and the Degraded forest. The prime objective of this analysis is to evolve the model parameters which best represent the runoff processes under these land covers.

In the present study, the daily rainfall, discharge and the meteorological parameters such as, maximum and minimum temperature, dry and wet bulb temperature readings are available for the study area from 2018 to 2021. Out of these 3 year period (2018 to 2020) was used for the calibration and one year i.e., 2021, has been used for validation. The meteorological parameters such as maximum and minimum temperature were used to compute the potential evapotranspiration by Turc method as suggested by Lakshman and Kavoor (2006). The calibration was done manually by varying each of the model parameters and by checking the various model evaluating techniques such as index of agreement, Nash-Sutcliff efficiency and RMSE. The statistics obtained for the optimized model parameters are tabulated in Table. 7.1.

The Table. 7.1, show a higher d index, and R^2 are greater than 0.8 and ranging between 0.9 and 0.7, and variance of simulated and observed flow does not show much difference, which is an indicative of good agreement. A lower RMSE values further support the good simulation by the model. The errors between observed and simulated flow are more of un-systematic ($RMSE_U$) than of systematic ($RMSE_S$). This indicates that, model simulations are not biased (dominated) by a particular phenomenon.

Table. 7.1. Results from statistical analysis of the comparison of modeled and measured Discharges

Criterion used for	Forest	Degraded	Acacia
d Index	0.826	0.8172	0.907
R^2	0.728	0.698	0.849
RMSE	0.0086	0.0123	0.0042
$RMSE_s$	0.00278	0.00532	0.00174
$RMSE_u$	0.00816	0.01108	0.00388
Pearson R^2	0.7277	0.6977	0.8484
Nash and Sutcliffe (E)	0.887	0.871	0.901

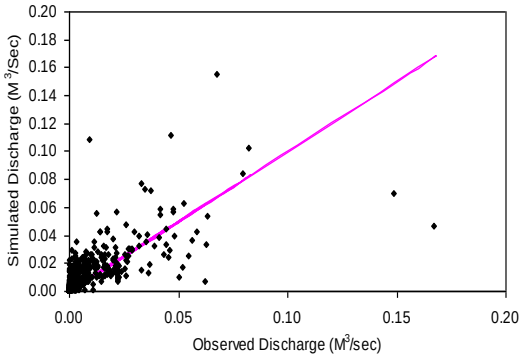

(a)

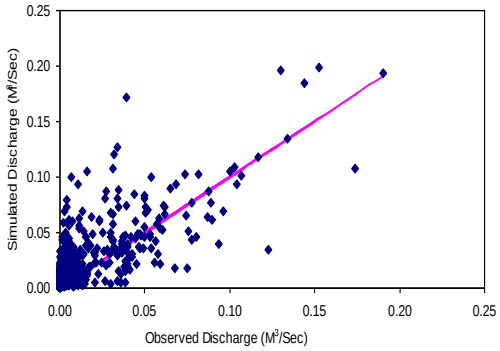

(b)

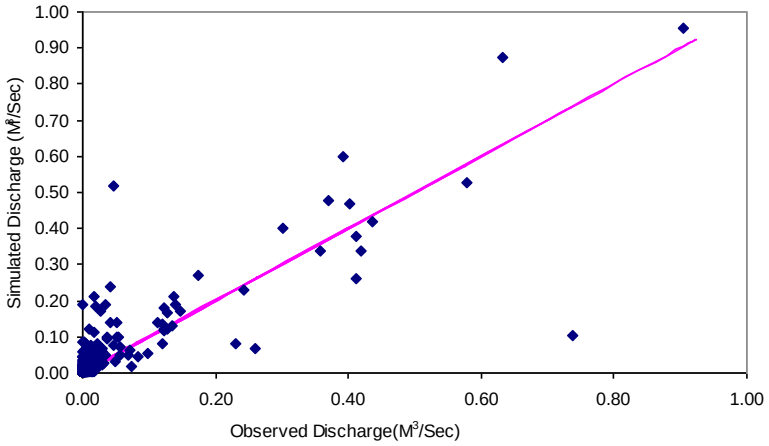

(c)

Figure.7.1 . Scatter plot of observed and simulated discharge for (a) Acacia, (b) Degraded and (c) Natural forest

A scatter plot comparing the simulated flow with observed flow for acacia, degraded and forested watersheds is shown in Figure.7.1. These plots indicate that the calibration procedure applied to model the flows has ensured to achieve the volume balance of the entire hydrological component. The scattering in Figure.7.1, may be the result of lumped values of input parameters considered while simulating the hydrological response of these watersheds. Inspite of this, the model is able to predict with good agreement of simulated flow to observed flow (as indicated by the index of agreement, '*d*' index).

The other model parameters such as deep percolation and the threshold value for baseflow (the baseflow component in the model is defined as the sub-component of deep percolation) are very high for forested watershed and lower for the degraded watershed. These two components in combination will act as controlling point in separating the baseflow and the deep percolation. Higher the moisture content, more baseflow and the deep percolation (recharge to ground water). This may due to the presence of higher moisture content in the deeper layer in forested watershed, suggesting a higher contribution towards the baseflow and consequently for deep percolation. This aspect is clearly seen in the runoff graph of forest and acacia watershed, where some flow is observed and the model is able to simulate that flow.

7.3. PREDICTION OF RUNOFF RESPONSE UNDER CHANGED LAND COVER SCENARIOS

In the present study, the monitoring of the hydrological parameters have been done in a meso scale watershed, namely Biligihole (28 km2). The water from this stream is being used for the irrigation during the monsoon and in lean season. Now, there has been lot of afforestation activities taking place in the catchment with monoculture species. The impact of such land cover on the water availability and their temporal distribution is not understood completely. There have been many studies carried out elsewhere to understand the impact of land cover changes on hydrological regime using various methods. For example, McVicar, et.al., (2007) used ET as a function of area weighted forest cover, Land Use Change modeling kit (D. Niehoff,et.al,2002); Physically based model (Legesse, et.al., 2003) and water balance model(Bowling and Strzepek, 1997).

Here in the present case, due to the complex land use condition, it is difficult to use the ET function as a base for evaluating impact of land cover changes. In order to assess

the impact, the water balance model, this is calibrated using the observed hydrological parameters (from the previous section) for simulating the flow at this scale. The flow chart for simulating the flow under the changing land cover scenario has been designed and is shown in Figure.7.2.

7.3.1. Quantification of the effect of land use changes on Flow

The impact of changes in vegetation type on flow regime can be depicted using flow duration curves (FDC). The flow duration curve for a catchment provides a graphical and statistical summary of the stream flow variability at a given location, with the shape being determined by rainfall pattern, catchment size and the physiographic characteristics of the catchment. The shape of the flow duration is also influenced by water resources development and land use type (Smakhtin, 1999). The FDC (cumulative distribution of the river flows) is widely used as a measure of the flow regime as it provides an easy way of displaying the complete range of flow at a particular location within a catchment. The FDC can also provide a useful measure of how the distribution of streamflow will change under different land use scenarios.

7.3.2 Parameterization of flow duration curve

Various methods have been used to parameterize the FDC (Cigizoglu and Bayazit, 2000). These methods have generally been used to produce regionalized FDC's (Meunier, 2001; Fennessey and Vogel, 1990) or to predict the FDC's for ungaguged catchments (Holmes, et.al. 2002). However, investigations into the changes in the FDC resulting from change in a catchment's vegetation are limited. Burt and Swank, (1992), used a regression model relating the percentile flow in the control and the treated basins during a seven year control period. This allowed the FDC for the treated catchment to be predicted using the FDC from the control catchment in the post-treatment period and an assessment of change in FDC under alternate vegetation type to be made. Recently however, it has also been suggested that flow duration curve may provide a hydrologic signature of a catchment. This hydrologic signature has been used in top-down modeling approaches to determine the appropriate level of complexity required in a rainfall-runoff models (Hothityangkoon et.al., 2001).

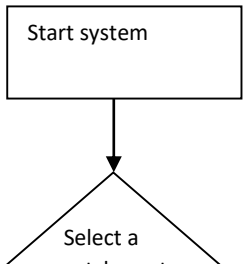

Figure. 7.2. Flow chart for simulating the impact of land cover changes using a water balance model.

7.3.3. Defining the flow duration curve

Following the procedure defined by Best et.al., (2003), streamflow was normalized by dividing it by the median discharge of the non-zero flow days. This ensures that the log of the normalized streamflow crosses the axis at the median streamflow of the non-zero flow days (since log(1)=0). Based on the shape of the curve and the data, a logarithmic

function appears to be most appropriate on to choose to represent it. The chosen function is

$Y = a X^b$

Where y: streamflow

X : percent exceedence

and ‘a’ and ‘b’ are the variable as follows

a = percent exceedence at the cease to flow value (for example, it a river flows for 90% of time, a = 90).

b= a constant controlling the slope of FDC.

7.4. SIMULATING IMPACTS OF LAND USE CHANGES ON ANNUAL RUNOFF

As explained in the previous section, the SWAT rainfall-runoff model was calibrated for watersheds using the measured flows and other meteorological parameters. Further, the calibrated model was used as a distributed model to simulate the flows at Biligihole watershed, within which, these small watersheds are located. In order to simulate the flow at the outlet of Biligihole watershed, initially the watershed was divided into number of smaller watersheds covering the natural forest, degraded forest and acacia plantation. The calibrated model was then applied to each of these small watersheds and the runoff was then routed to the outlet where the flows have been monitored.

7.4.1. Land cover scenarios

Here we have performed simulations under different land cover scenario conditions in order to analyse the impact on the catchment hydrology of possible changes in the land covers in the future.

In order to facilitate task of, a hypothetical land cover scenarios were developed in two fold. At first, land cover scenario’s is “assuming the entire watershed has only two land cover” such as (a) forest and degraded land scape; (b) Acacia and Degraded and (c) forest and Acacia. The simulation of flow was done by varying % of land cover which finally leads in replacing the other land cover (ex. Acacia is replacing entire degraded land scape, i.e., entire 28 km^2 will be covered by Acacia plantation). The changes in flow caused

by the change in land cover are quantified by fitting the equation mentioned earlier to flow duration curve. The coefficient of the equation of fitting FDC such as ‘a” and ‘b” obtained for different percent of land cover are tabulated in the following Table.7.2 to Table.7.8.

The value of “a” in equation represents the ‘cease to flow point”. That is, a perennial river would have a value of 100, while a river that flows for 80% of the time would have a value of 80.

From the Table.7.2 to Table.7.8, it can be seen that, as the forest cover goes on decreasing, a simultaneous decrease in the value of “a” is noticed. This indicates that, flow in the river get reduced as forest cover is being replaced either by degraded land or by acacia plantation. The magnitude of decreasing in % of time the flow occur in the stream quite higher uto 63%, when the entire area has been degraded from acacia plantation and by clearing the natural forest. Also, other combinations of land cover changes indicate that, if the entire area is under natural forest cover, the flow in the stream will lost upto 90% of time, and flow upto 85% of time, when the whole of the catchment is under acacia plantation. Under these two contrasting land cover, the model more or less behave similarly, probably due to the improvement in the soil properties and lower utilization of water by the acacia plantation (Kallarakkal, 2008).

Secondly, the other scenario considered for the simulations includes all the 3 major land cover of the watershed. These land covers are changed such as way that, one land cover in the catchment is considered to be unchanged, and the other two are changed by increasing one of the land cover to replace the other one completely. The cases considered for the analysis are; (i) when the forest cover is unchanged and acacia plantation is completely replaced by degraded land; (ii) forest cover is unchanged and degraded land is completely planted with acacia plantation; (iii) degraded land is unchanged and acacia is replaced by natural forest and (iv) acacia plantation remains unchanged and forest is cleared and left as degraded land. The results obtained for these simulations are tabulated in Table.7.2 to Table.7.9. From the tables, it is clear that, as the % of degraded land increase, the % of time of flow decreases. The decrease in the flow % is as low as 48%, when the forest land was completely replaced by degraded land. Whereas, same % increase in the area of acacia plantation has resulted in an increase in the flow occurring in the

stream upto 65%. Similarly, when the acacia plantation was completely replaced by degraded land has resulted in a decrease of value 'a' upto 53%. But the highest value of 'a' was obtained when the forest was increased by more than 50% of present forest cover in the catchment (89%). These simulations are an indicative of how even a small change in land cover can bring in about a major change in the flow condition of the stream. An important point to be noted from the simulation is that, when the catchment is devoid of all the forest cover, the impact on the flow was higher (45%), and the same impact was seen when the acacia plantation were cleared (53%). On the other hand, when the acacia plantation was increased by over 100% of area, a greater improvement was seen.

7.5. CHARACTERISTICS OF DAILY SIMULATED FLOWS UNDER CHANGING LAND COVER SCENRIOS

As described in the previous paragraphs, the simulated flows were used to construct the flow duration curve for various scenarios of land cover change. These, FDCs can be potentially used as a tool in understanding and solving a variety of water resources problems. Here in the present study, we are interested in quantifying how the changing land cover has an impact on the daily flows. In order to quantify these effects, the flow quantile from Q_{10} to Q_{90} were selected and are tabulated in Table.7.2 to Table.7.8. Further to examine daily stream flow variability, we defined high flows as flows which exceed 10%, i.e., Q10, and a ratio which is termed as high flow index (Q_{10}/Q_{50}) and low flows as being 90%, i.e., Q90, the low flow index (Q_{90}/Q_{50}) . The ratio of these extreme flows to median stream flow (Q50) is a measure of stream flow variability; these ratios along with their percentage changes with corresponding changes in the percent land cover are listed in Table.7.2 to Table.7.8.

Table. 7.2. Regression coefficient of flow duration model and the flow quintiles when the forest landscape is converted into degraded landscape

Sl. No	Degraded	Forest	Model Parameter		Flow Quantiles for various duration									Indices for various duration flows			
			A	B	Q_{10}	Q_{20}	Q_{30}	Q_{40}	Q_{50}	Q_{60}	Q_{70}	Q_{80}	Q_{90}	High flow index	Low Flow index	% change in HFI	% Change in LFI
1	0	28	89.95	-9.86	25.70	9.09	3.163	1.60	0.996	0.636	0.379	0.129	0.029	25.80	0.03		
2	2.8	25.2	84.50	-9.48	25.94	9.27	3.27	1.65	0.999	0.654	0.384	0.119	0.028	25.97	0.03	0.63	-6.32
3	5.6	22.4	82.49	-9.22	25.24	9.36	3.29	1.64	0.995	0.639	0.377	0.108	0.025	26.03	0.03	0.88	-14.68
4	8.4	19.6	81.30	-9.02	25.93	9.40	3.16	1.63	0.998	0.635	0.327	0.101	0.023	25.88	0.02	0.30	-22.64
5	11.2	16.8	80.34	-8.86	26.73	9.64	3.30	1.72	0.997	0.645	0.372	0.927	0.021	26.81	0.02	3.90	-29.60
6	14	14	75.13	-8.73	27.81	10.11	3.54	1.906	0.999	0.675	0.380	0.086	0.020	27.84	0.02	7.89	-33.09
7	16.8	11.2	67.00	-8.52	30.56	10.28	3.72	2.09	0.996	0.64	0.36	0.083	0.019	30.68	0.02	18.91	-36.24
8	19.6	8.4	64.08	-8.29	35.21	12.18	4.52	2.58	0.954	0.62	0.31	0.068	0.010	36.91	0.01	43.04	-64.97
9	22.4	5.6	56.08	-7.23	30.83	14.94	4.40	3.06	0.866	0.58	0.27	0.058	0.000	35.60	0.00	37.97	-100.00
10	25.2	2.8	53.12	-5.56	43.20	19.15	6.45	2..06	0.967	0.311	0.11	0.017	0.000	44.67	0.00	73.13	-100.00
11	28	0	37.982	-5.23	47.52	28.80	13.36	1.79	0.917	0.158	0.062	0.00	0.00	51.82	0.00	100.83	-100.00

Table.7.3. Regression coefficient of flow duration model and the flow quantiles when the Acacia plantation is converted into degraded landscape

Sl. No	Degraded	Acacia	Model Parameter		Flow Quantiles for various duration									Indices for various duration flows			
			A	B	Q_{10}	Q_{20}	Q_{30}	Q_{40}	Q_{50}	Q_{60}	Q_{70}	Q_{80}	Q_{90}	High flow index	Low Flow index	% change in HFI	% Change in LFI
1	0	28	84.572	-9.86	16.61	9.87	5.18	2.09	1.02	0.613	0.70	0.80	0.90	16.28	0.88		
2	2.8	25.2	73.979	-9.15	12.59	8.74	3.40	1.84	0.9	0.63	0.44	0.70	0.72	13.99	0.80	-14.10	-9.43
3	5.6	22.4	65.909	-8.73	10.53	7.96	3.27	1.79	0.66	0.55	0.42	0.50	0.49	15.95	0.74	-2.03	-15.95
4	8.4	19.6	60.302	-8.41	18.96	8.96	3.50	1.94	0.988	0.65	0.41	0.36	0.45	19.19	0.46	17.85	-48.44
5	11.2	16.8	55.978	-8.13	23.60	8.36	3.47	1.93	0.963	0.622	0.392	0.25	0.10	24.51	0.10	50.49	-88.24
6	14	14	52.369	-7.91	24.57	8.86	3.42	1.91	0.927	0.591	0.359	0.13	0.03	26.50	0.04	62.76	-95.73
7	16.8	11.2	50.036	-7.71	25.41	9.01	3.48	2.04	0.998	0.558	0.338	0.11	0.01	25.46	0.01	56.35	-98.87
8	19.6	8.4	46.561	-7.52	26.28	9.20	3.68	2.12	0.97	0.53	0.30	0.09	0.00	27.09	0.00	66.37	-100.00
9	22.4	5.6	43.378	-7.35	33.46	9.51	4.01	2.04	0.94	0.51	0.26	0.02	0.00	35.60	0.00	118.59	-100.00
10	25.2	2.8	40.314	-7.19	37.19	9.95	4.15	2.70	0.89	0.45	0.22	0.00	0.00	41.79	0.00	156.61	-100.00
11	28	0	37.340	-7.04	47.52	28.04	13.36	2.08	0.991	0.174	0.062	0.00	0.00	47.95	0.00	194.46	-100.00

Table.7.4. Regression coefficient of flow duration model and the flow quantiles when the forested landscape is replaced by Acacia plantation

Sl. No	Acacia	Forest	Model Parameter		Flow Quantiles for various duration									Indices for various duration flows			
			A	B	Q_{10}	Q_{20}	Q_{30}	Q_{40}	Q_{50}	Q_{60}	Q_{70}	Q_{80}	Q_{90}	High flow index	Low Flow index	% change in HFI	% Change in LFI
1	0	28	89.950	-9.86	25.72	9.09	3.163	1.64	0.995	0.636	0.379	0.129	0.0298	25.85	0.03		
2	2.8	25.2	81.317	-8.15	25.27	8.95	3.19	1.58	0.990	0.065	0.400	0.134	0.032	25.53	0.03	-1.25	7.92
3	5.6	22.4	68.554	-8.02	24.51	9.01	3.25	1.54	0.990	0.664	0.415	0.145	0.035	24.76	0.04	-4.22	18.04
4	8.4	19.6	65.194	-7.89	23.76	8.28	3.32	1.73	0.997	0.634	0.39	0.136	0.05	23.83	0.05	-7.81	67.45
5	11.2	16.8	61.209	-7.77	23.45	9.03	3.20	1.67	0.99	0.70	0.45	0.168	0.04	23.69	0.04	-8.37	34.91
6	14	14	59.740	-7.65	23.69	9.25	3.42	1.74	0.998	0.727	0.480	0.171	0.04	23.74	0.04	-8.17	33.82
7	16.8	11.2	57.900	-7.54	25.34	9.40	3.72	1.83	0.997	0.740	0.502	0.18	0.04	25.42	0.04	-1.68	33.96
8	19.6	8.4	53.862	-7.42	23.26	10.74	3.80	1.86	0.997	0.780	0.540	0.20	0.05	23.33	0.05	-9.75	67.45
9	22.4	5.6	50.621	-7.30	21.15	11.10	3.53	1.72	0.998	0.70	0.510	0.180	0.01	21.19	0.01	-18.02	-66.54
10	25.2	2.8	48.854	-7.18	21.00	11.39	3.46	1.75	0.997	0.68	0.48	0.21	0.01	21.06	0.01	-18.52	-66.51
11	28	0	45.430	-7.04	19.08	8.18	3.32	1.73	0.997	0.63	0.44	0.21	0.05	19.14	0.05	-25.97	67.45

Table. 7.5. Regression coefficient of flow duration model and the flow quantiles when the Acacia plantation is replaced by Degraded landscape

Sl. No	Acacia	Degraded	Forest	Model Parameter		Flow Quantiles for various duration									Indices for various duration flows			
				A	B	Q_{10}	Q_{20}	Q_{30}	Q_{40}	Q_{50}	Q_{60}	Q_{70}	Q_{80}	Q_{90}	High flow index	Low Flow index	% change in HFI	% Change in LFI
1	7	10	11	80.46	-8.88	26.46	9.83	3.53	1.93	0.999	0.692	0.430	0.119	0.029	26.49	0.03		
2	5.6	11.4	11	64.68	-8.18	27.48	10.15	3.56	1.98	0.999	0.696	0.435	0.115	0.029	27.51	0.03	3.85	0.00
3	4.2	12.8	11	61.64	-8.03	28.08	11.81	3.95	2.18	0.999	0.662	0.419	0.10	0.027	28.11	0.03	6.12	-6.90
4	2.8	14.2	11	58.19	-7.89	33.43	12.98	4.24	3.13	0.997	0.510	0.370	0.09	0.01	33.53	0.01	26.60	-65.45
5	1.4	15.6	11	54.96	-7.71	39.41	15.67	8.59	4.92	0.997	0.480	0.263	0.06	0.00	39.53	0.00	49.24	-100.00
6	0	17	11	52.51	-7.64	48.51	23.25	9.68	6.01	0.992	0.210	0.090	0.01	0.00	48.90	0.00	84.63	-100.00

Table. 7.6. Regression coefficient of flow duration model and the flow quantiles when the degraded landscape is brought under Acacia plantation while forested landscape is not disturbed

Sl. No	Acacia	Degraded	Forest	Model Parameter		Flow Quantiles for various duration									Indices for various duration flows			
				A	B	Q_{10}	Q_{20}	Q_{30}	Q_{40}	Q_{50}	Q_{60}	Q_{70}	Q_{80}	Q_{90}	High flow index	Low Flow index	% change in HFI	% Change in LFI
1	7	10	11	80.468	-8.88	26.46	9.83	3.53	1.93	0.999	0.692	0.430	0.119	0.029	26.49	0.03		
2	9	8	11	76.086	-8.71	25.88	9.88	3.61	1.91	0.997	0.745	0.466	0.137	0.035	25.96	0.04	-2.00	20.93
3	11	6	11	72.770	-8.56	25.40	9.78	3.58	1.89	0.997	0.753	0.480	0.151	0.038	25.48	0.04	-3.81	31.30
4	13	4	11	69.410	-8.42	24.73	9.78	3.60	1.10	0.997	0.760	0.502	0.167	0.043	24.80	0.04	-6.35	48.57
5	15	2	11	66.670	-8.30	24.11	9.68	3.56	1.85	0.997	0.755	0.501	0.174	0.045	24.18	0.05	-8.70	55.48
6	17	0	11	64.689	-8.18	23.10	9.37	3.51	1.78	0.997	0.748	0.504	0.186	0.048	23.17	0.05	-12.52	65.85

Table.7.7. Regression coefficient of flow duration model and the flow quantiles when Acacia plantation is brought under forested landscape while degraded landscape is not disturbed.

Sl. No	Acacia	Degraded	Forest	Model Parameter		Flow Quantiles for various duration									Indices for various duration flows			
				A	B	Q_{10}	Q_{20}	Q_{30}	Q_{40}	Q_{50}	Q_{60}	Q_{70}	Q_{80}	Q_{90}	High flow index	Low Flow index	% change in HFI	% Change in LFI
1	7	10	11	80.46	-8.88	26.46	9.83	3.53	1.93	0.999	0.692	0.430	0.119	0.029	26.49	0.03		
2	5.6	10	12.4	84.19	-8.26	26.48	9.65	3.46	1.88	0.999	0.681	0.412	0.112	0.13	26.51	0.13	0.08	348.28
3	4.2	10	13.8	85.54	-8.33	25.94	9.76	3.40	1.80	0.997	0.669	0.39	0.210	0.14	26.02	0.14	-1.77	383.73
4	2.8	10	15.2	86.22	-8.41	25.74	9.55	3.21	1.72	0.997	0.655	0.376	0.253	0.183	25.82	0.18	-2.53	532.30
5	1.4	10	16.6	87.21	-8.49	25.39	9.63	3.17	1.69	0.994	0.641	0.373	0.283	0.201	25.54	0.20	-3.56	596.59
6	0	10	18	88.89	-858	24.56	9.11	3.15	1.55	0.994	0.681	0.423	0.324	0.235	24.71	0.24	-6.71	714.42

Table.7.8. Regression coefficient of flow duration model and the flow quantiles when forested landscape is brought under degraded landscape while Acacia plantation is not disturbed

Sl. No	Acacia	Degraded	Forest	Model Parameter		Flow Quantiles for various duration									Indices for various duration flows			
				A	B	Q_{10}	Q_{20}	Q_{30}	Q_{40}	Q_{50}	Q_{60}	Q_{70}	Q_{80}	Q_{90}	High flow index	Low Flow index	% change in HFI	% Change in LFI
1	7	10	11	80.46	-8.88	26.46	9.83	3.53	1.93	0.999	0.692	0.430	0.119	0.029	26.49	0.03		
2	7	12.2	8.8	73.12	-8.25	28.01	10.10	3.55	2.01	0.999	0.688	0.426	0.117	0.029	28.04	0.03	5.86	0.00
3	7	14.4	6.6	68.72	-8.31	30.58	12.12	3.93	2.34	0.999	0.653	0.403	0.111	0.027	30.61	0.03	15.57	-6.90
4	7	16.6	4.4	57.88	-8.39	33.07	15.61	5.36	3.83	0.999	0.593	0.366	0.099	0.00	33.10	0.00	24.98	-100.00
5	7	18.8	2.2	51.54	-8.47	38.31	19.33	8.50	4.61	0.999	0.544	0.325	0.011	0.00	38.35	0.00	44.78	-100.00
6	7	21	0	48.09	-8.56	46.37	28.91	11.45	7.01	0.994	0.465	0.281	0.0	0.0	46.65	0.00	76.13	-100.00

It is observed from Table.7.2 to Table. 7.8, is that, median flow (Q_{50}) is more or less independent and does not have any influence of changes in land cover occurring in the catchment. However, the high flow index (Q_{10}/Q_{50}), and low flow index (Q_{90}/Q_{50}) exhibits a very high variability in all the cases. These observations indicates that, the hydrological simulations carried out for various combination of land covers have influenced either the higher and lower flows not the median flows.

Case-I : When forested area in completely degraded: as the forested watershed is getting degraded (increasing percent of degraded landscape), the flow at 10% duration registering an increasing trend (Table.7.2). The low flow at 90% duration are decreasing and ceases to flow when forest area is less than 5.6 km^2 (degradation level of 80%). Similarly, high flow index is increasing and is as high as 51% when forest is completely replaced by the degraded landscape (at 100% degradation of forest landscape). At the same time, low flow index has declined in amount and registered 100% change.

Case-II: When acacia plantation are cleared and allowed the landscape to degrade : The high flow index decreases inspite of the clearing the acacia plantation upto 20% (Table.7.3). However, a 200% change in high flow index is observed when the acacia plantation is completely converted into degraded landscape. On the other hand the low flow index has decreased by 100% when the degraded level is at 70%.

Case-III; When Forested landscape is brought under Acacia Plantation : The high flow index show a decreasing trend as the acacia is replacing the forested landscape (Table.7.4). Simultaneously, an increasing trend is noticed in the low flow index is noticed. This clearly indicates that, the acacia plantation will help in sustaining the flow for a longer period of time.

Case-IV; When Acacia Plantation converted into degraded landscape, while Forested landscape is retained un-disturbed: The results under this class, is comparable with the case-II with less degree of variation in both high flow and low flow index (Table.7.5). Here in this case, the variation in high flow index is 84% and low flow index is decreasing in nature and registered a change of 100%. The presence of forested landscape might have played a role in moderating the high flows.

Case-V; When degraded landscape converted into Acacia Plantation, while Forested landscape is retained un-disturbed: Here in this case, we can notice a decreasing trend in the high flow index with an increasing trend of low flow index (Table.7.6). The combination of both Acacia plantation with Forested landscape can act complete forested landscape.

Case-VI; When Acacia Plantation converted into Forested landscape, while Degraded landscape is retained un-disturbed: The slow conversion of the Acacia plantation into a forested landscape can initially yield an increase in the high flow index and once it is stabilized, can act as good as a forested landscape (Table.7.7). This is clearly seen in this case along with the case-V.

Case-VII; *When Forested landscape converted into Degraded landscape, while Acacia Plantation is retained un-disturbed*: The high flow index is noticed an higher percentage changes as high as 75% along with the decreasing of low flow index of 100%. This is clearly evident as the catchment is getting degraded higher and higher over a period of time (Table.7.8).

7.6 SUMMARY and IMPORTANT OBSERVATIONS

Many studies have investigated the impact of afforestation on water yield at the catchment scale. But no such study has been carried out so far in the shayadri region, which is head water catchment for most of the peninsular India. The understanding the impact of land cover changes has been so important, due to the intensive afforestation efforts in this area. This study makes an attempt towards this cause.

In the present study, a water balance model namely, ARNO model is used. Initially, the model is calibrated and validated to the watersheds which cover the most dominant land cover of the area. The calibration and validation of the model was done using the monitored data. Then the calibrated model is used as distributed model to predict the flow at the outlet of a meso scale watershed and compared with the measured flow.

CHAPTER-VIII UP-SCALING STUDIES

8.0 Introduction

8.1 BARCHI NALA CATCHMENT

The Barchi nala watershed is located on the lee-ward side of the Western Ghats and is a sub basin of Kali river. It lies in the Haliyal taluk of Karwar (North Kanara) district in Karnataka. The BarchiNala stream originates from Thavargatti in Belgaum district at an altitude of about 734 m, 20 km north of Dandeli and flows through North Kanara district of Karnataka state. The catchment is relatively short in width and river flows in southerly direction and joins the main Barchi River near the gauging site. The watershed covers a total geographical area of 14 km^2. The watershed lies between 74° 36' and 74° 39' east longitudes and between 15° 18' and 15° 24' North latitudes (Figure 8.1). High land region consists of dissection of high hills and ridges forming parts of the foot hills of Western Ghats. It consists of steep hills and valleys intercepted with thick vegetation. The slope of the Ghats is covered with dense deciduous forests. The forest occupies around 80% of the study area. The watershed is mainly covered in Bamboo, Teak and mixed plantations. The brownish and fine-grained soils are the principal types of soils found in the area.

Figure 8.1. Location of Barchi watershed from Google Earth

The stream gauging site is located at an elevation of 480 m, where the Nala crosses the Dandeli-Thavargatti road, about 5 km from Dandeli. The stream is a 4th order stream and joins the main Barchi River downstream of the gauging site. The Barchi raingauge station is located at 15° 18' N and 74° 37'

E. Average annual rainfall for the watershed is about 1500 mm, majority of which occurs during the south-west monsoon period.

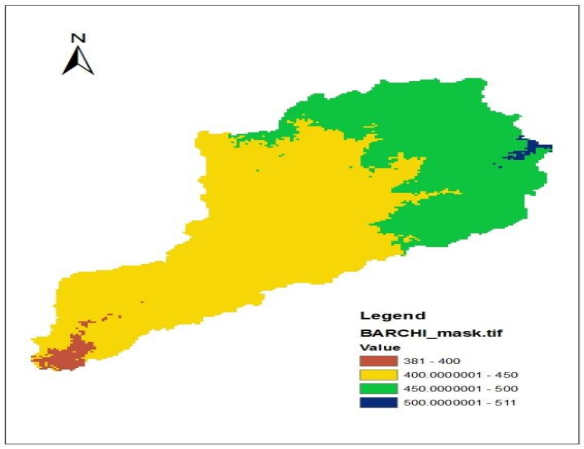

Figure 8.2. Color-coded elevation map of Barchi watershed

The ground surface elevation in the study area varies from 381 m to 511 m above msl (Figure 8.2). The summary of the topography and slope of the region as obtained from the DEM is shown in the Table 8.1. Table 8.2 shows the slope distribution in the Barchi Nala catchment, while Table 8.2 discusses the area covered under various land use/ land cover in the region (Figure 8.4 to Figure 8.5).

Table 8.1 Elevation distribution in Barchi Nala catchment

ELEVATION	% AREA UNDER ELEVATION
Below 400 m	1.33%
400 - 450 m	60.91%
450 - 500 m	37.16%
Above 500 m	0.60%

Table 8.2 Slope distribution in Barchi Nala catchment

SLOPE	% AREA UNDER SLOPE
0 to 5	27.85%
5 to 10	46.94%

10 to 15	20.75%
15 to 20	3.85%
Above 20	0.61%

Table 8.3 Land use pattern in Barchi Nala catchment

LAND USE	AREA
Savannah	**47.46%**
Deciduous broad-leaf forests	**24.29%**
Evergreen broad-leaf forests	**28.25%**

The Barchi rain gauge station is located at 15° 18’ North and 74° 37’ east. Average annual rainfall in the region is 1500 mm, majority of which occurs during the southwest monsoon period. Depth to water table varies between 4 to 12 m during pre- and post-monsoon periods. The yield of bore-wells in the study area is found to vary between 120 gallons per hour to 1170 gallons per hour.

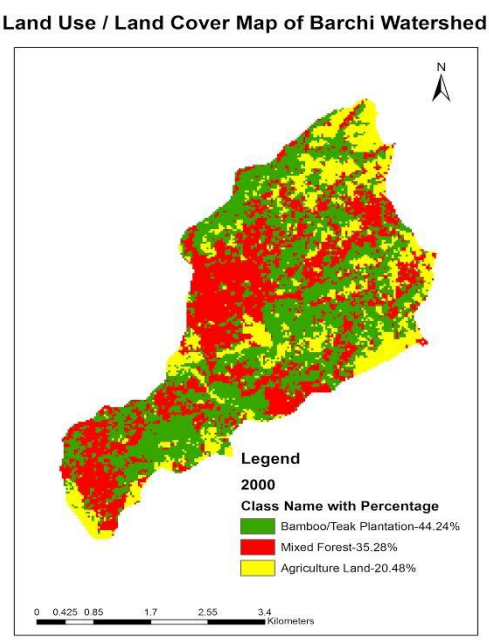

Figure 8.3: Land use/land cover map in 2000

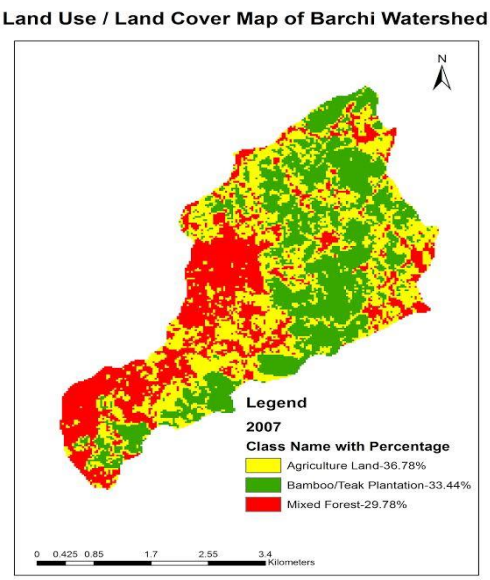

Figure 8.4: Land use/land cover map in 2007

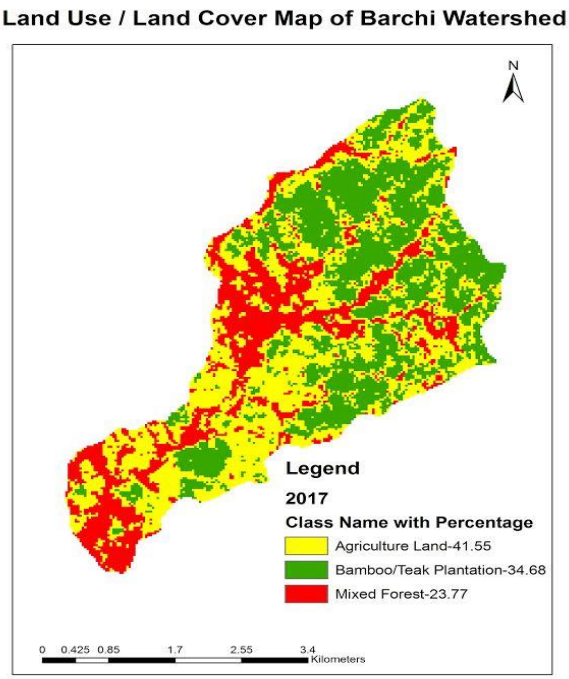

Figure 8.5: Land use/land cover map in 2020

The Barchi Nala catchment is a small, narrow catchment located in the foot hills of Western Ghats, covering an area of 21.12 sq. km. The entire study area was divided into various sub-units, which were further classified in to several HRUs based on the land use, soil and slope distribution. The sub-units of the Barchi Nala catchment are shown in the figure 8.6.

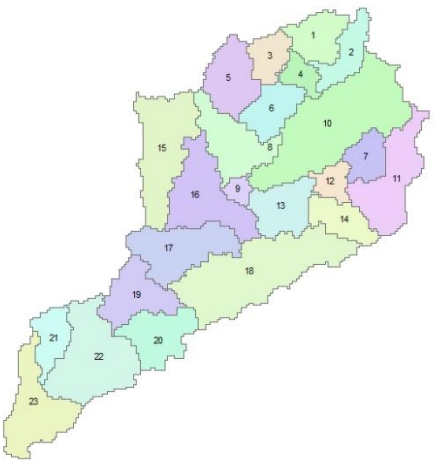

Figure 8.6. HRU of the Barchi Nala catchment

8.1.1 Rainfall characteristics of Mid Ghat watersheds, Barchi

Table. 8.4 presents a summary of recorded rainfall pattern of the study region. In Mid-Ghat region total rainfall was 1383.8 mm 1280.4 mm during 2019-20 and 2020-21 respectively. Analysis of the daily rainfall shows that total number of rainy days during 2019-20 was 98 and the maximum in a day was 108.4 mm and in the year 2020-21, total rainy days were 95 with a maximum of 105 mm in a day. However, average daily rainfall varied between 4mm and 6 mm with a standard deviation (SD) of 10.34 and 9.25 respectively.

Table 8.4 Rainfall characteristics for (a) year 2019-20 and (b) year 2020-21 for Mid Ghat(Barchi) region, Haliyal/Supa

Station	Year	Total Rainfall (mm)	# of rainy days	Maximum rainfall (mm) in a day	Average daily rainfall (mm)	Standard Deviation
Barchi (Haliyal/Supa)	2019-20	1383.8	98`	108.4	3.26	10.34
	2020-21	1280.4	95	75.8	3.85	9.25

Table 8.4 describes seasonal and monthly rainfall pattern of the Mid Ghat region during 2019 to 2021. In Mid-ghat region, rainfall trend during monsoon period (June to September) was found to be increasing where in dry winter and post-monsoon (October to May) it is almost constant in both the year. The annual average rainfall over the study period, i.e. 2019 to 2021, an average annual rainfall observed was 1332.1 mm of which about 80% occurred during south west monsoon (June to September), 12.5% during north east monsoon (October- December) and 7.5% distributed during remaining months. The distribution of rainfall pattern has a significant influence over the vegetation and also on water availability for crops during critical periods.

The details of monthly rainy days and respective total rainfall are given in following Table 5.15. During 2019-2020, rain occurred in all months except in the month of December and February and in the year 2020-21, no rainfall was observed in January, February and March. As expected most of the rain occurred during south west monsoon (June-September) as the normal pattern in central Western Ghats, Karnataka.

From the Table. 8.5 describes the event classified rainfall for 2019 to 2021 by magnitude of daily depths of Mid Ghat region. Results showed that the year 2020-21 was an exceptionally wet year with significant rainfall occurring over 97 days and giving rise to rainfall of 1371.8 mm. whereas year 2019-20, was a relatively drier year with a total of 1165 mm received in 78 days. In the year 2020-21, there were frequent rainfall events of higher (<40 mm) amount 73.9% of the annual rainfall (74 days). But

the small amount rainfall (>40 mm) has occurred for about 4 day's contribution about 26.1% of the annual rainfall. In the year 2019-21, higher amount of rainfall was accounted only for 20% whereas the smaller rainfall events have contributed for 80% of the rainfall. From the Table 8.6., we can notice that, the rainfall events exceeding >20 mm of rainfall have contributed about 33% of the annual rainfall in the year 2021 in comparison to that of 28% in 2019. This analysis highlights the importance of investigating intra-annual variability rather than classification based on annual rainfall totals

Table 8.5: Monthly rainfall characteristic of Mid-Ghat (Barchi) Regions, UK, Karnataka (2019 to 2021)

Year	No of Rainy days	Total Rainfall (mm)	Year	No of Rainy days	Total Rainfall (mm)
Jun-19	16	196.8	**Jun-20**	14	207.6
Jul-19	30	650.4	**Jul-20**	21	462.8
Aug-19	16	219.4	**Aug-20**	17	174.6
Sep-19	1	74	**Sep-20**	17	182
Oct-19	3	45.4	**Oct-20**	8	141.4
Nov-19	6	67.8	**Nov-20**	10	106.8
Dec-19	0	0	**Dec-20**	1	2.6
Jan-20	1	9.8	**Jan-21**	0	0
Feb-20	0	0	**Feb-21**	0	0
Mar-20	1	21.6	**Mar-21**	0	0
Apr-20	6	72.2	**Apr-21**	8	69.8
May-20	3	26.4	**May-21**	1	24.2

Table 8.6 Rain runoff characteristics under different land-use type for (a) year 2019-20 and (b) year 2020-21 in Mid Ghat watersheds (Barchi), UK, Karnataka

Class of rainfall depth (mm)	Days		Amount		% of Annual Rainfall		Cumulative Annual Rainfall (%)	
	2019-20	2020-21	2019-20	2020-21	2019-20	2020-21	2019-20	2020-21
>80	2	0	215.60	0	18.5%	0.0%	18	0
40.1 to 80	2.00	5.00	88.2	276.6	7.6%	20.2%	26	20
20.1 to 40	12.00	16.00	331.6	450.8	28.4%	32.9%	55	53
10.1 to 20	22.00	23.00	318.2	349.4	27.3%	25.5%	82	78
5.1 to 10	20.00	28.00	138.8	203.4	11.9%	14.8%	94	93
2.5 to 5.1	20.00	25.00	73.2	91.6	6.3%	6.7%	100	100
Annual Total	78	97	1165.60	1371.8	100	100		

8.1.2 Runoff Estimation under different land use land cover

Annual Run-off

The salient features of the observed discharge from natural and degraded forest land-use types are shown Table 8.3 for year 2019-20 and 2020-21. This table also depicts the percent of runoff of the selected watersheds, specific discharge and specific peak discharge. During 2019-20, it was observed that the highest runoff found in degraded forest and lowest in natural forest. The total discharge in degraded forest is 352.94 mm (or 45.61%), while this was found only 265.7 mm (or 22.8%). Similar to previous year in 2020-21 also higher rate (893.04 mm or 63.5%) of discharge was seen in degraded forest and minimum (352.94 mm or 25.07%) discharge was found with degraded forest. compared to earlier year, during 2020-21 the net increase of discharge under degraded forest is 39.8% and it was 24.7% in natural forest. With respect to specific and specific peak discharge highest specific discharge and the specific peak discharge were observed in degraded forest but whereas it is minimum in natural forested watershed. However, specific peak discharge values are almost equal with respect to temporal variation in the all the watersheds. On an average 24.8 percent increase in the specific discharge natural forest and 39.07% in degraded forest as compared to 2019-20. Rainfall-Runoff relationship of Barchi watershed is shown in Figures 8.7 & 8.8.

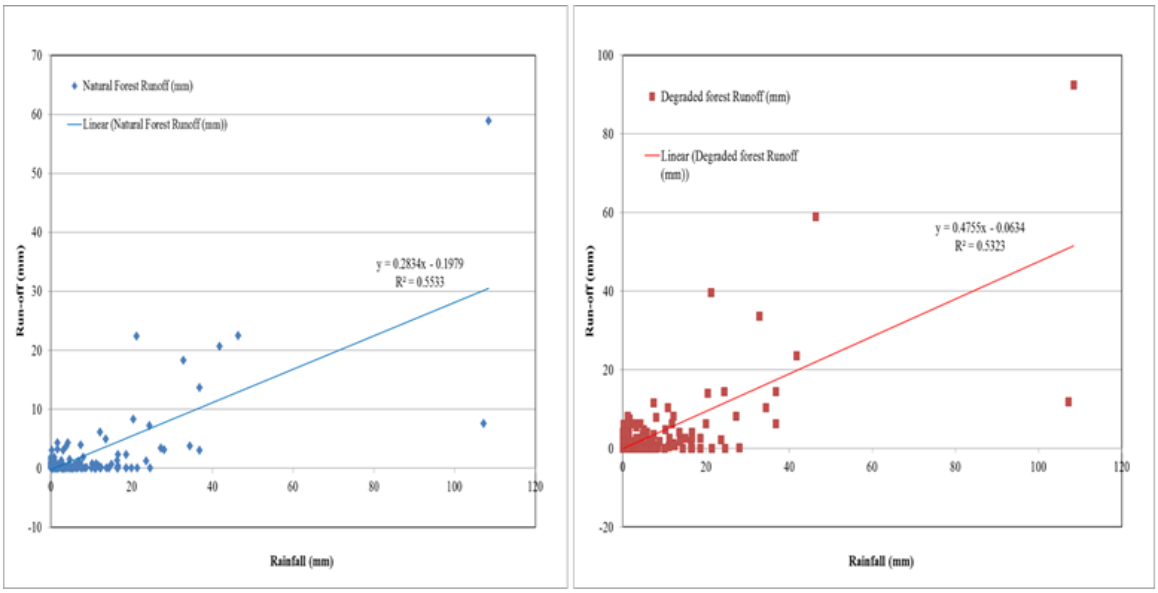

Figure 8.7. Daily Rainfall-Runoff in Barchi watershed of Midghat Region (2019-2020)

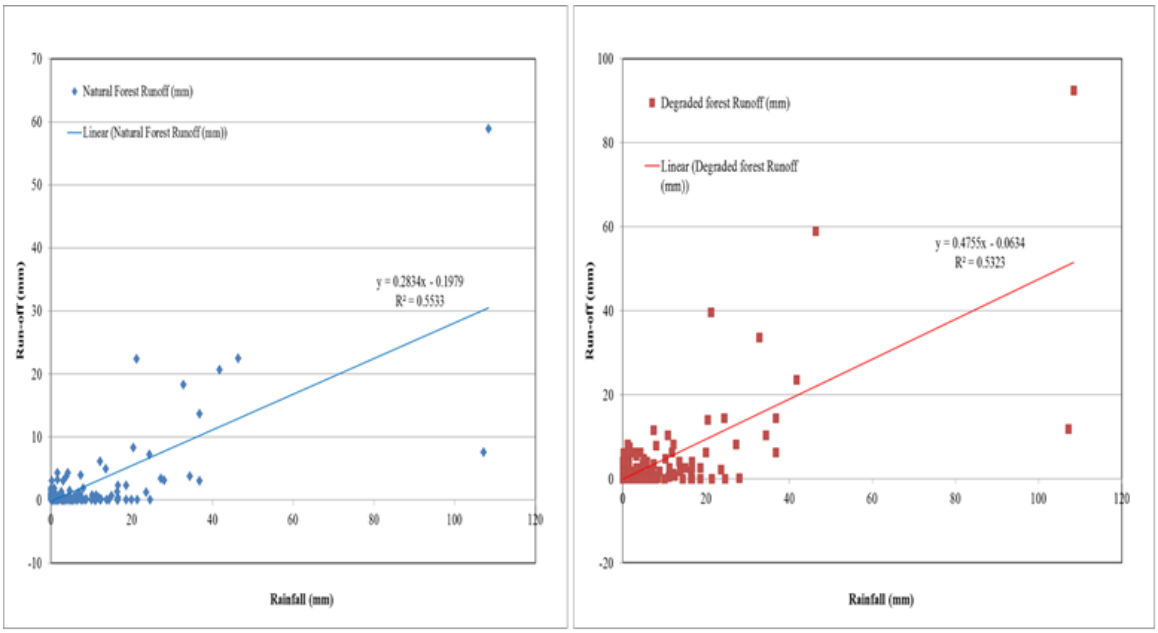

Figure 8.8. Daily Rainfall-Runoff in Barchi watershed of Mid Ghat Region (2020-2021)

8.1.3 Groundwater Recharge Estimation using HYDRUS-1D

The study of soil water is being given the top priority in the present era. Several attempts have been done from the past to contribute towards the estimation of the soil water by the best methods. HYDRUS1-D model which has been used in the project is one of the most sophisticated hydrological models. This model has been used in various parts of the world and its applications are published in various journals.

HYDRUS 1-D is a software package for simulating water, heat and solute movement in one-dimensional variably saturated or unsaturated media. The software consists of the HYDRUS computer program, and the HYDRUS 1-D interactive graphics-based user interface for both data preparation and graphical post-processing in Windows. The HYDRUS program is a finite element model designed to numerically solve the Richards' equation for variably saturated water flow and convection-dispersion type equations for heat and solute transport.

The flow region may be composed of non-uniform soils. Flow can occur in the vertical, horizontal, or a generally inclined direction. The upper boundary condition includes standard constant pressure and constant flux conditions in addition to meteorological forcing. Options for the lower boundary condition include unit gradient and seepage face. This model has been developed as a collaborative effort of the U.S. Salinity Laboratory and University of California at Riverside.

8.1.4 SIMULATION OF GROUNDWATER RECHARGE

Input Data

Rainfall: Daily rainfall for the period 2008-2017 for the Barchi raingauge station located in Barchi watershed was considered for the study. The annual rainfall distribution for the considered period has been represented in Figure 8.9.

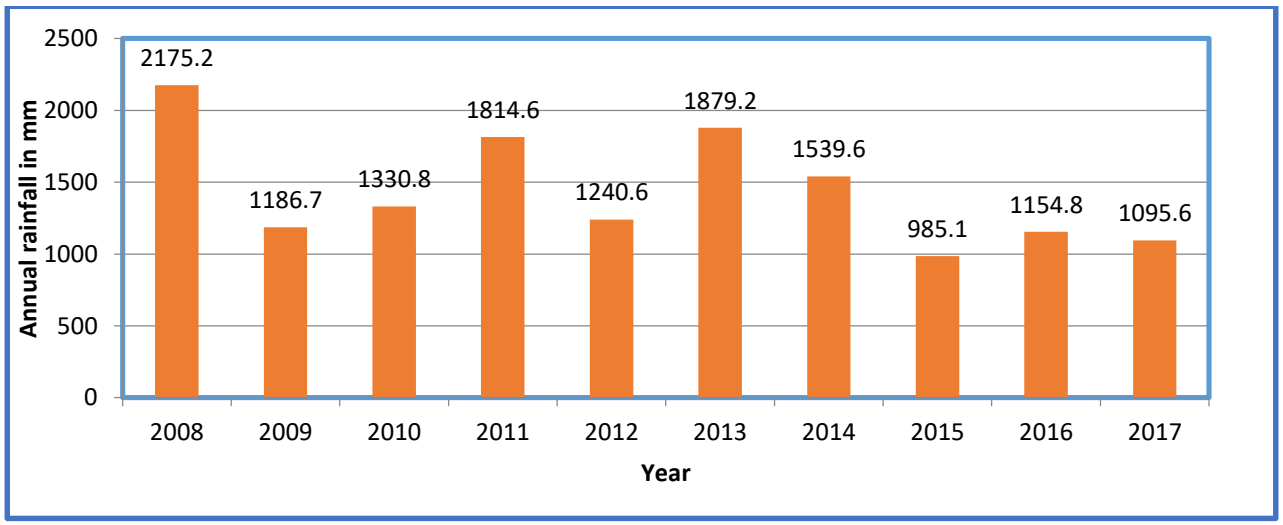

Figure 8.9: Rainfall Distribution in Barchi Watershed during 2008-2017

Evaporation: Daily evaporation data of Barchi watershed for the period 2008-2017 was considered for the analysis.

Saturated Hydraulic Conductivity: To model the retention and movement of water in the unsaturated zone, it is necessary to know the relationships between soil water pressure (h), water content (θ) and hydraulic conductivity (K). It is often convenient to represent these functions by means of relatively simple parametric expressions. The problem of characterizing the soil hydraulic properties then reduces to estimating parameters of the appropriate constitutive model (Table 8.7 and Table 8.8).

Table 8.7: van Genuchten model parameters α and n for upper soil layer

Station	Ks (cm/hour)	θ_r	θ_s	Van Genuchten Parameters	
				α	n
1	0.58	0.08	0.37	0.0073	1.434
2	0.57	0.14	0.37	0.0023	1.509
3	0.60	0.09	0.38	0.0021	1.465
4	0.18	0.30	0.53	0.0067	1.523
5	0.20	0.28	0.53	0.0129	1.373
6	0.18	0.28	0.53	0.0235	1.300
7	0.24	0.25	0.52	0.0020	1.580
8	0.16	0.30	0.54	0.0019	1.552
Average	0.339	0.215	0.471	0.0047	1.4385

Table 8.8: van Genuchten model parameters α and n for lower soil layer

Station	Ks (cm/hour)	θ_r	θ_s	Van Genuchten Parameters	
				α	n
1	1.66	0.11	0.38	0.0148	1.563
2	0.60	0.09	0.32	0.0045	1.760
3	0.007	0.06	0.43	0.0154	1.358
4	0.58	0.14	0.41	0.0134	1.310
5	0.58	0.16	0.43	0.0070	1.444
6	0.18	0.28	0.53	0.0235	1.300
7	0.58	0.13	0.31	0.0120	1.596
8	0.60	0.20	0.45	0.0125	1.688
Average	0.648	0.121	0.394	0.0095	1.4212

8.1.5 Simulation Results

Using the above data, HYDRUS 1-D was run for the period 2008-2017. Infiltration, Runoff, Groundwater Recharge, Evapotranspiration and Soil Water Storage were computed from the model as given in Table 8.9. Annual rainfall varied between 985mm to 2180mm during the study period, mostly occurring in the monsoon season (June-October). Simulated runoff at Barchi gauging site was found to vary between 24.6 mm to 1038.45 mm. The ground water recharge varied between 239.56 mm to 45.16 mm, evapotranspiration between 418mm to 651 mm and soil water storage between 136 mm to 186 mm.

Table 8.9: Estimated Water Balance in Barchi Watershed using HYDRUS 1-D

Year	Rainfall (mm)	Infiltration (mm)	Runoff (mm)	Recharge (mm)	Evapotranspiration (mm)	Soil water storage (mm)
2010	1331.2	927.83	403.31	307.52	463.91	156.39
2011	1814.6	851	963.25	239.56	425.5	185.94
2012	1240.6	835.93	404.68	248.01	417.96	169.96
2013	1879.2	840.75	1038.45	268.35	420.38	152.03
2014	1539.6	862.25	677.35	282.8	431.13	148.33
2015	1985.1	1060.42	924.61	400.59	423.28	236.26
2016	1754.8	810.2	944.6	268.53	408.09	133.59
2017	1955.95	1088.61	867.34	450.39	476.39	161.84
2018	1882.44	1095.76	786.35	428.87	487.88	165.65
2019	2456.76	1434.45	1022.31	639.56	515.35	279.34
2020	2944.78	1555.75	1388.87	676.35	530.44	348.45
2021	3015.38	1580.86	1434.5	564.67	694.65	321.49
Average	1983.368	1078.651	904.635	397.933	474.58	204.939

It is well known that thick soil cover and forest cover facilitates percolation. The study also indicates that the soils under forest cover exhibit higher values of infiltration. The higher infiltration is attributed to the proliferation of macropores particularly in the surface layers due to the high density of roots and soil fauna activity. Such macropores allow water to pass the unsaturated matrix and allow preferential flow to reach the saturated zone more quickly than through the unsaturated soil matrix. In general, abundance of large pores and macropores associated with aggregation and micro-aggregation of the clay particles would account for the relatively higher values of Ks and would be expected to strongly influence the movement of water.

It is observed from land use/land cover maps in the year 2000, the watershed is mainly covered with the Bamboo plantation / Teak plantation – 44.24%, Mixed forest – 35.28% and Agricultural land – 20.48%. Hence the study carried out by Purandara et al. (2000) indicated that the yearly rainfall varied between 1241 mm to1887 mm and evapo-transpiration being 33%. The groundwater recharge varied from 38% to 47% with the average value being 42%.The runoff was found to vary between 12% (low rainfall year) to 32% (high rainfall year) with the average value being 24%. The forested watershed has higher amount of soil water flux than any other land cover type. It is a well-known fact that the forest holds more water in their soil strata and allows water to percolate downward and recharges the groundwater table. The forested watershed considered for the study had a good amount of leaf litter on the floor and was covered with tree species with different ages and therefore had more capacity for groundwater recharge.

However in the study period (2010-2020) carried out by the authors, the variations in land use/land cover changes were distinctly observed as indicated in Figure 8.3 to 8.5. The watershed is covered with Bamboo plantation / Teak plantations around 34.68%, mixed forest around 23.77% and agricultural land being 41.55% thus indicating deforestation of 10% in tree plantations and 8% in mixed forests thereby increasing the agricultural activities by 18%. The results clearly indicated that the evapo-transpiration increased to 39% and the groundwater recharge decreased to 35%.

The temporal variations of annual groundwater recharge for the period 2008 to 2017 in the study area for the eight stations are shown in figure 8.10. Also superimposed in this plot are the rainfall values during the same periods. From these results, it can be seen that the groundwater recharge follows the rainfall pattern observed at the site. The difference observed at each of the locations under the selected watershed is due to soil moisture extraction, evapotranspiration and runoff.

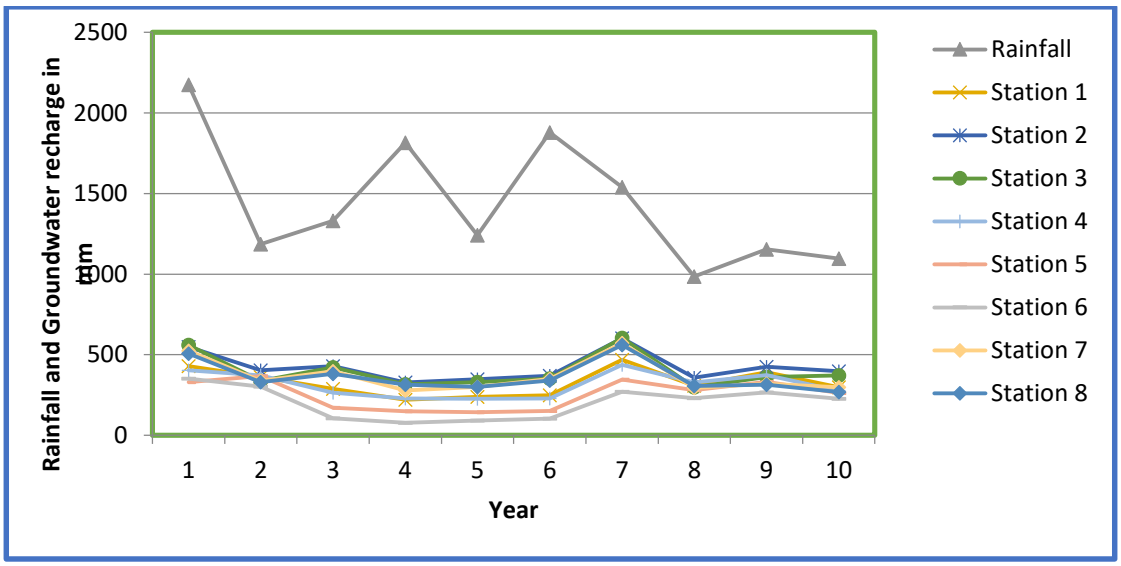

Figure 8.10: Groundwater recharge distribution in Barchi Watershed during 2010-2020

The estimated groundwater recharge at the eight stations is averaged for the study period 2008 to 2017 in the Barchi watershed. The mean and standard deviation of such spatially averaged groundwater recharge were computed for the study period and is given in Table 8.10.

Table 8.10: Mean GW recharge (mm) and standard deviation of Barchi watershed

Station	Mean (mm)	Standard deviation (mm)	Mean of spatially averaged groundwater recharge (mm/year)	Standard deviation of spatially averaged groundwater recharge

				(mm/year)
1	307.52	87.83	397.51	89.23
2	239.56	83.93		
3	248.01	99.07		
4	268.35	75.21		
5	282.8	86.11		
6	400.59	94.43		
7	268.53	96.53		
8	450.39	90.71		
9	428.87	89.56		
10	639.56	91.32		
11	676.35	94.45		
12	564.67	90.22		
Mean	397.933	89.23		

Spatial variations in computed groundwater recharge were evaluated by analyzing data for the eight stations in the Barchi watershed. This was achieved by calculating the groundwater recharge deviation D_j^i defined as the difference between the groundwater recharge estimated at occasion i at location j (J_j^i) nd the average of groundwater recharge estimated at all the locations in the watershed on the same occasion ($\check{j}i$). The computed deviation are then used to compute the basic statistics such as the mean and standard deviation. It is noticed that some of measuring locations in the selected watershed show a negative average values. This implies that these locations are below the catchment average during most part of the study period. As it is reported by Famiglietti et al. (1998) and Cosh et al. (2004), the measurement done on the slopes are always below the catchment and measurements on the plains or mild slopes are more on the higher side. This may be the reason under the present case also, as some of these measuring locations are on the slope and few are on the valley part of the watershed.

Model Calibration

The SWAT model for Barchi catchment was calibrated using observed daily discharge values of the Barchi raingauge station for a period of four years from 1994 to 1997 by the application of SUFI2 algorithm in SWAT-CUP. Figure 8.11 and 8.12 shows the results of the calibration process:

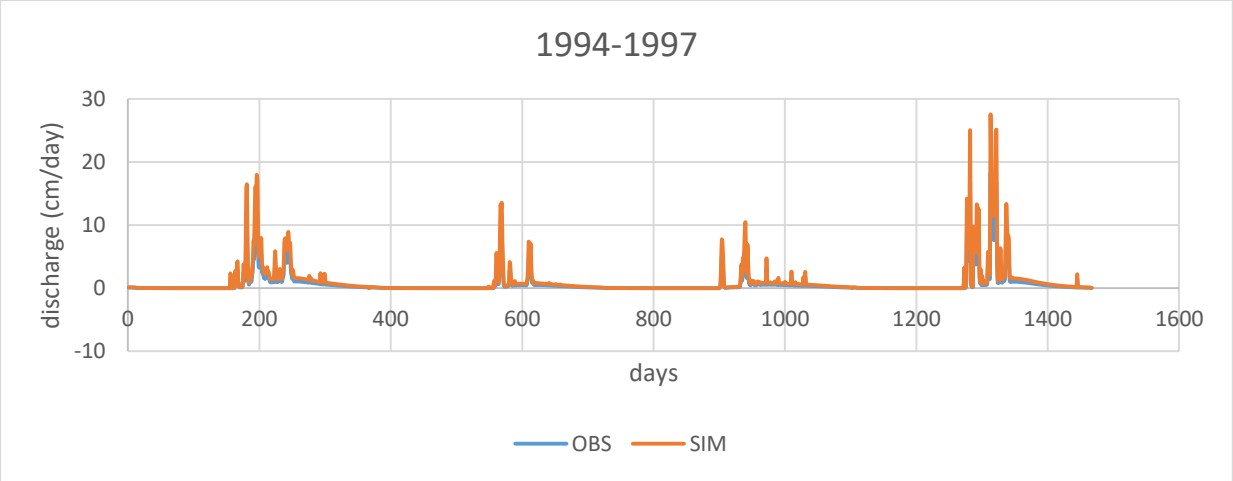

Figure 8.11. Observed and simulated discharge values for the calibration period

The fitted values for the different parameters obtained after calibration are shown in Table 8.11.

Table 8.11 Calibrated parameters of SWAT model

S. No.	Parameter_Name	Fitted_Value	Min_value	Max_value
1	R__CN2.mgt	-0.080000	-0.200000	0.200000
2	V__ALPHA_BF.gw	0.700000	0.000000	1.000000
3	V__GW_DELAY.gw	38.400002	30.000000	450.000000
4	V__GWQMN.gw	0.440000	0.000000	2.000000

The parameters refer to the following:

CN2 = Initial SCS runoff curve number for moisture condition II

ALPHA_BF = Baseflow alpha factor

GW_DELAY = Groundwater delay (days)

GWQMN = Threshold depth of water in the shallow aquifer for return flow to occur Additional information about the various parameters in SWAT model can be obtained in the official SWAT documentation. It can be downloaded from www.swat.tamu.edu.

Model Validation

The SWAT model was validated for a period of four years from 1998 to 2001 using observed daily discharge values at the Barchi raingauge station. The calibrated values of the SWAT parameters as

shown in table 8.12, were used in the model for validation process. Figure shows the results of the validation process.

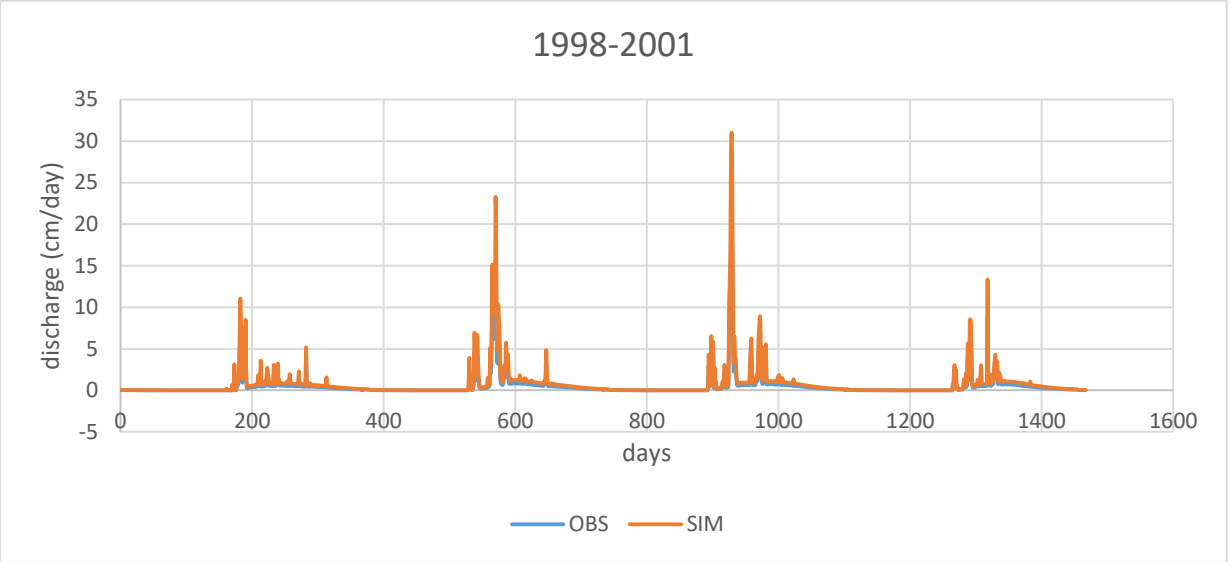

Figure 8.12. Observed and simulated discharge values for the calibration period

Model output

The SWAT model utilizes elevation, land use and soil maps, as well as meteorological parameters such as daily precipitation, temperature, wind speed, relative humidity and solar radiation for calculating the flow parameters. During SWAT run, the study area was divided into 23 sub-basins, for which the groundwater recharge and evapotranspiration was estimated individually.

The simulated annual values of recharge for the model simulation period from 1994 to 2001 are shown in the Table 8.12:

Table 8.12 Simulated Annual Recharge from 2014 to 2021

Sum of GW_Qmm	Years							
Sub-basins	2014	2015	2016	2017	2018	2019	2020	2021
1	495.61	331.683	147.946	470.918	325.62	373.596	637.681	363.408
2	498.216	333.756	148.726	473.298	327.429	375.589	641.256	365.65
3	499.797	344.359	150.189	483.664	333.953	385.397	659.884	370.323
4	503.178	373.186	153.854	511.044	351.068	411.488	710.576	382.939
5	507.526	409.586	158.659	545.923	372.862	444.657	774.196	398.512
6	502.603	416.871	158.214	551.346	375.667	450.82	787.332	398.517
7	493.406	329.949	147.23	468.671	323.925	371.737	634.617	361.581

8	505.768	396.384	156.916	533.31	364.969	432.689	751.086	392.703
9	497.351	333.074	148.458	472.686	327.041	374.99	640.493	365.188
10	495.282	344.839	149.086	482.594	332.656	385.1	660.838	368.09
11	493.236	329.787	147.143	468.387	323.708	371.508	634.358	361.392
12	492.079	328.88	146.814	467.437	323.015	370.713	632.809	360.442
13	492.819	329.505	147.081	468.241	323.608	371.395	633.852	361.027
14	486.013	338.078	144.982	470.809	325.231	379.861	649.411	372.254
15	506.544	403.81	157.828	540.236	369.254	439.335	764.06	395.835
16	497.863	333.488	148.654	473.135	327.327	375.474	640.812	365.272
17	465.764	371.441	141.032	489.898	336.055	411.337	709.188	396.379
18	443.903	358.038	132.061	465.369	319.804	399.689	686.603	400.379
19	489.311	403.071	151.9	530.565	362.416	439.386	763.692	402.3
20	443.319	357.576	131.998	465.226	319.702	399.571	685.806	399.688
21	510.152	423.495	160.741	559.572	381.488	457.522	798.582	405.042
22	464.89	379.02	141.432	496.207	339.888	418.212	722.527	400.01
23	499.686	355.378	151.269	493.717	340.065	395.217	679.284	374.399

Similarly, the simulated annual values of evapotranspiration for the same simulation period are shown in the table 8.12: The SWAT result shows that the surface runoff in the region is about 27.20%, while the total aquifer recharge is about 35.98 %. The evapotranspiration in the Barchi catchment is found to be 37.0195% of the average rainfall. The higher values of recharge and evapotranspiration may be possible due to greater forest cover in the region.

Table 8.12 Water balance components in Barchi basin

S. NO.	PARAMETER	VALUE (mm)	Percentage of rainfall
1	Precipitation	1251.5	
2	Surface Runoff Q	340.47	27.20495406
3	Lateral soil Q	6.86	
4	Shallow Aquifer Recharge	413.53	33.0427487
5	Deep Aquifer Recharge	22.52	1.799440671
6	Total Aquifer Recharge	450.32	35.98242109
7	Evapotranspiration	463.3	37.01957651
8	Potential ET	1838.3	

8.1.6 Application of MODFLOW

The groundwater flow simulation was carried out using Visual MODFLOW, where the values of recharge and evapotranspiration were assigned as input, along with various other parameters. The model was run for a period of 8 years. The groundwater table contour map for the simulation is shown below in figure 8.13:

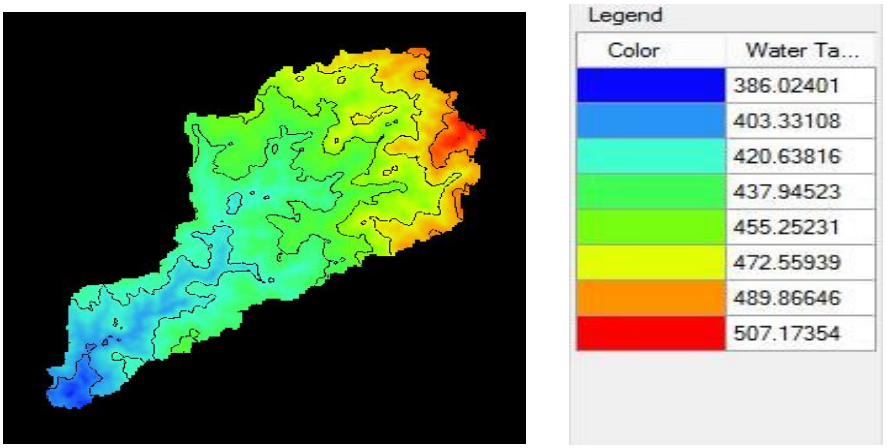

Figure 8.13 Groundwater table contour map obtained from Visual MODFLOW

8.1.7 Summary

Variations in land use land cover brought on by anthropogenic disturbances have impacted various hydrological parameters such as recharge and runoff throughout the past few decades. It is noticed that there is a significant variation in infiltration and soil moisture distribution over Barchi watershed. These variations are attributed to large scale disturbance occurred due to change in land use/land cover, i.e. conversion of original forest land to teak plantation (gap filling/afforestation). Though in some of the afforested land have shown improvement in infiltration rates and saturated hydraulic conductivity, however, the region is dominated by infiltration excess overland flow as it is covered black and mixed soils. Anthropogenic activities have an increased impact on impervious surfaces and storm drain, which divert precipitation away from recharge areas. Groundwater recharge is found to be maximum in forested landscapes as compared to agriculture land and degraded patches. Groundwater levels are relatively deeper in major part of the watershed which could be due to the presence of deeper roots spread over the watershed.

8.2 MALAPRABHA SUB-BASIN UPTO KHANAPUR

The Malaprabha sub-basin lies in the extreme western part of the Krishna basin. It extends between 74° 20’ and 74° 30’ longitudes and 15° 20’ and 15° 40’ latitudes and encompasses an area of 540 sq. km. of the Belgaum district in Karnataka state. Digital elevation map Malaprabha catchment up to Khanapur is shown in figure 8.14.

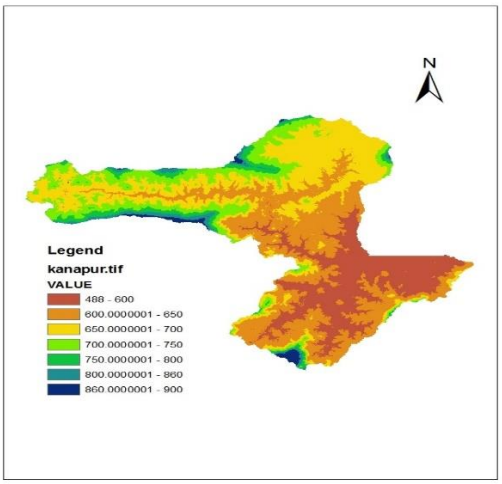

Figure 8.14 Location of the Malaprabha sub-basin

This sub-basin is the major source of water yield for the Naviluteerth dam constructed at 35-45 km downstream of its mouth. This dam impounds about 1377 MCM water and provides water for irrigation approximately for 2.17 lakh hectare lands. Elevation classification and slope variation in the catchment up to Khanapur (Gauging site) is given in Table 8.13 & 8.14 respectively.

8.2.1 Hydrometeorological Network

There are five raingauge stations and two hydro-meteorological stations consisting of Stevenson screens (to record temperature and humidity), pan evaporimeter, anemometer, windvane, self-recording and ordinary rain-gauges at different places in the Malaprabha basin.

Table 8.13 Topography of the Malaprabha up to Khanapur

ELEVATION	% AREA UNDER ELEVATION
Below 600 m	15.61
600-650 m	30.94
650-700 m	30.07

700-750 m	15.48
750-800 m	4.58
800-850 m	1.88
850-900 m	1.13
Above 900 m	0.31

Table 8.14. Slope distribution in the Malaprabha (up to Khanapur)

SLOPE	% AREA UNDER SLOPE
0 to 5	30.29
5 to 10	32.84
10 to 15	18.68
15 to 20	9.83
Above 20	8.36

8.2.2 Basin characteristics

A brief description of the Malaprabha sub-basin characteristics, i.e. geology, soils, land use pattern and geomorphological parameters are given below:

Geology: Geologically, the malaprabha sub-basin comprises of two main geological formations (i) tertiary basalts (ii) sedimentary formations of the Pre Cambrian age

(i) ***Tertiary basalts-*** A major portion (96 %) of the sub-basin is covered in tertiary basalts. The hydrology of basalts is different from that other types of hard rocks. One of the main differences is that the various basalt flow units can form multi-aquifer system somewhat similar to a sedimentary rock sequence, having alternate pervious and impervious horizons.

(ii) ***Sedimentary rocks-*** The sedimentary rock formation is of pre-Cambrian age. This types of rocks are confined in the south eastern part of the study area. Sedimentary rocks generally act as good aquifer if it is not interrupted by intertrappean clays and other impermeable rocks.

Soils- Pedologically speaking, the basin rocks are covered by thin (0.5 m) to thick (10 m) layer of soils, which are divisible into two major groups. These are red loamy soils and medium black soils.

(iii) ***Red loamy soils-*** the upper reaches of the basin, i.e. on crest and gently sloping mid-crest regions, viz., pediplains are characterized by red loamy soils. The top soil texture varies between sandy loam to clayey loam underlain by gravel and sandy loam, sub-soil horizon. About 80% area of the Malaprabha sub-basin is covered by red loamy soils.

(iv) ***Medium black soils-*** this type of soil occurs extensively in parts of Khanapur taluk. Soils are moderately deep to very dark greyish brown, dark reddish brown or black in colour, usually calcerous cracking and clayey. These are moderately well drained with low permeability.

Land use pattern: Land use pattern of the Malaprabha sub-basin is very complex comprising of forest, agriculture, shrubs and barren land. A brief description of the different land use is given below (Figure 8.15):

Forests- About 62.65% of the Malaprabha sub-basin, that includes Kanakumbi, Jamboti and Gunji areas are covered by dry tropical forests. The major species are covered by teakwood, rosewood, jackwood, bamboo etc. The ground of these forests are covered by shrubs (2-4 m high) and grasses.

Shrubs- the eastern facing watershed of the area having steep slope (20-30) are covered by shrubs and small trees and bushes (3-5 m high). The most important feature of this class is that these are relatively shallow soil areas. About 19.3% area of the basin is covered by shrubs.

Agricultural land- the gentle slopes and level valley bottom areas, where the most fertile soil is confined, have been occupied by man for the cultivation of various cereals (paddy, ragi etc) and cash crops (cotton, sugarcane). About 16.85 % of the total basin falls under agricultural land.

Barren land- About 1.15% of the area is in form of small patches, on steep slopes and on gentle slopes having very thin film of soil, is in form of barren land. This land is used for the grazing purpose of cattles.

Table 8.15: Land use pattern in the Malaprabha up to Khanapur

LANDUSE	% AREA UNDER LAND USE
DRYLAND CROPLAND AND PASTURE	8.9

IRRIGATED CROPLAND AND PASTURE	2.85
CROPLAND/GRASSLAND MOSAIC	11.27
CROPLAND/WOODLAND MOSAIC	9.05
SHRUBLAND	2.68
SAVANNA	53.92
DECIDUOUS BROADLEAF FOREST	2.46
EVERGREEN BROADLEAF FOREST	8.77
MIXED FOREST	0.1

8.2.3 LU/LC and Soil Moisture Distribution

Infiltration event is followed by redistribution of soil water within the soil profile. There is a continued downward redistribution of the infiltrated water, together with an evaporative loss from the soil surface, and extraction of water from the depth of soil which is exploited by the roots of transpiring vegetation. Therefore, the redistribution of soil moisture is a very complicated process and need a systematic study. Even in uniform, non-swelling soil the water movement process is complicated by severe non-linearity and hysteresis phenomenon.

In the present study, Soil moisture percentage in different land covers is estimated by gravimetric method. Monitoring of soil moisture is done once in two months and in most of the cases soil samples were collected only up to depth of 5 to 6 ft. The moisture content observed and corresponding rainfall pattern for available stations. The results indicate that soil moisture variation is quite varied and depend upon various factors such as land use, soil type, type of plantation, rainfall intensity and duration. Further results indicate that there is no marked variation in soil moisture distribution if the region falls under the same agro-climatic conditions. Along the Gunji- Khanapur belt the moisture observation showed almost a similar trend irrespective of the land use and plantation. However, it is noted that the moisture content remains for longer duration under forest and plantation covers when compared to degraded lands. Similar observations were also made for Jamboti- Khanapur belt and Belgaum – Jamboti belt. It is also noted that along Belgaum – Jamboti belt the moisture distribution is higher than in other two zones. This is mainly because of the red loamy soil and comparatively higher thickness of the soil layer. Site specified observations of soil moisture distribution are discussed below

Gangavali Forest

Figure 4.4 shows the variation of moisture content with depth under forest cover. Steady increase of moisture was observed from June to October at 0.5m depth. In the deeper layers (1 m and 1.5m, the higher moisture was observed only during August, i.e during heavy rainfall period and decreased

steadily. The observations on the bottom soil layer and below 1m depth there is no significant variation in moisture content. This could be due to the deeper roots present in the forests, which draws water from deeper layers without affecting the top layers.

Figure 8.15 shows the variation of soil moisture at Kankumbi (forest) i.e. at the upper most part of the catchment. At this location, distribution of soil moisture showed significant variation from that of Gangavali. Very high moisture content was observed, particularly during psot-monsoon season. The drastic change in moisture percentage could be attributed to high rainfall (more than 5000 mm) occurring in and around Kankumbi. The relatively higher forest cover observed in this part of the study area may lead to increased interception and stem flow. This kind of dissipation of rainfall energy influences soil moisture redistribution after the process of infiltration. This also demonstrated the fact that the distribution of moisture content not only depends on the land use/land cover changes but also on the rainfall pattern and intensity.

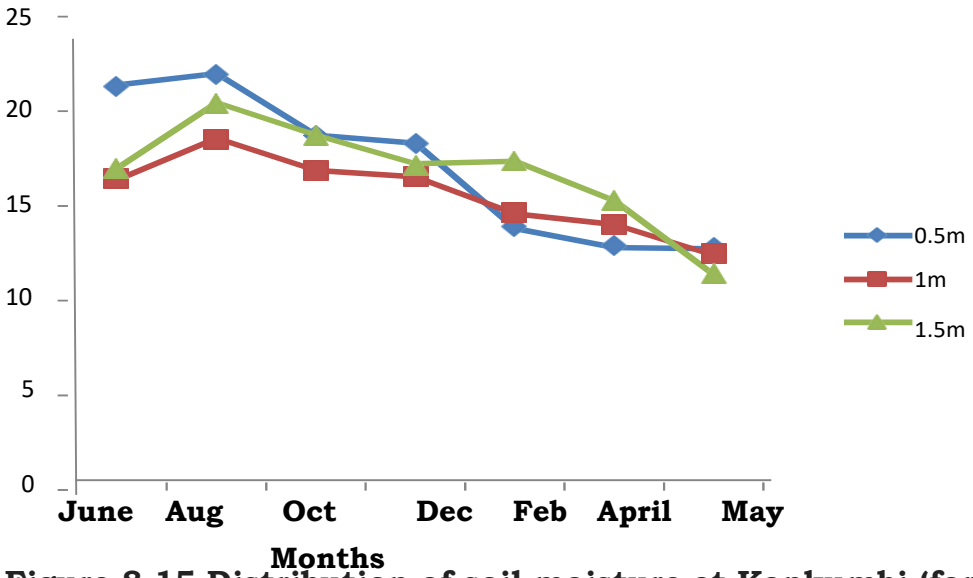

Figure 8.15 Distribution of soil moisture at Kankumbi (forest)

Degraded Forest: Figure 8.16 show the variation of moisture content with depth in degraded forest in Kankumbi (a high rainfall region) and a moderate rainfall area (between Jamboti and Khanapur). Degraded forests in Kankumbi in spite of having high rainfall (more than 5000mm) showed comparatively lower moisture content than in forest cover. Variation of moisture in a degrded land Jamboti and Khanapur also showed similar trend. This clearly indicated that, irrespective of the rainfall pattern, the moisture content varies considerably in the degraded forests which could be attributed to higher runoff and lower recharge taking place in the scrubs.

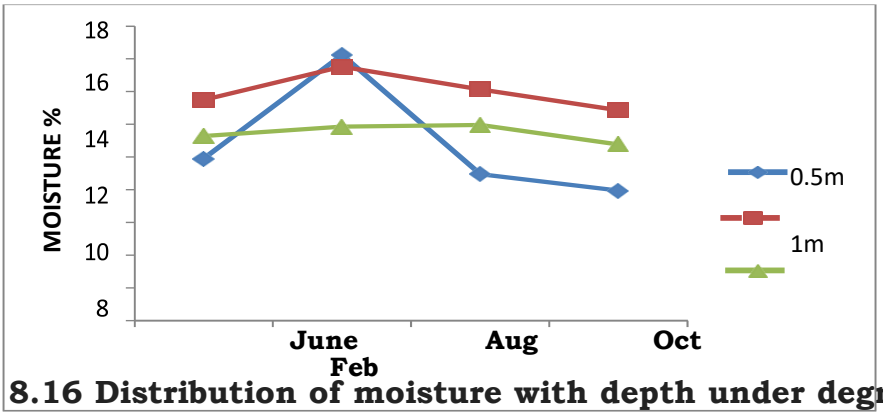

Figure 8.16 Distribution of moisture with depth under degraded forest (Kankumbi)

Barren land

In the case of barren land it is found that the average moisture content is much higher than the forest and scrubs. The maximum percentage varies from 20% to 35% at Kankumbi and 11 to 18% at Santibastwad. This could be attributed to change in rainfall pattern. Kankumbi receives very high rainfall whereas Santibastwad, receive less than 50% of Kankumbi. The higher moisture content observed in the barren land could be attributed to low rate of evapotranspiration. In addition, the type of soil and its physical and chemical characteristics play a significant role in deciding the moisture holding capacity. Figure 8.17 show the distribution of moisture with depth in a barren land at Kankumbi.

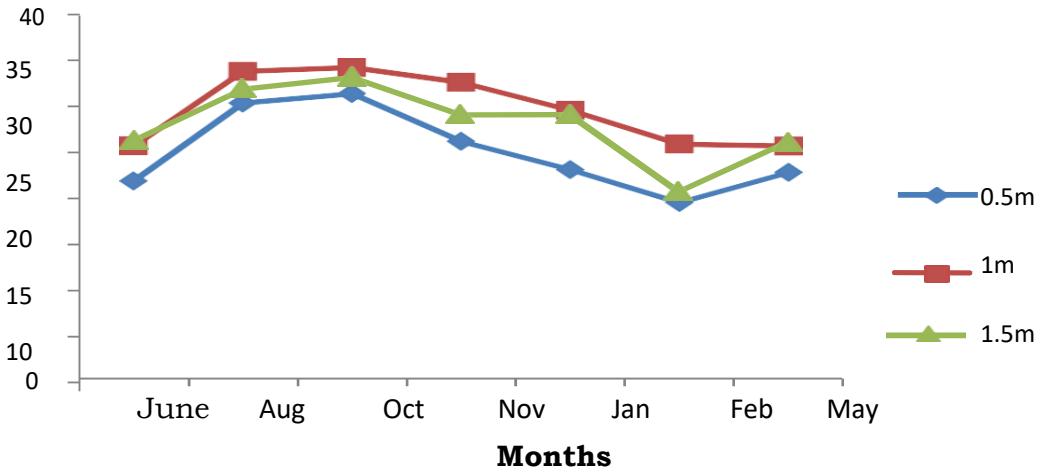

Figure 8.17 Distribution of Moisture with depth in a barren land (Kankumbi)

Acacia plantations

Figure 8.18 and 8.19 show the variation of moisture content with variety of plantation, i.e. Eucalyptus and Acacia. It is noticed that the moisture content is significantly high in acacia plantation as compared to eucalyptus. This is true as reported by number of earlier researchers. In eucalyptus plantation, the maximum moisture content is less than 18% whereas in acacia, it is more than 30%. This variation could be explained based on the horizontal growth of roots observed in acacia. Due to the spreading of surficial roots horizontally, acacia plantation does not draw much water from deeper layers. In the case of eucalyptus, it is noticed that the roots are deeper and draw much more water than acacia.

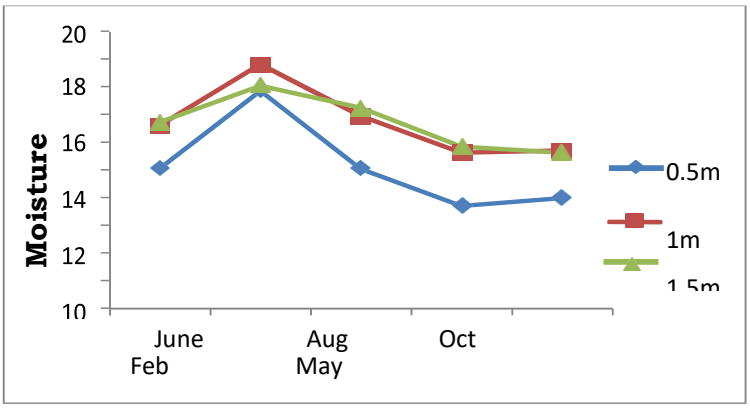

Figure 8.18 Soil moisture distribution in an Eucalyptus plantation

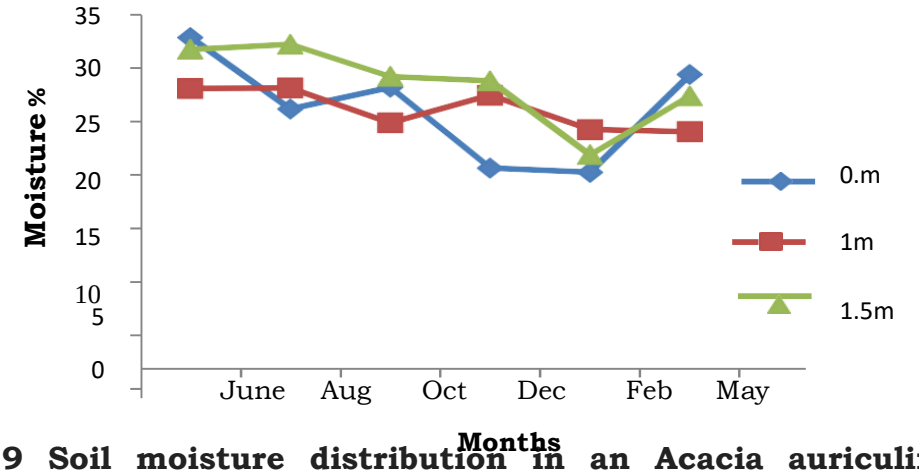

Figure 8.19 Soil moisture distribution in an Acacia auriculiformis plantation

Teak plantations

One of the interesting observation made in the present study is with regard to the distribution of moisture in teak plantation. Teak plantation showed minimum rate of infiltration as compared to other afforested areas. However, distribution of moisture under two different land covers showed a reasonably good match with that of forest. This could be attributed to the deep roots present in the teak which draws

water from deeper layers without affecting the surface layers. Further, the leaf litter present in the teak plantation give rise to high organic matter which acts as sponge and slowly transmits water to soil layers. Apart from the said reason, wider leaves and comparatively higher interception, moisture can be held for longer time. In order to conclude, it is essential to have a detailed analysis of soil moisture, ecology and hydrological processes. Figure 8.20 and 8.21 indicates the variation of moisture content in two teak plantations one at high rainfall region and another at relatively lower rainfall area.

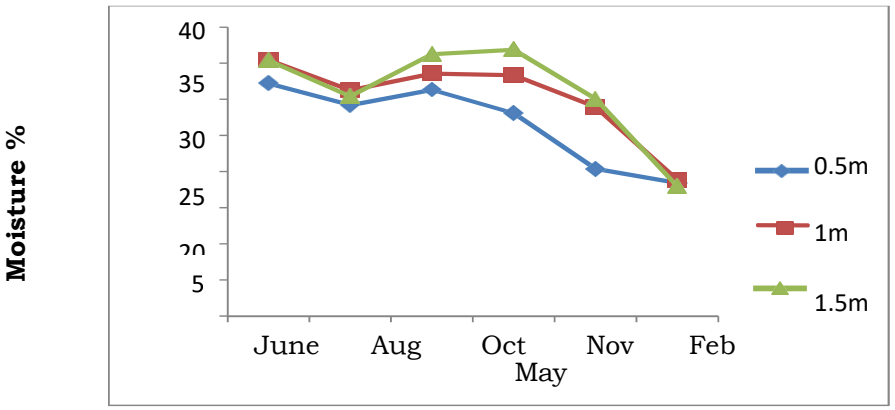

Figure 8.20 Soil moisture distribution in teak plantation at Jamboti

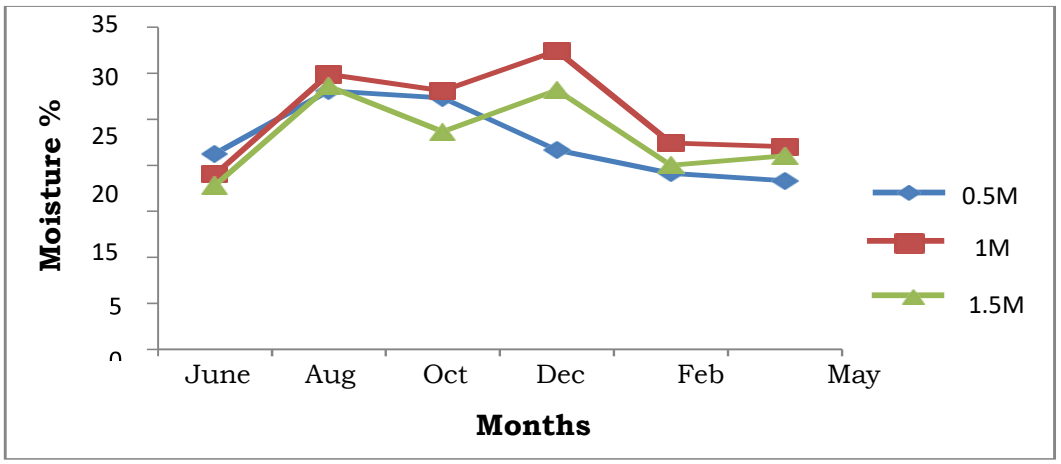

Figure 8.21 Soil moisture distribution in Teak plantation at Khanapur

Agriculture Land

Figure 8.22 and 8.23 shows the variation of moisture content in two agriculture plots located in two rainfall regimes. In the agriculture land the role of moisture plays a significant role as it may help to grow more crops. Therefore, in agriculture land the conservation of moisture is the priority. The observations made in two agriculture sites (4.30 &4.31) shows two different kinds of scenario. In the first case moisture varies between 10 and 15% (except in the month of May) whereas in the second

case, moisture varies from 20% to 25%. The variation in the moisture distribution could be attributed to the following reasons.

- Impact of agriculture activity on soil hydraulic properties
- Type of crops plays a significant role in moisture redistribution
- Rainfall intensity, erosivity and type of activity.

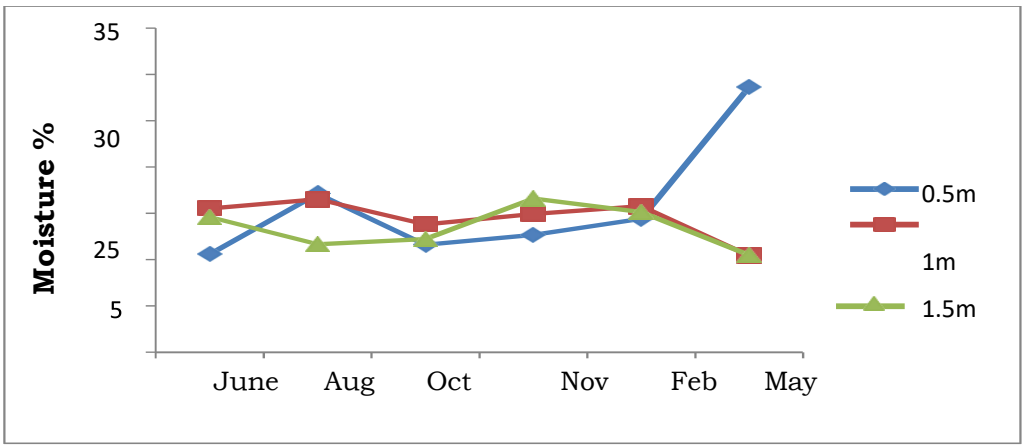

Figure 8.22 Soil moisture distribution in Agricultural land

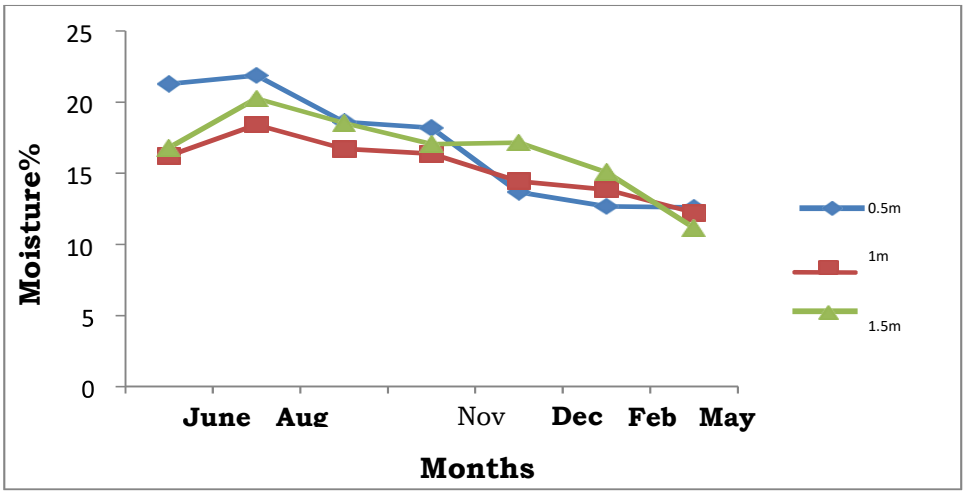

Figure 8.23 Soil moisture distribution in Agricultural land

8.2.4 Moisture retention characteristics

Table 8.16 presents the moisture retention characteristics of soils in Malaprabha sub-basin (up to Khanapur) under different land covers.

Table 8.16. Soil moisture retention characteristics of Malaprabha soil

Land use/Land covers	Pressure in bars							
	0.33	1	3	5	7	10	12	15
	Variation of Moisture content with pressure							
Degraded	0.28	0.24	0.22	0.19	0.15	0.13	0.12	0.09
Degraded	0.21	0.18	0.14	0.13	0.12	0.1	0.09	0.07
Agriculture	0.48	0.44	0.42	0.39	0.37	0.35	0.33	0.32
Agriculture	0.25	0.24	0.23	0.21	0.2	0.18	0.17	0.16
Forest	0.3	0.21	0.19	0.17	0.14	0.12	0.11	0.07
Forest	0.34	0.32	0.3	0.27	0.24	0.22	0.19	0.17
Grassland	0.25	0.24	0.23	0.21	0.2	0.18	0.17	0.16
Grassland	0.28	0.26	0.22	0.21	0.19	0.15	0.13	0.1
Teak	0.2	0.16	0.15	0.13	0.13	0.12	0.1	0.07
Teak	0.26	0.24	0.22	0.21	0.18	0.15	0.12	0.1

From the above results it is understood that for a given land, the parameters show significant variations for each of the soil samples (taken at different times); implying temporal variability in soil water retention characteristics. The higher water content at saturation and lower residual water content of these soils suggest that soils are wholly underdeveloped and contain some coarse fragments (i.e. higher % sand).

8.3 Estimation of Rainfall Recharge to Groundwater

8.3.1 Empirical Methods

Groundwater Recharge has been estimated for various stations in Malaprabha sub basin to understand the variation recharge with rainfall. An empirical equation developed by KL Rao was applied as it was found to be more reasonable to peninsular part of India.

Krishna Rao Method: Krishna Rao gave the following empirical relationship in 1970 to determine the groundwater recharge in limited climatological homogeneous areas (Table 8.17):

Rr = K (P - X) …(4.1)

The following relation is stated to hold good for different parts of Karnataka:

Rr = 0.20 (P - 400) for areas with annual normal rainfall (P) between 400 and 600 mm Rr = 0.25 (P - 400) for areas with P between 600 and 1000 mm
Rr = 0.35 (P - 600) for areas with P above 2000 mm where, Rr and P are expressed in millimetres.

Table 8.17 Ground water recharge estimated using Empirical Formula (K. L. Rao method)

SL.No	RAINFALL in mm	RECHARGE in mm	% Recharge
1	2789.296	766.25	27.6
2	3176.825	901.880	28.3
3	2238.11	573.33	25.6
4	2806.437	772.05	27.4
5	1942.302	469.8	24.1
6	3200.500	910.175	28.4
7	2713.667	739.83	27.26
8	2834.640	782.124	27.6
9	2795.760	768.51	27.4
10	2465.625	652.68	25.4
11	2206.380	562.23	25.4
12	1760.351	406.12	23.07
13	1531.163	325.9	21.2
14	2696.043	733.61	27.2
15	1997.929	489.27	24.4
16	2335.855	607.54	26
17	2225.986	569.09	25.5
18	2526.757	674.36	26.6
19	2690.344	920.62	34.2
20	3526.929	1024.42	29
21	1894.229	452.98	23.9
22	2036.593	502.8	24.6
23	1733.629	396.77	22.8
24	2060.471	511	24.8
25	2530.657	675.72	26.6
26	2021.529	497.53	24.6
27	1974.193	480.96	24.4
28	1766.529	408.28	23..10
29	2449.257	647.23	26.4

8.4 Application of SWAT

The SWAT model was applied to Malaprabha sub-basin for the estimation of recharge and evapotranspiration. The model was set up in a GIS environment and run for a simulation period of 14 years from 1980 to 1993, with the help of land use, soil and elevation maps. Weather parameters such as daily precipitation and temperature were used as an input to the model, and other parameters (relative humidity, solar radiation and wind speed) were simulated using IMD weather generator database. The

model was then calibrated using SWAT-CUP for a period of nine years from 1980 to 1988 using observed daily runoff data at the Khanapur gauging station.

In the first phase of the SWAT simulation, the model divided the catchments into number of sub-units and further classified the sub-units into HRU's based on soil, land use and slope characteristics (Figure 8.24).

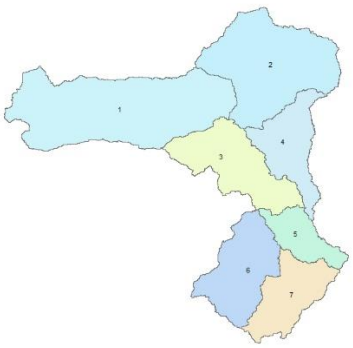

Figure 8.24. Malaprabha catchment demarcated into sub-units by using SWAT model

8.4.1 Calibration of the SWAT model

The model was calibrated with the observed daily discharge of Khanapur gauging station for a period of 9 years (1980-1988) by using SWAT-CUP. The results obtained from the calibrated model is shown in figure 8.25.

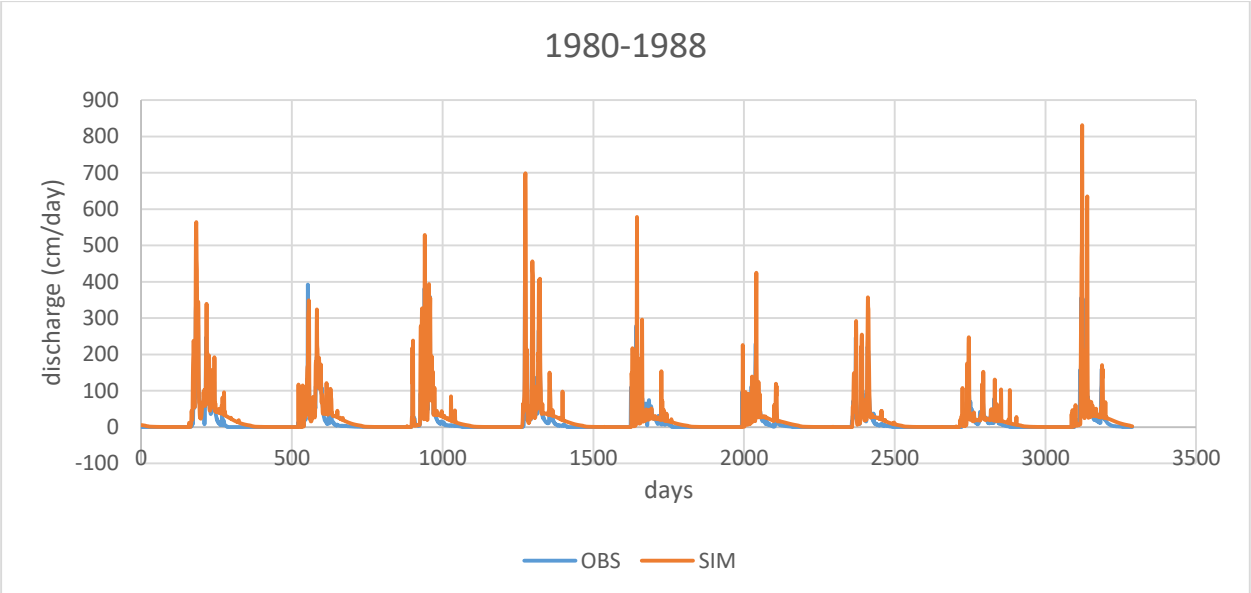

Figure 8.25 Observed and simulated discharge values for the calibration period

The calibrated parameters for the Malaprabha sub-basin is presented in Table 8.18.

Table 8.18: Fitted values of the parameters as obtained after the calibration

S. No.	Parameter_Name	Fitted_Value	Min_value	Max_value
1	R__CN2.mgt	-0.140000	-0.200000	0.200000
2	V__ALPHA_BF.gw	0.550000	0.000000	1.000000
3	V__GW_DELAY.gw	51.000000	30.000000	450.000000
4	V__GWQMN.gw	0.500000	0.000000	2.000000

Here, the parameters refer to the following:

CN2 = Initial SCS runoff curve number for moisture condition II

ALPHA_BF = Baseflow alpha factor

GW_DELAY = Groundwater delay (days)

GWQMN = Threshold depth of water in the shallow aquifer for return flow to occur (mm H_2O)

Additional information about the various parameters in SWAT model can be obtained in the official SWAT documentation. It can be downloaded from www.swat.tamu.edu.

8.4.2 Validation of the Model

The model was validated for the remaining five years i.e. 1989 to 1993. The graph plotted between the observed and simulated daily runoff values for the year 1993 is as follows (Figure 8.26):

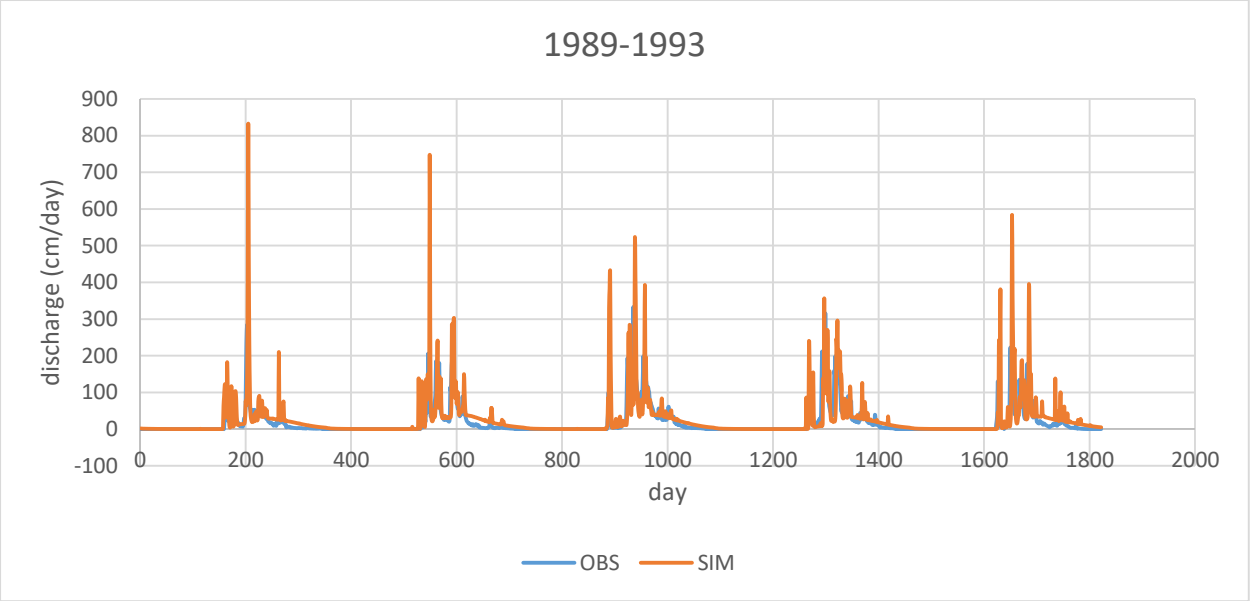

Figure 8.26 Observed and simulated discharge values for the validation period

8.4.3 Output of the Model

The results of the water balance components such as surface runoff, groundwater recharge and evapotranspiration for the Malaprabha sub-basin (up to Khanapur) is shown in Table 8.19

Table 8.19 Estimated Water balance components using SWAT model

S. NO.	PARAMETER	VALUE (mm)	Percentage of rainfall
1	Precipitation	2282	
2	Surface Runoff Q	1159.9	50.82822086
3	Lateral soil Q	21.94	
4	Shallow Aquifer Recharge	602.52	26.40315513
5	Deep Aquifer Recharge	32.46	1.422436459
6	Total Aquifer Recharge	649.28	28.45223488
7	Evapotranspiration	456.8	20.01752848
8	Potential ET	1738.8	

Based on the results obtained for the Malaprabha sub-basin, it is evident that the study area receives an average annual rainfall of 2282 mm/year. The surface runoff in the sub-basin was found to be 50.82% of the total rainfall. The total aquifer recharge in the region was 28.45% of the rainfall, while the evapotranspiration was found to be 20.017%.

Based on estimated groundwater recharge, flow models were developed using MODFLOW.

8.4.4 Application of MODFLOW

The groundwater flow simulation was carried out using Visual MODFLOW, where the values of recharge and evapotranspiration were assigned as input, along with hydraulic conductivity, porosity and specific yield etc. A total of 14 wells were taken in to consideration for this model. Figure 8.27 shows the locations of the observation wells in the Malaprabha catchment up to Khanapur.

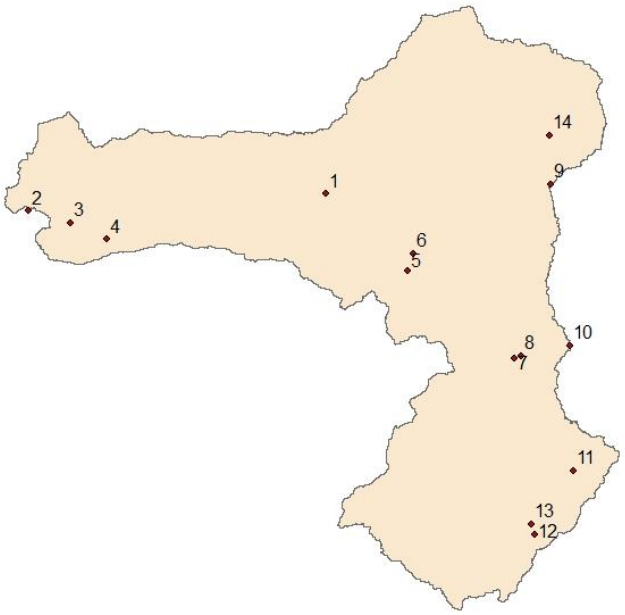

Figure 8.27 Malaprabha catchment up to Khanapur with locations of Obs. wells

The model was run for a period of 10 years from 2011 to 2020. The observed and simulated water levels (RL in meters) is presented in figure 4.38. It is found that the groundwater level varies between 570.74m and 749.77m. The simulated results followed the similar trend with that of the observed groundwater fluctuations. The observed and simulated groundwater levels are given in Table 8.28.

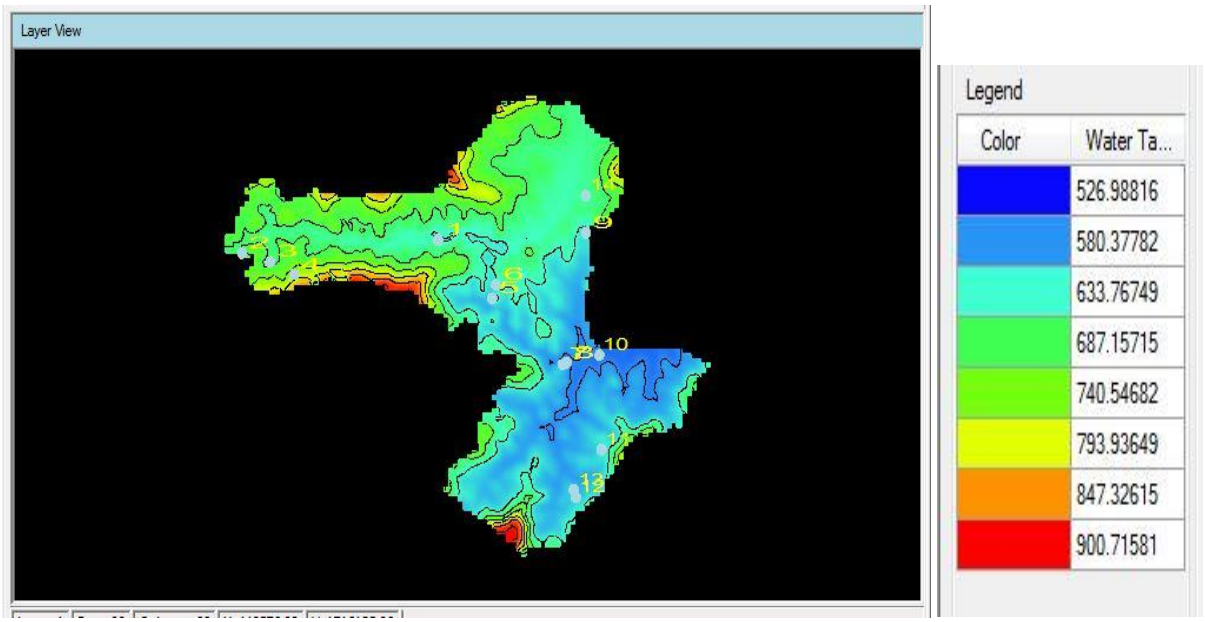

Figure 8.28 Groundwater flow model of Malaprabha sub-basin

Table 8.20: Observed and Simulated groundwater levels in the Malaprabha catchment up to Khanapur.

WELL ID	OBSERVED	SIMULATED
1	628.3246	626.58
2	674.6277	673.78
3	658.8538	663.16
4	749.7691	744.75
5	635.358	631.19
6	635.1163	638.61
7	589.7	592.185
8	574.7784	571.02
9	627.3825	629.206
10	570.7369	569.9
11	614.503	609.18
12	598.9759	599.002
13	607.1281	609.368
14	658.0391	656.833

Based on the model results, it is evident that the simulated water levels for nine wells were found to be matching with the observed water levels, with the difference in observed and simulated water levels being in the range of 0.7 to 3 meters. Whereas the model was unable to predict the water levels in the remaining five wells, where the difference was found to be more than 3 meters. This is attributed to the uneven groundwater draft occurring in the region. Figure 8.29 shows the groundwater table fluctuations

in the study area. It is noticed that the water table is higher in the headwaters as compared to the downstream areas.

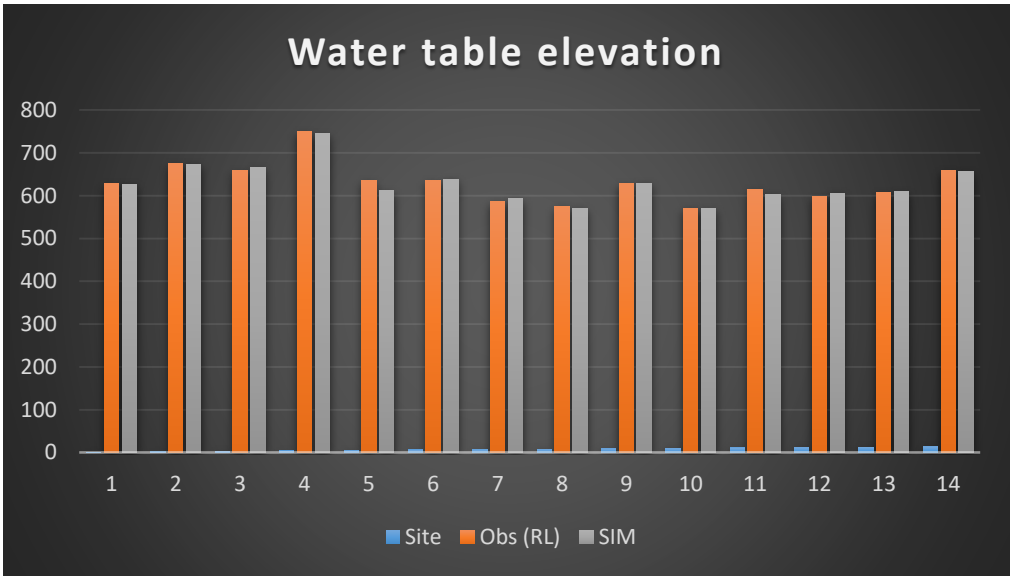

Figure 8.29 Groundwater table variations in Malaprabha catchment up to Khanapur

An evaluation of the MODFLOW results is shown in figure 8.30. From the above analysis it is evident that the MODFLOW simulated the groundwater levels to more than 80% accuracy.

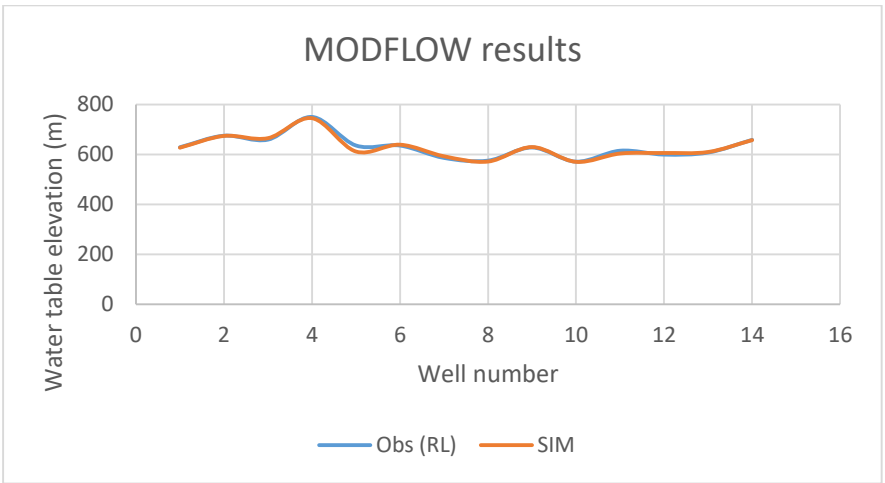

Figure 8.30 Plot of the observed and simulated water levels

CHAPTER – IX : SUMMARY AND CONCLUSION

9.1. SUMMARY and CONCLUSIONS

Based on a review of a rather limited research and partly extrapolating from hydrological studies in the other parts of the world, it is reported that our understanding of prospects for the enhanced rainfall and augmented base flows as a consequences of forestation in the humid tropics are generally very poor, but dependent on site-specific factors. In terms of being able to predict the hydrological effects of land use changes it is especially important to understand the local hydrology, at least in terms of the dominant processes governing the runoff generation, erosion and sediment production from degraded landscapes. These processes may readily moderate and stabilized at very low levels by forestation.

Initially the influence of rainfall, temperature, evapotranspiration and other hydro meteorological parameters on runoff dynamics and soil moisture building up mechanism were studied for these selected watersheds. Hydro-meteorological measurements taken at study area such as rainfall and temperature were subjected to detailed analysis. Studies on rainfall amount and intensities and their spatio-temporal variations indicated that the area is under the influence of monsoon and receive major part of rainfall during the months of July and August. The rainfall intensity analysis show that, the study area receive higher intensity rainfall for short duration and medium intense rainfall for longer duration which eventually influences the runoff generation mechanism. High intense short duration spells contribute to maximum amount of rainfall to yearly totals and mainly goes as runoff whereas the less intense spells gets evaporated faster. Moderate intensity spells which are prolonged for sufficient durations are mainly responsible for soil moisture build up. The evaporation computed using the Turc method show that, summer months recorded higher evapotranspiration with a secondary maximum during post-monsoon months. The lower evapotranspiration rates were observed during monsoon months. The T-M method classify the climate in the region generally is humid and moist but witness water deficits during December to May after the cessation of rains which are evidenced from the water balance studies.

Soil moisture measurements were taken at 4 locations within each of the selected land covers at different soil depths and slopes to arrive at soil moisture fluxes. Both temporal and spatial variations were studied. The soil moisture variability was quite pronounced in degraded watershed compared to acacia and forested watersheds where trees are more or less uniformly distributed. The temporal variation of soil moisture was influenced by rainfall and peak soil

moisture generally preceded by peak rainfall. Degraded watershed responded relatively steeper for the rainfall events, whereas acacia and forest responded slowly and soil moisture built up was slower. The vertical profile soil moisture variation indicated that the soil moisture under acacia plantation below 1.0m depth are higher in comparison with the pattern observed under forest and degraded watersheds. This suggests the notion that the acacia trees do have a shorter root system and utilize the soil moisture available within the top soil layer. Whereas under forest, there is uniform utilization of soil moisture across the soil profile up to a depth of 1.5m.

Runoff from three land covers revealed a significantly different runoff generation mechanism. Runoff was higher from degraded forests and did not last much longer whereas acacia watershed had runoff till the end of October. Under similar conditions, runoff were more from degraded and less from forested watershed which may be due to higher water holding capacity and slow release compared to degraded forest soils. It is also observed that, despite the differences in the annual rainfall quantity, the percentage of precipitation converting into runoff remains consistent during the study period within each of the land covers. The cumulative plots of rain and runoff show a rank of degraded forest<acacia<forest in runoff generation. However, the residual cumulative plots (rainfall – runoff) indicate the reversal of the rank, i.e., forest<acacia<degraded forest. These plots provide information about the quantity of water available as a catchment storage for the processes such as evapotranspiration and ground water storage. The afforestation done on the degraded landscape has lead to an increased water availability (there is an increase of 25% of yield due to afforestation on degraded land). This increased availability of water may contribute to the building up of soil moisture, which further increase the possibility of enhanced ground water recharge. The improved catchment storage might have contributed towards low flows observed during the later part of monsoon from the acacia watershed.

The observed discharge series were used to calibrate and validate a conceptual rainfall-runoff model for the selected watersheds under forest, degraded forest and acacia plantation. The calibrated model, was then used to simulate the impact of changing land cover on the daily flow in a meso-scale watershed namely, Biligi hole with a catchment area of 28 km^2. The Biligi hole is feeding the water for the summer paddy crop in the region. In order to predict the impact, the land cover was steadily varied to replace one with another. The flows then realized from the varying land cover were characterized using the flow duration curve and by defining the

indices such as low flow index (Q_{90}/Q_{50}) and high flow index (Q_{10}/Q_{50}). The results reveal that, the Biligi hole stream may flow only for 35% of time with increased peak flows, when the entire catchment is completely degraded. On the contrary, the combination of forest and acacia plantation can sustain the flow upto about 85% of the time with a moderated peak discharge

The observed groundwater levels were used in MODFLOW model to calibrate and to verify, how the steadily changing land uses would influence the rate of groundwater recharge. The estimated rate of groundwater recharge for forest vary between 25% to 28%, Acacia 20-23% and for degraded forest 18% to 21%. Since the selected watershed were very small to evaluate the changes, the results obtained through this work has up-scaled for relatively larger basins, namely Malaprabha and Barchi catchment. These two catchments possess similar basin characteristics and with land use covers. The simulations of MODFLOW carried out for these basins with model parameters as derived from the experimental watersheds, indicates an error of 10-12% in estimating the water levels at observed sites. This exercise validates the rate of groundwater recharge estimated for experimental watersheds are more or less govern across the western Ghats region.

The results so far discussed in the preceding paragraphs suggests that, the afforestation using the exotic species such as acacia can help in

1. Restoring the hydrologic processes which were deteriorated due to the degradation of landscape to the level of natural forest over a period of time
2. Moderating the peak flow and increase the low flow quantities
3. The highest rate of groundwater recharge is observed in forest and lowest in Degraded forest.

Finally it can be concluded that, the acacia plants can be considered as a replacement for the natural forest from the hydrological perspective. However, it needs to be further verifying its utility from the point of view of bio-diversity and eco-hydrological services provided by the acacia plantation for the local community in the region which are as essential as that of the water for life.

REFERENCES

Al-Dousari A., Milewski A., Ud Din S., Ahmed M., 2010, 'Remote sensing input to SWAT model for groundwater recharge estimated in Kuwait', Advances in Natural and Applied Sciences, Volume 4, No. 1, pp. 71-77, 2010.

Amurtha Rani H. R., Shreedhar R., 2014, 'Study of rainfall trend and variability for Belgaum District', International Journal of Research in Engineering and Technology, Volume 3, no 6, May 2014.

Anibas, C. et al., 2012. A hierarchical approach on groundwater-surface water interaction in wetlands along the upper Biebrza River, Poland. *Hydrology and Earth System Sciences*, 16(7), pp.2329–2346.

Arnold, J.G. et al., 1998. Large area hydrologic modeling and assesment Part I: Model development. *JAWRA Journal of the American Water Resources Association*, 34(1), pp.73–89.

Baier J., Uhlik J., Datel J. V., 2013, 'Mathematical modelling of the groundwater and heat flow in the complicated hydrogeology structures', International journal of engineering research and technology, Volume 2, No. 11, November 2013.

Bailey, R.T. et al., 2016. Assessing regional-scale spatio-temporal patterns of groundwater- surface water interactions using a coupled SWAT-MODFLOW model. *Hydrological Processes*, 30(23), pp.4420–4433.

Barthel, R., 2014. HESS Opinions "integration of groundwater and surface water research: An interdisciplinary problem?" *Hydrology and Earth System Sciences*, 18(7), pp.2615–2628.

Barthel, R. & Banzhaf, S., 2016. Groundwater and Surface Water Interaction at the Regional-scale – A Review with Focus on Regional Integrated Models. *Water Resources Management*, 30(1), pp.1–32.

Bonell, 1993, "*Progress in understanding runoff generation dynamics in forests*," Journal of Hydrology, vol 150(2-4 Special issue on water issues and forests today): pp 217-276.
Bonell, M., 1998, "Possible impacts of climate variability and change on tropical foresthydrology," Climatic Change, 39(2-3): 215-272.

Bruijnzeel, L. A., 1989, "(De)forestation and dry season flow in the tropics: A closer look," Journal of Tropical Forest Science, 1(3): 229-243.

Bruinjzeel, L A, 1991, "Hydrology of moist tropical forests and effects of conversion: State ofknowledge review," International Association of Hydrology, UNESCO, and Free University, Amsterdam.

Bruinjzeel, L A, 1993, "Land use and hydrology in warm humid regions: Where do westand?," Journal of Hydrology, 216: 3-34.

Brunner, P. et al., 2010. Modeling surface water-groundwater interaction with MODFLOW: Some considerations. *Ground Water*, 48(2), pp.174–180.

Calder, Ian R., 1979, "The Balquhidder catchment balance and process experiment resultsin context - What do they reveal?," Journal of Hydrology, 145: 467-480.

Chinnasamy, P. & Hubbart, J.A., 2014. Potential of MODFLOW to model hydrological interactions in a semikarst floodplain of the Ozark border forest in the central United States. *Earth Interactions*, 18(20).

Condappa D., Barron J., Tomer S. K., Muddu S., 2012, 'Application of SWAT and a groundwater model for impact assessment of Agricultural Water Management interventions in the Jaldhaka watershed: data and setup of models', Technical report, Stockholm Environmental Institute, Sweden, March 2012.

Chandramohan T., Venkatesh B., Jain S. K., Singh R. D., 'Derivation of GIUH for small catchments in the hard rock region', National Institute of Hydrology, Roorkee, 1999-2000.

Douglas, E.M. et al., 2009. The impact of agricultural intensification and irrigation on land-atmosphere interactions and Indian monsoon precipitation - A mesoscale modeling perspective. *Global and Planetary Change*, 67(1-2), pp.117–128. Available at: http://dx.doi.org/10.1016/j.gloplacha.2008.12.007.

Durbude D., Rao P. R. S., Kumar C. P., 'Comprehensive hydrological studies of Malaprabha and Ghataprabha representive basins', Technical Report, National Institute of Hydrology, Roorkee, 2000-2001.

Fleckenstein, J.H. et al., 2010. Groundwater-surface water interactions: New methods and models to improve understanding of processes and dynamics. *Advances in Water Resources*, 33(11), pp.1291–1295. Available at: http://dx.doi.org/10.1016/j.advwatres.2010.09.011.

Gleeson, T. et al., 2012. Water balance of global aquifers revealed by groundwater footprint. *Nature*, 488(7410), pp.197–200.Available at: http://www.nature.com/doifinder/10.1038/nature11295.

Harbaugh, Arlen, W., 2005. MODFLOW-2005 , The U . S . Geological Survey Modular Ground-Water Model — the Ground-Water Flow Process. *U.S. Geological Survey Techniques and Methods*, p.253.

Haque M. A. M., Jahan C. S., Mazumder Q. H., Nawaz S. M. S., Mirdha G. C., Mamud P., Adham M. I., 2012, 'Hydrogeological condition and assessment of groundwater recharge usin Visual MODFLOW

modeling in the Rajshahi city aquifer, Bangladesh', Journal Geological Survey of India, Volume 79, pp.77-84, January 2012.

Huang, J. et al., 2016. Global semi-arid climate change over last 60 years. *Climate Dynamics*, 46(3-4), pp.1131–1150.

Jurado, K.Y.G. et al., 2017. Surface Water and Groundwater Interactions in Traditionally - Irrigated Fields in Northern New. , pp.1–14.

Kilb N. D., 2005, 'Models of ponding in two flooded recharge basins', Undergraduate research report, Geology department, Stony Brook University, New York (USA), Fall 2005.

Kim, N.W. et al., 2008. Development and application of the integrated SWAT-MODFLOW model. *Journal of Hydrology*, 356(1-2), pp.1–16.

Kim N. W., Chung I. M., Won W. S., Arnold J. G., 2008, 'Development and application of the integrated SWAT-MODFLOW model', Journal of Hydrology, February 2008.

Kumar C. P., 2013, 'Numerical modelling of groundwater flow using MODFLOW', Indian Journal of Science, Volume 2, number 4, February 2013.

Kumar C. P., Purandara B. K., 'Simulation of soil moisture movement in a hard rock watershed using SWIM model', Technical Report, National Institute of Hydrology, Roorkee, 2000-2001.

Lélé, Sharachchandra, 1993, "Degradation, Sustainability, or Transformation: A case study of villagers' use of forest lands in the Malnaad region of Uttara Kannada district, India," Ph.D. Thesis, University of California, Berkeley.

Lélé, Sharachchandra, 1994, "Sustainable use of biomass resources: A note on definitions, criteria, and practical applications," Energy for Sustainable Development, 1(4): 42-46.

Leta, O.T. et al., 2013. Evaluating the simulation of evapotranspiration and groundwater surface water interaction using SWAT : the river Zenne (Belgium) case study.

Liu, C. et al., 2015. Studying groundwater and surface water interactions using airborne remote sensing in Heihe River basin, northwest China. *Proceedings of the International Association of Hydrological Sciences*, 368(August 2014), pp.361–365. Available at: http://www.proc-iahs.net/368/361/2015/.

Ljungberg V., Qvist S., 2004, 'Assessment of groundwater flow and pollutant transport through modelling- a pilot study in the Sulur watershed, Coimbatore district', Master of Science thesis, Stockholm, Sweden, 2004.

Mondal N. C., Singh V. S., 2008, 'Mass transport modeling of an industrial belt using Visual MODFLOW and MODPATH: A case study', Journal of geography and regional planning, Volume. 2(1), pp.001-019, January 2009.

Mondal N. C., Singh V. P., Sankaran S., 2011, 'Groundwater model for a tannery belt in Southern India', Journal of Water Resources and Protection, Volume.3, page 85-97, 2011.

Mridhula K., 2014, 'Impact of lined/unlined canal on groundwater recharge in the lower Bhavani basin', International journal of engineering research and technology, Volume 3, No. 9, September 2014.

Needhidasan S., Nallanathel M., 2013, 'Application of Visual MODFLOW and GIS in groundwater modelling', International Journal of Civil Engineering , Volume 2, No. 3, 41-50, July 2013.

NRSC, 2011. Evaluation of Indian National DEM from Cartosat-1 Data. *Indian space Research Organization-NRSC*, 1(September 2011), pp.1–19.

Paul, S. et al., 2016. Weakening of Indian Summer Monsoon Rainfall due to Changes in Land Use Land Cover. *Nature Publishing Group*, (August), pp.1–10. Available at: http://dx.doi.org/10.1038/srep 32177.

Pradeep Kumar G. N., Kumar A. P., (2014), 'Development of groundwater flow model using Visual MODFLOW', International Journal of Advanced Research, Volume 2, No. 6, pp. 649-656, 2014. China - A synthesis. *Hydrology and Earth System Sciences*, 17(7), pp.2435–2447.

Pattanayak, S. K. and R. A. Kramer, 2001a, "Pricing ecological services: Willingness to pay for drought mitigation from watershed protection in eastern Indonesia," Water Resources Research, 2001 Mar, 37(3): 771-778.

Pattanayak, S. K. and R. A. Kramer, 2001b, "Worth of watersheds: a producer surplus approach for valuing drought mitigation in Eastern Indonesia," Environment &Development Economics, 2001 Feb, 6(1): 123-146.

Pattanayak, Subhrendu, 2004, "Valuing watershed services: concepts and empirics from southeast Asia," Agriculture, Ecosystems & Environment, September, 104(1): 171- 184.

Purandara, B. K. and C. P. Kumar, 2000, "Simulation of soil moisture movement in afforested watershed," in R. Mehrotra, B. Soni and K .K. S. Bhatia, eds., *Proceedingsof International Seminar on Integrated Water Resources Management forSustainable Development*, New Delhi, India, pp.833-839.

Purandara, B. K. and C. P. Kumar, 2003, "Hydrologic characteristics of soils under different land covers in Ghataprabha basin," *Journal of Civil Engineering, Institution ofEngineers, India*, **84**: 1-5.

Purandara, B. K., B. Venkatesh, B. Soni, R. Jayakumar and M. Bonell, 2006, I*mpact of afforestation on soil hydraulic properties: A case study In : Hydrology and watershed services in the western ghats of India: effects of land use and land cover change*, Tata-Mc-Graw Hill Publication, New Delhi.

Putty, M. R. Y. and R. Prasad, 2000, "*Understanding run off processes using a watershed model: A case in the Western ghats in South India*," Journal of Hydrology,vol 228: pp (215-227).

Rajamanickam R., Nagan S., 2010, 'Groundwater quality modeling of Amravati river basin of Karur district, Tamil Nadu, using Visual MODFLOW', International Journal of Environmental Sciences, Volume 1, no 1, 2010.

Rani, A. & Shreedhar, R., 2014. Study of Rainfall Trends and Variability for Belgaum district. *International Journal of Research in Engineering and Technology*, 03(06), pp.148–155.

Rostamian R., Jaleh A., Afyuni M., Mousavi S. F., Heidarpour M., Jalalian A., Abbaspour K. C., 2014, 'Application of SWAT model for estimating runoff and sediment in two mountainous basins in central Iran', Hydrological Sciences Journal, No. 53, no 5, December 2014.

Reshmidevi, T. V. & Nagesh Kumar, D., 2014. Modelling the impact of extensive irrigation on the groundwater resources. *Hydrological Processes*, 28(3), pp.628–639.

Rodríguez Estrella, T., 2014. The problems of overexploitation of aquifers in semi-arid areas: characteristics and proposals for mitigation. *Boletín geológico y minero*,125(1), pp. 91-109.https://dialnet.unirioja.es/servlet/articulo?codigo=4677518&info=resumen&idioma=SPA.

Shope, C.L. et al., 2014. Using the SWAT model to improve process descriptions and define hydrologic partitioning in South Korea. *Hydrology and Earth System Sciences*, 18(2), pp.539–557.

Takounjou A. F., Rao V. V. S., Ngoupayou J. N., Nkamdjou L. S., Ecodeck G. E., 2009, 'Groundwater flow modeling in the upper Anga'a river watershed, Yaounde, Cameroon', African Journal of Environmental Science and Technology, Volume 3, No. 10, pp. 341-352, October 2009.

Tian, Y. et al., 2015. Modeling surface water-groundwater interaction in arid and semi-arid regions with intensive agriculture. *Environmental Modelling and Software*, 63, pp.170–184. Available at: http://dx.doi.org/10.1016/j.envsoft.2014.10.011.

Vishal V., Kumar S., Singhal D. C., 2014, 'Estimation of groundwater recharge in the national capital territory, Delhi using groundwater modelling', Journal of Indian Water Resources Society, Volume 34, No. 1, January 2014.

Wake J. S., 2008, 'Groundwater–surface water interaction modelling using Visual MODFLOW and GIS', Master of Science thesis report, Universiteit Gent, Vrije Universiteit Brussel, Belgium, June, 2008.

Youssef T., Gad M. I., Ali M. M., 2012, 'Assessment of groundwater resources management in Wadi El Farigh area using Visual MODFLOW', IOSR Journal of Engineering, Volume 2, No. 10, pp 69-78, October 2012.

Zare M., Koch M., 2014, '3D groundwater flow modeling of the possible effects of the construction of an irrigation/drainage network on water logging in the Miandarband plains, Iran', Basic Research journals of Soils and Environmental Science, Volume 2, No. 3, pp. 29-39, June 2014.

Zeng, R. & Cai, X., 2014. Analyzing streamflow changes: Irrigation-enhanced interaction between aquifer and streamflow in the Republican River basin. *Hydrology and Earth System Sciences*, 18(2), pp.493–502.

Zhou, Y. et al., 2013. Groundwater-surface water interactions, vegetation dependencies and implications for water resources management in the semi-arid Hailiutu River catchment,

Hydrological Investigations in parts of Kodagu District

The study area

Situated in the cradle of the Western Ghats, Kodagu is 'a land ofmillion hills' (Richter 1870). The district is characterised by landwith elevation varying between 900 and 1750 m (Kodagu District Disaster Management Plan 2017–2018).The following mountain ranges run through the district.

- The Brahmagiri range running south-east–north-west allalong the Kerala border and forming the ridge line between the west flowing Barapole and the east flowing Lakshmanatirtha and Kaveri;

- The Pushpagiri range in north running nearly south-north, forming the divide line between Kumaradhara and the east flowing Harangi and Hemavathi;

- The Benganadu (Madikeri-Galibeedu) range running nearly normal to (i), interlinking the above two, and forming the ridge line between the west flowing streams Payaswini and Kumaradhara and the Kaveri;

- A few other minor ranges, branching off from the main ranges.

As is the case with the whole of the central and southern Western Ghats, Kodagu is underlain by Precambrian Igneous rocks, intrusive granites and granitic gneiss forming the basic types (Pascal 1984). The district experiences annual rainfall in the range of 1700 to 7200 mm, with an average of about 120 rainy days/year all over. Over 80% of rain in the district is of the orographic type (Putty 2010) resulting due to a continuous north-east flow of moisture from the Indian Ocean and the Arabian Sea obstructedby the mountain barriers. As a consequence, even though the daily rainfall depths are very high, short-duration intensities are only moderate.

The rare combination of very heavy moderate intensity rainfall and a hard rock base material has resulted in development of a huge regolith of soil (Bourgeon 1989) in the region—the mantlesare often greater than 50 m in depth in mid-slope areas (Darshan2016). Also, the streamflow in the region is dominated by subsur- face runoff. The mechanism of runoff generation here is best explained by the variable source area theory (Putty 2010), accord- ing to which overland flow is limited to saturated areas riparian tothe streams and to small patches of land devoid of vegetation.

The district, a major portion of which probably was covered with rainforests prior to the nineteenth century (Richter 1870) has undergone a lot of land-cover changes. There have been appre- hensions of these changes casting ill effects on the hydrology and the ecology of

the land since the period of the British (Bidie 1869). An unaccounted extent of prime forest land seems to have been exploited for commercial crops, coffee in particular. Still, the district is host to a dense vegetation cover.

All the above features, together with steep slopes, render the area landslide prone. Yet, landslides have not been a very regular feature, except for the road-side mud falls that disrupt traffic for just a few hours, in the district. The slides of 2018 have been exceptional, both in number and sizes. Hence, a study on them is interesting. The area most affected during the year lies mainly in the Benganadu hill range, covering mainly the sub-basin of Harangi and upland areas of the basin of Payaswini (Fig. 2).

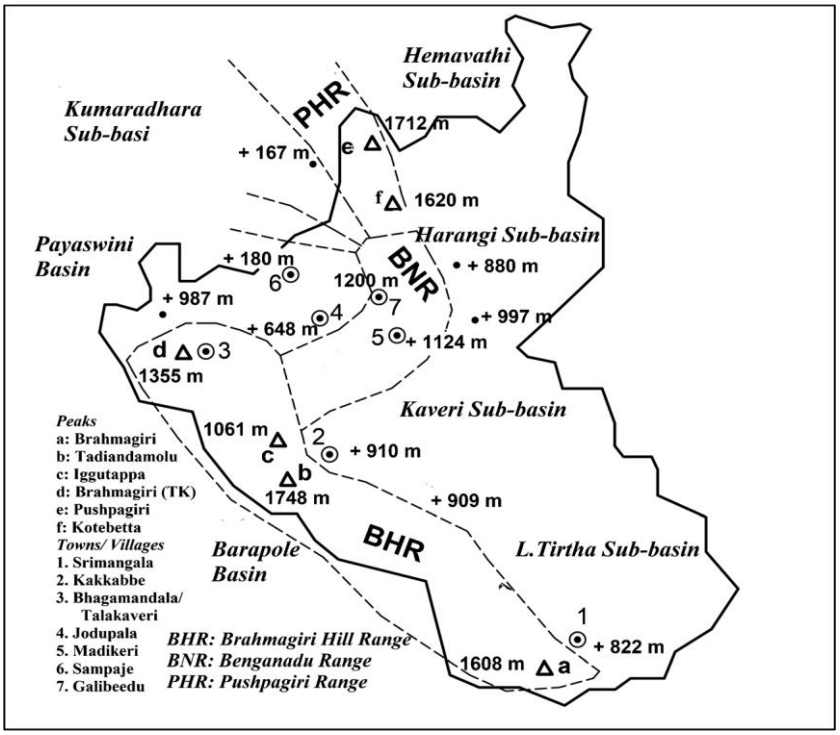

Fig. 2 Location of the study area in the district of Kodagu, Karnataka

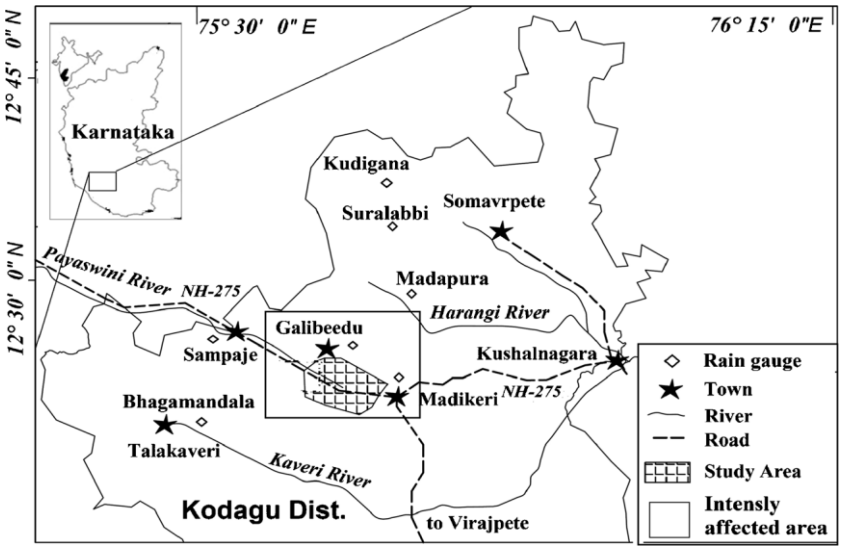

Fig. 3 The major mountain ranges and drainage basins in Kodagu

Methodology

Locational features of the sites affected

In order to understand the features of the land that has been most commonly affected, location of all the landslides sites adjoining NH-275 and the Payaswini valley was delineated and investigated (Fig. 4). Only those slides which could be identified on 'Google Earth' were included in the study. A reconnaissance survey was also carried out in order to ascertain the location of these sites. It was observed during the survey that many small slides, mostly in the valleys and a few others adjoining the road, could not be recognised on the image. These were not included in the study. Those in the valleys have gone out of the reckoning since they remain covered by thick vegetation that characterises the valleys and are away from the roads. The following features pertaining to the so spotted landslides were delineated:

(1) A reconnaissance survey of all the slides adjoining the Na- tional Highway NH-275 and the slopes draining into the valley of the river Payaswini (in which NH-275 runs) in between Madikeri and Sampaje, a distance of about 20 km, in order to establish the most commonly affected landscape;

(2) An intensive study of the selected sites to understand the topographic features and other characteristics that influence the vulnerability of land;

(3) Studies on selected ten landslide sites to understand the soil characteristics in the region;

(4) Studies on the rainfall records pertaining to 2018 in order to establish the severity of rainfall that led to the disasters; and,

(5) A study on the variations in the location of the ground water table and the growth of the saturation zone in a typical catchment during rainfall, using a watershed model.>

The details concerning the methodology adopted and the work done under each of these cases is furnished after presenting a description of the study area, the district of Kodagu.

Topographic feature of the site—valley, with contours concaved/s; the watershed divide, with contours convex d/s; or the mid-slope, with almost straight contours;

- Length and area covered on the image by the slide portion and the area affected d/s;
- Distance of the highest point (the crown) from the road, if found nearby;
- Distance of the crown of the slide from the ridge;
- Gradient upslope (from the crown to the peak/ridge)—computed as the ratio of the difference in RL (called relief) to the distance between the two points;
- Local slope obtained using the DEM;
- Land cover and human interference at the crown and in a major portion of the slide.

This information was obtained from a study of the topo-sheets, the Google Earth and a reconnaissance survey of the region approachable. The land cover is classified as forest, scrub, tree clad area, plantation and barren/ urban. The density of vegetation is also included in terms the words dense, open and sparse. Human interference is identified in terms.

Delineation of these features was accomplished using the Google Earth, the Survey of India Topo-sheets and a 30.5-m resolution DEM furnished by NRSC, ISRO. A total of 25 landslides were identified and listed. The above features pertaining to the sites are presented in Table 1. Figure 4 shows the location of these sites. The following are the important inferences that can be drawn from the illustrations:

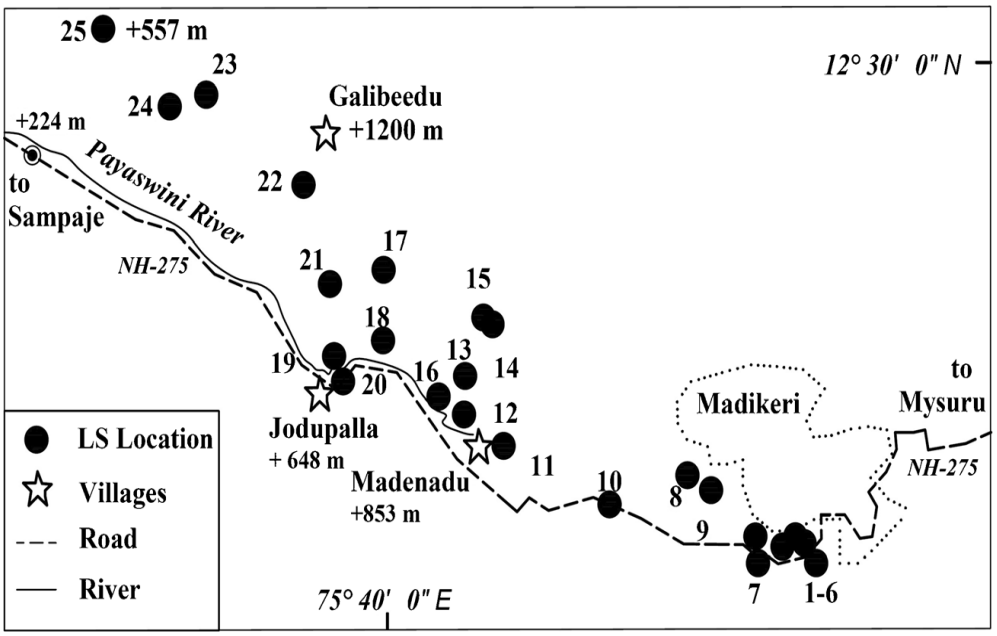

Fig. 4 Location of the sites investigate

Plate : Field investigations in Kodagu region

- The general perception that landslides are caused by anthropogenic activities like land-cutting, for road building in particular, is ill founded—most of the landslides studied are found to have been initiated far removed from the roads. Also, those adjoining the road are very small in size.
- Land slope at all the sites, except a couple, is very high ranging from about 30% to over 60%—the study area is on the western slopes of the ranges, which in general is very steep, and hence no inference could be drawn specifically on the influence of slope on the slides.
- Sites with all sorts of land cover, including grasslands, open scrub, plantations and dense forest lands, have been affected.

  This fact opens up a Pandora's Box—it renders the argument that vegetative cover with deep-rooted trees and shrubs can reduce the occurrence of rapidly moving landslides by strengthening soil layers and improving drainage. There have been arguments (Hamilton 2008) that Deep landslides resulting from continuous heavy rainfall or earthquakes are less likely to be affected by vegetation. According to Bruijnzeel (2004), whereas a well-developed tree cover can prevent shal- low landslides up to about 1 m in depth, landslides of depth more than 3 m are not appreciably affected by forest cover. The present one is a very strong case in support of these arguments. It is interesting to note that vegetation cover increases infiltra- tion, which only helps build up of the ground water table in the valley portions, enhancing the chances of sliding. Facts also go to support the theory that hefty trees on unsupported cut slopes even may go counterproductive (Forbes and Broadhead 2011), often leading to small land slips. In cases of extreme climatic events such as hurricanes, trees may actually increase slope instability due to the trees' weight and the susceptibility of particularly high trees to uprooting due to extreme storms, damaging the soil matrix (Bruijnzeel 2004).
- Very few landslides are located near the watershed divide andridges; valleys are the zones prone to slides, meaning that hydrology is the subject matter most pertinent to a study of landslides in this region. This observation is in conformity with the experiences reported by Kuriakose et al. (2008), who have carried out extensive studies on landslides of Kerala.
- As mentioned earlier, many more slides that occurred in the valleys during the critical period of 2018 could be sited during the reconnaissance. This fact highlights the

importance of subsurface water in causing slides. The present work gains importance since it focuses on hydrology pertaining to the deluge of 2018. Rainfall, topographical characteristics and sub- surface flow mechanisms are the aspects of hydrology that can be supposed to influence the vulnerability of the land to slide. Field surveys show that all the landslides have been removal and movement of huge masses of soil, along with the vegetative cover on the surface and that the debris consisted of very few rock masses. Hence, investigations on soils carried out in selected sites will be presented first. Rainfall and other hydro- logical aspects of the deluge will be looked in to subsequently.

Soil characteristics

A glimpse of the depth of soil in the region can be had from the road side cuttings on highways and from the vertical cuts caused due to the landslides—which are often deeper than 10 m. The information about soil mantles in Kodagu made available by the Dept. of Mines and Geology is presented in Fig. 5. The subsurface profiles shown here are from places namely Madapura, Somavarapete and Napoklu. Places around Madapura experienced innumerable slides in 2018. It is seen that soil thickness at these three places is as high as 22 m, 28 m and 42 m, respectively, and the hard base rock is present only below these depths. Soils so deep are not exclusive to Kodagu alone. Data on subsurface profiles furnished by the Karnataka Power Corporation Ltd., obtained from their project sites, confirm that deep soils feature all highly wet regions of Western Ghats in Karnataka (Darshan 2016). Sankar et al. (2017) have detected and investigated tunnels produced due to soil piping 30 to 40 m below the ground level in the district of Kannur, in the state of Kerala (Fig. 1), adjoining Kodagu. This explains why landslides in the region have been removal of only soil. Sajinkumar et al. (2011), who have carried out preliminary studies on landslide occurrences in Ernakulam and Idukki districts of Kerala, also opine that presence of very thick weathered

Table 1 Locational, topographic and land cover characteristics of the sites

No.	Topography	Length[a] (m)	Area[b] (ha)	Dist.[c] road (m)	Land[d] cover	Human interference	Dist.[e] ridge (m)	Slope[f] (%)	Local slope (%)
1	Mid-slope	13	6	12	OS	D	29	44.8	55.8
2	Valley	20	4	166	OS	D	103	34.0	49.0
3	Mid-slope	123	5	117	TC-S	D	31	26.9	56.6

4	WS divide	100	14	155	BU	D	71	35.2	40.4
5	WS divide	29	12	30	TC-S	D	271	28.5	51.0
6	Valley	67	6	195	TC-S	D	307	29.6	28.7
7	Mid-slope	18	4	28	TC-S	D	495	29.7	30.6
8	Valley	910	444	1016	OS+ Pl.	D	248	21.4	32.5
9	Valley	738	202	1059	OS	PD	230	39.1	21.3
10	Valley	31	28	39	Pl.	D	129	30.2	61.3
11	Valley	943	974	800	TC-D	PD	64	34.4	55.4
12	Valley	447	179	454	Pl.	D	330	36.4	22.2
13	Valley	1181	1143	4042	TC-D	SD	990	25.5	30.6
14	WS divide	2040	751	1852	OF/ DS	SD	53	15.1	21.3
15	Mid-slope	1885	404	1862	DS	U	40	17.5	34.4
16	Mid-slope	140	61	347	Pl.	D	1550	26.9	44.5
17	WS divide	247	90	584	Pl.	D	1490	32.9	48.3
18	Valley	2276	1044	2314	DMJ	U	685	36.6	36.0
19	Mid-slope	78	20	42	TC-D	PD	160	45.0	40.4
20	Valley	206	42	340	TC-D	PD	2246	24.8	44.5
21	Valley	798	394	1230	DMJ	U	1516	31.9	40.8
22	Valley	2180	1761	2290	DMJ	U	540	53.3	48.1
23	WS divide	2743	1175	2594	DMJ	U	810	49.9	73.2
24	Valley	1846	813	2094	DMJ	U	56	38.8	60.1
25	Valley	183	75	2360	DMJ	U	1278	32.0	14.1

a Length of the landslide plus the area affected, as seen on the image

b Area affected in square meters

c Distance of the highest point (crown) from the nearest road in meters

d Land cover in the vicinity of the slide

e Dist. of the crown from the ridge (m)

f Average slope from nearest peak/ridge to the crown

Notations: *FDS*, fairly dense scrub; *OS*, open scrub; *DS*, dense scrub; *Pl.*, cardamom/coffee plantation; *TC-S*, sparsely tree clad; *TC-D*, densely tree clad; *DMJ*, dense mixed jungle (forest); *B/U*, barren/urban; *D*, disturbed (regularly accessed); *PD*, partly disturbed (often accessed, but not much activity); *SD*, slightly disturbed (seldom accessed); *U*, undisturbed (no access) zones is the main cause of landslides in the region. Detailed studies on landslides in such deep soil regions are not available and general studies on landslides attach only a secondary impor- tance to soil characteristics (Sharma et al. 2012; Fonseca et al. 2017). Most studies deal with soils of thickness of the order 1 to 2 m and classify them as shallow (< 50 cm), moderately shallow, moderately deep and deep (> 100 cm). Generally, soils on granite are believed to be shallow with low storage and high permeability, resulting in relatively high slope instability (Walker and Shiels 2013). Hence, deep landslides are considered rooted in bedrock. Commonly, studies on deep slides presume that landslides are a direct result of

structural deficiencies in the strength of the rock and emphasise on the presence of weak zones like faults and consider lineaments an important factor in mapping hazard zones (Anbalagan 1992; Chawla et al. 2018). Therefore, a study on land- slides in Kodagu is important—it can be expected to throw new light on this natural disaster in very deep soils.

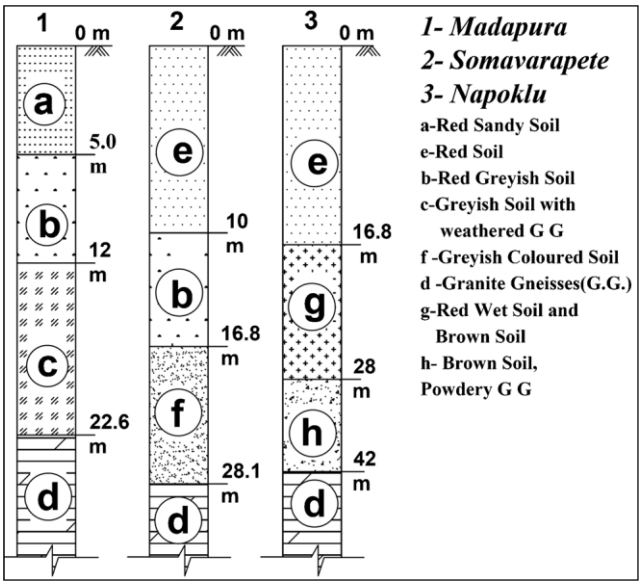

Fig. 5 Subsurface profiles showing the soil depth and type in the study area(Source: Dept. of Mines and Geology, Madikeri)

In the present work, soil characteristics of the region of the landslides were analysed using soil samples collected from ten slide sites. These sites were selected through a reconnaissance survey in the region keeping in view the facilities available for collection and transport of the samples. At each of the ten selected sites, soil samples were collected at two points—one near the crown and the other near the base. At the crown, samples were collected on the surface. At the base, sampling was done at undisturbed portions of the land nearest possible to the slide, so as to get information on the in situ soil. Samples were collected 3–6 m below the surface either on the vertical face of the slide or at tall road cuttings adjoining the slide. Both core and bulk samples were collected to facilitate laboratory tests for density, permeability and texture.

Results from the tests are presented in Table 2. This table furnishes the textural classification, the fraction of silt and clay present, the density and the permeability of the soil. A few important observations from the table are as below:

- Soils are dominated by the silt fraction—soils at the bottom layers are all sandy silts, while those at the surface are either
  sandy silts or silty sands;
- Clay percentages are low—they vary between 2.3 and 12.7 in the bottom layers. This renders the soil highly stable, permitting
  vertical unsupported road cuttings;
- Dry densities are generally low, ranging between 900 and 1400 kg/m3. Considering the specific gravity of solids as 2.6, the
  corresponding porosities work out to be between 65 and 45%. This means the soils are highly porous, capable of storing large quantities of water;
- Soils are generally highly permeable at the surface, the values of coefficient of permeability (K) going up to 250 mm/h.
  Results from infiltration tests reported by Putty et al. (1997) and Chaitra et al. (2015) support this observation. However, permeability values in the subsurface layers indicate that drainage rates are low, ranging between 1 and 4.8 cm/h. The high infiltration capacity of the terrain along with a low per- meability soil matrix can be expected to result in high amounts of soil water storage during prolonged rainfall spells, leading to excessive pore pressures. Extensive studies in the region (Putty and Prasad 2000; Putty 2006; Sankar et al. 2017) have established that the soil mantles in the Sahyadris are characterised by pipes that drain subsurface water quickly to the streams. Piping renders the slopes stable (Jones 1994) in the usual case. But, under exceptionally heavy continuous spells of rain, the soil matrix may get saturated in the valley portions, into which soil moisture converges. An inves- tigation of the rainfall of 2018 and an analysis of the soil water storage pattern on a typical slope can hence be expected to reveal the cause of the devastation that struck Kodagu during the year. A discussion of the rainfall pattern is presented first.

Studies on the rainfall of 2018

The work on rainfall included (i) studies on progress of monsoon rainfall in the year, with data on cumulative rainfall, (ii) probability analysis of indices of extreme rainfall and (iii)

analysis of short-duration intensities on the days of the deluge. The first two components were accomplished using daily rainfall data, made available by Karnataka Directorate of Economics and Statistics (KDES), from stations in the affected area. Intensity studies pertained to the data from the Self Recording Rain Gauge (SRRG) at Kudigana being maintained by NIE-WRC.

Progress of the monsoon rain

It has been observed that the catchment of Harangi (Fig. 2) was the most affected due to the excess rainfall of 2018. Hence, studies on rainfall pertained to the data from this region. Daily data from stations at Surlabbi, Galibeedu and Kudigana were used. It has been found from the records that since 2000, 2013 and 2018 have been the years of excess rainfall while, 2011 has been the one recording the normal amount. Hence, the rainfall series during these years were mutually compared by plotting cumulative rainfall against time. Figure 6 shows the facts. It is clearly observed from the illustration that the progress of rainfall in 2013, which received almost the same amount as in 2018, has been very steady, whereas 2018 saw an extremely heavy spell during the period between the 5th and 16th of August, which led to the greatest damage. This inference is in coherence with the observations of Ibsen and Casagl (2004) that a two-stage pattern of precipitation, comprising a preparatory period and a triggering period, is necessary for inducing most landslides.

Probability analysis of extreme values

Most of the landslides in the region were reported to have oc- curred on the 15th, 16th and 17th of August. Hence, an attempt was made to quantify the rainfall of this spell by means of a probability analysis, using records from four stations in the Harangi catch- ment and two other prominent stations in Kodagu. For the pur- pose, indices of extreme rainfall, 1-day, 2-day, 3-day, 5-day and 10-day extreme values were computed for sufficient lengths of period (Table 3), and the series were subjected to probability analysis. Suitability of the normal, log-normal and Gumbel distributions was studied on data from the station of Somavarpete, whose record length is over 100 years. It was found that the Gumbel distribution fits the data the best (Nitish 2019). Hence, the return periods of extreme rainfall for the year 2018 were estimated using the Gumbel function. The results are

presented in Table 3. It is observed from the table that for the stations in the Harangi basin, while the 1-day, 2-day and 3-day extreme values for 2018 show return periods of 3 to 28 years, the 5-day and 10-day extremes have been highly excessive with return periods exceeding 50 years. It is also seen that in the case of Galibeedu, the 2018 rainfall has been exceptionally high, with the extreme values showing return periods of 150 to over 500 years. Consequently, it has been observed that it is the region close to Galibeedu (Fig. 2) which was the worst affected by landslides. On the other hand, data from Bhagamandala, which is situated in the wettest part of Kodagu, shows that the 2018 rainfall in that region is not exceptionally different from the normal year.

Table 2 Soil characteristics at landslide sites

Sampling site	Silt (%)	Clay (%)	Texture	Density (g/cm^3)	K_s (cm/h)
Site 1					
Top	44	9	Sandy silt	1.35	4.6
Bottom	36.7	6.5	Sandy silt	1.06	4.8
Site 2					
Top	27	7	Gravelly sand	1.35	19.6
Bottom	36	3	Sandy silt	1.28	2.1
Site 3					
Top	36.6	10.2	Sandy silt	1.13	8.6
Bottom	39.6	2.4	Sandy silt	1.37	1.1
Site 4					
Top	29.6	14	Sandy silt	1.00	25.3
Bottom	21.8	9	Sandy silt	1.03	2.3
Site 5					
Top	51	11	Silty sand	1.24	14.7
Bottom	57	12.7	Silty sand	1.25	3.5
Site 6					
Top	27.7	3.5	Sandy silt	1.27	13.3
Bottom	32.8	2	Sandy silt	1.37	1.6
Site 7					
Top	27	6	Sandy silt	0.9	4.3
Bottom	31.5	10.5	Sandy silt	1.3	1.3
Site 8					

Top	32.2	10	Sandy silt	1.05	20
Bottom	32.4	8	Sandy silt	1.39	2.1
		Site 9			
Top	27.2	5	Gravelly sand	1.2	5.4
Bottom	38.7	9.5	Sandy silt	1.2	4.6
		Site 10			
Top	33.1	11.9	Sandy silt	1.27	13.3
Bottom	30.5	2.3	Sandy silt	1.37	1.6

Interestingly, few slides have been reported from this region. Further, data from the station at Kudigana shows that the 5-day extreme for the year (during the period 13th to 17th of August) is equal to 1686 mm and is the highest ever recorded in the history of Kodagu. The earlier highest 5-day extreme for any location in the District has been 1462 mm, recorded in 1964 at Bhagamandala, a station receiving rainfall similar to Kudigana. This spell of unprecedented rain fol- lowing a highly wet 2-month period seems to have been behind the devastation caused in the region. Yet, the short-duration intensities, which are always higher than the intensities for longer durations, are usually considered to be more important in causing overland flows and landslides. The following is an analysis of intensities on the 3 days of the deluge. The data analysed has been procured from the SRRG being maintained by the NIE-WRC at Kudigana. rainfall intensity is higher than the infiltration rates. The duration for which the various intensities were exceeded on the most intense rainy day is shown in Fig. 9. It can be observed from here that intensities greater than 50 mm/h lasted only about 10 intervals (of 15 min) on the day. Con- sidering the infiltration rates of the order of 100 mm/h, as explained in 'Soil characteristics' above, it can be seen that most of the rainfall gets infiltrated in this region. Hence, excessive overland flow cannot be expected to have been the cause of the landslides.

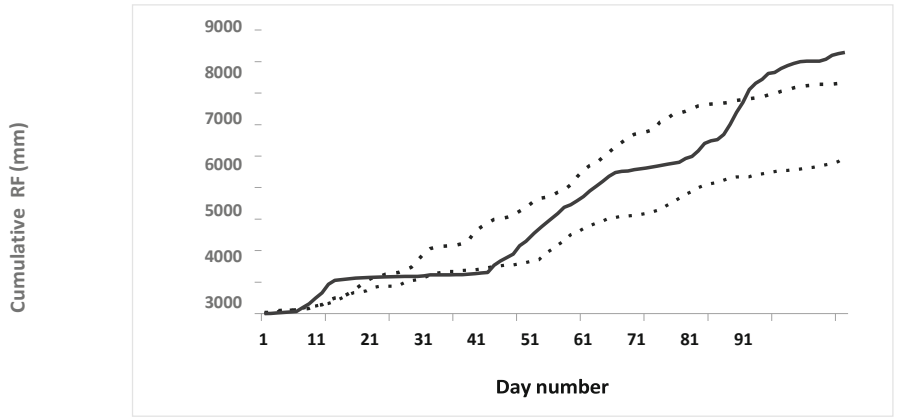

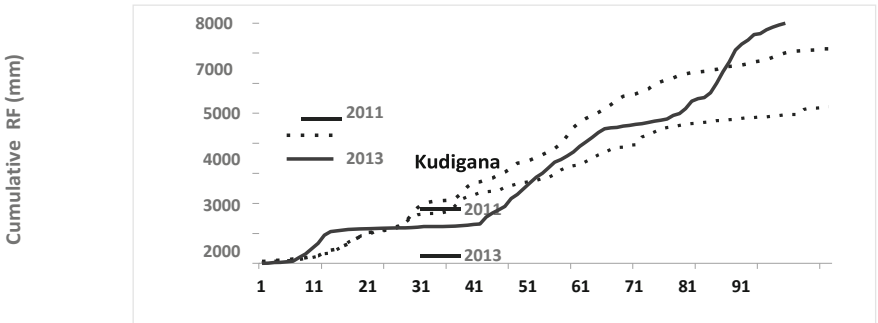

Fig. 6 Progress of monsoon rainfall (from 1st June to August end) of 2011 (normal), 2013 (highly wet) and 2018 (highly wet) in the Harangi basin

Short-duration intensities on the days of deluge

Figure 7 shows the 15-min rainfall values recorded at Kudigana on the 16th of August. It is interesting to note that the rainfall is nearly continuous on days like this, and the intensities are not extraordinary. Figure 8 shows the intensity–duration curves obtained from the data of the 3 days (13th, 15th and 16th) of excessive rainfall at the station. The following observations are important:

(i) The maximum 15-intensity for the days are 60, 80 and 102 mm/h, respectively;
(ii) The hourly maximum is about 60 mm/h;
(iii) Three-hour maximums are just about 35 mm/h;
(iv) Intensities for durations longer than 10 h are nearly same at around 15–25 mm/h.

These intensities are not unusually high. Very commonly, floods resulting due to overland flow are attributed to be the cause for landslides (Parkash 2019) and mitigation measures prescribed include provision for draining overland flow properly.

Overland flow occurs when On the other hand, high rates of infiltration lead to excessive storage and result in flow of large quantities of subsurface water on highly wet days. Subsurface flow from the landslide locations has been documented by GSI (2018a) also. As reported by Jain et al. (2019), GSI states thus: 'Clean water flow in force from inside the slope: it was observed that considerable volume of very clean water was coming out from the middle parts of the landslides. This continuous flow of the water in force inside the slope in fissures and cracks will decrease the stability of the slope and eventually will act as a triggering factor for slope failure'. Probably, GSI has wrongly attributed 'continuous flow of the water in force' to flow through fissures in rocks. Studies (Jones 1994; Tsukamoto et al. 1982) have established that piping, in spite of being a mechanism of draining water out quickly, results in the soil mantle near the valleys grow weaker than the rest of the land. Under prolonged heavy downpour lasting days together, as it happened during the second week of August 2018, the valleys may get saturated and yield under extreme conditions. The simulations of a hydrological model can be used to throw light on the growth saturation in valleys. An attempt in this regard is presented below.

A model to study subsurface flow and surface saturation

In order to investigate the build-up of the water table and the growth of the saturated zone during rains, the simulations of a ground water flow model, applied on a typical micro-catchment in the region are used. The model used is MODFLOW (Harbaugh 2005), which is available as an open-source software (Winston 2006). This three-dimensional distributed physically based model takes recharge at the land surface as input and simulates variations in the ground water table and ground water outflow as the outputs. It uses aquifer parameter values that can be obtained from field measurements. When coupled with a surface runoff model, which estimates overland flow and infiltration amounts, MODFLOW can be used as a watershed model to simulate runoff from the catchment. Ghanshyam (2019) modified this model to facilitate application in variable source area regions (Putty 2010), in which the recharge zone is a dynamic one. In this type of applications, the catchment will comprise two parts, the saturated and the unsaturated. Rainfall on the saturated zone, which usually lies riparian to the stream channels, will immediately runoff as 'source area flow' and rainfall on the unsaturated part, in excess of initial abstractions, will get infiltrated completely. The infiltration recharges subsurface storage and augments ground water in course of time.

Mountainous and forested/grassed areas of Sahyadris belong to this category of catchments. In the method developed by Ghanshyam (2019) for applying MODFLOW to suit the dynamic nature of the recharge zone, information on the variable saturated area has to be input manually to the model in steps, at the end of each of which the model outputs the ground water levels and ground water flow. The source area runoff is estimated as equal to the rainfall on the fraction of the catchment which is saturated. The model can be run, for convenience, using steps of 5 or 10 days each, when daily rainfall data is used. The model simulates daily runoff and water table level. Further details of the model are not furnished here for want of space, but can be obtained from the authors.

Table 3 Magnitude and return period of extreme rainfall values for the year 2018 compared with highest ever in the records

Station/data length	RF (mm)/return period	1 day	2 days	3 days	5 days	10 days
Madikeri (1960–2018)	2018 RF	184.2	320.6	440.8	681.6	1139.8
	T (years)	7.2	9.5	13.0	28.3	68.8
	Highest RF	250.8	371.6	462.6	681.6	1139.8
Madapura (1970–2018)	2018 RF	206.0	373.6	487.2	749.6	1066.6
	T (years)	28.6	49.3	40.1	74.0	65.6
	Highest RF	262.4	386	502.4	749.6	1066.6
Suralabbi (1998–2018)	2018 RF	400.4	778.4	1101.4	1693.4	2826.4
	T (years)	18.2	48.7	57.9	65.6	57.9
	Highest RF	482	778	1101	1693	2826

Galibeedu (1970–2018)	2018 RF	352	702	932.2	1263	1966.9
	T (years)	142.9	369.1	475.4	447.6	561.5
	Highest RF	352	702	932.2	1263	1966.9
Sampaje (1960–2018)	2018 RF	177.6	320.6	469.8	729.4	1124.2
	T (years)	3.5	6.0	11.5	41.9	62.9
	Highest RF	275.6	447.5	608.5	729.8	1124.2
Bhagamandala (1960–2018)	2018 RF	252.0	502.4	667.8	979.0	1397.0
	T (years)	2.1	3.5	3.5	4.5	4.2
	Highest RF	530	790	1061.8	1452.2	1968.6

In the present work, the model has been applied on a micro- catchment of area at 0.53 km2, located in the Kumaradhara Field Hydrological Laboratory in Kodagu, a facility being maintained by the Water Resources Centre of The National Institute of Engineering (N.I.E., Musuru), to which the authors are affiliated. The model has been applied using daily rainfall data from Galibeedu for 3 years—2011, 2013 and 2018 ('Progress of the mon-soon rain') and the simulations are studied. A 30-m resolution DEM is used to obtain the topography of the watershed. The catchment is assumed to be made up of two layers vertically, with the total soil thickness varying from 2 m adjoining the streams to 40 m near the ridges. Parameter values used by Ghanshyam (2019) for a nearby catchment, on which the model was applied in order to test its performance and found to be reliable, have themselves been used for the present case also. The initial level of the ground water table is fed in to the model, based on the experience of the authors and has been assumed to vary between 3 and 10 m below the ground level. The simulations of the model are presented in Fig. 10 and in Table 4. The way the saturated source area expanded during the monsoon of 2018 is shown in Fig. 10. The elevation and slope map of the catchment are presented in Fig. 11. Table 4 presents the pattern of growth of saturation during the 3 years and the rainfall during the corresponding period. It can be ob- served from these illustrations that the saturation area lies in the flat valley portions of the catchment during the first few fortnights after the beginning of the monsoon (assumed to be by 1st of June), while it grows to rise to higher elevations and cover steeper slopes during the wetter days. It is observed that by 9th of August 2018, the saturation zone had grown to about 54% of the catchment and covered very steep portions of the land. The rainfall in the 1-week period following it has been over 1500 mm, an

extreme combina-tion probably unprecedented in the recent history of Kodagu. It can be argued that such a combination of extreme conditions resulted in the disastrous landslides of the year. Table 4 shows that 2013 also saw extreme conditions of saturated areas growing to over 45% by 9th of August. However, the rainfall by this time of year is found to have decreased, not having led to disasters of the kind of 2018.

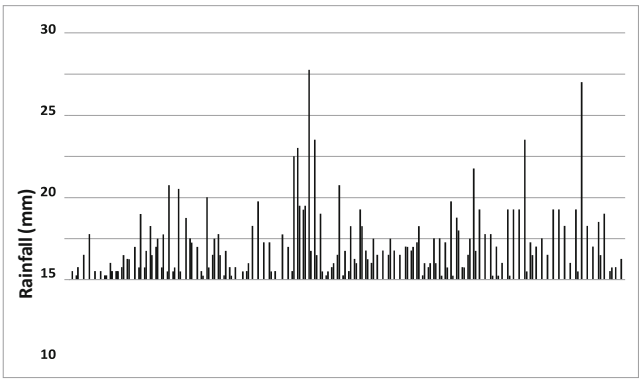

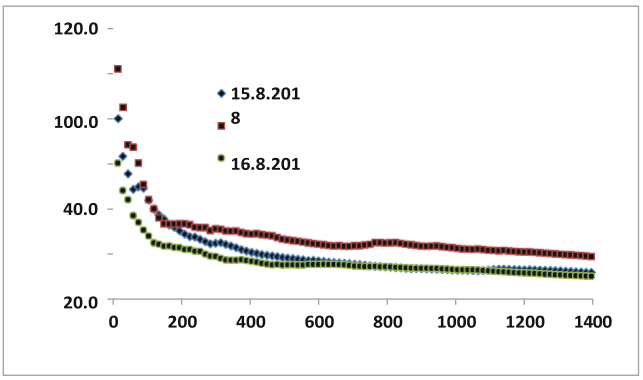

Fig. 7 Fifteen-minute rainfall recordings of days 15th–16th August at Kudigana (time beginning at 0830 hours on the 15th). Fig. 8 Intensity–duration curves of 3 days of excessive rainfall

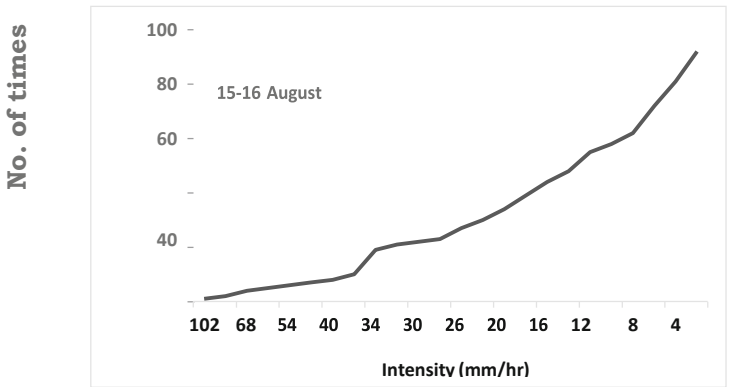

Fig. 9 Intensity prevalence—the No. of 15-min intervals with higher intensities

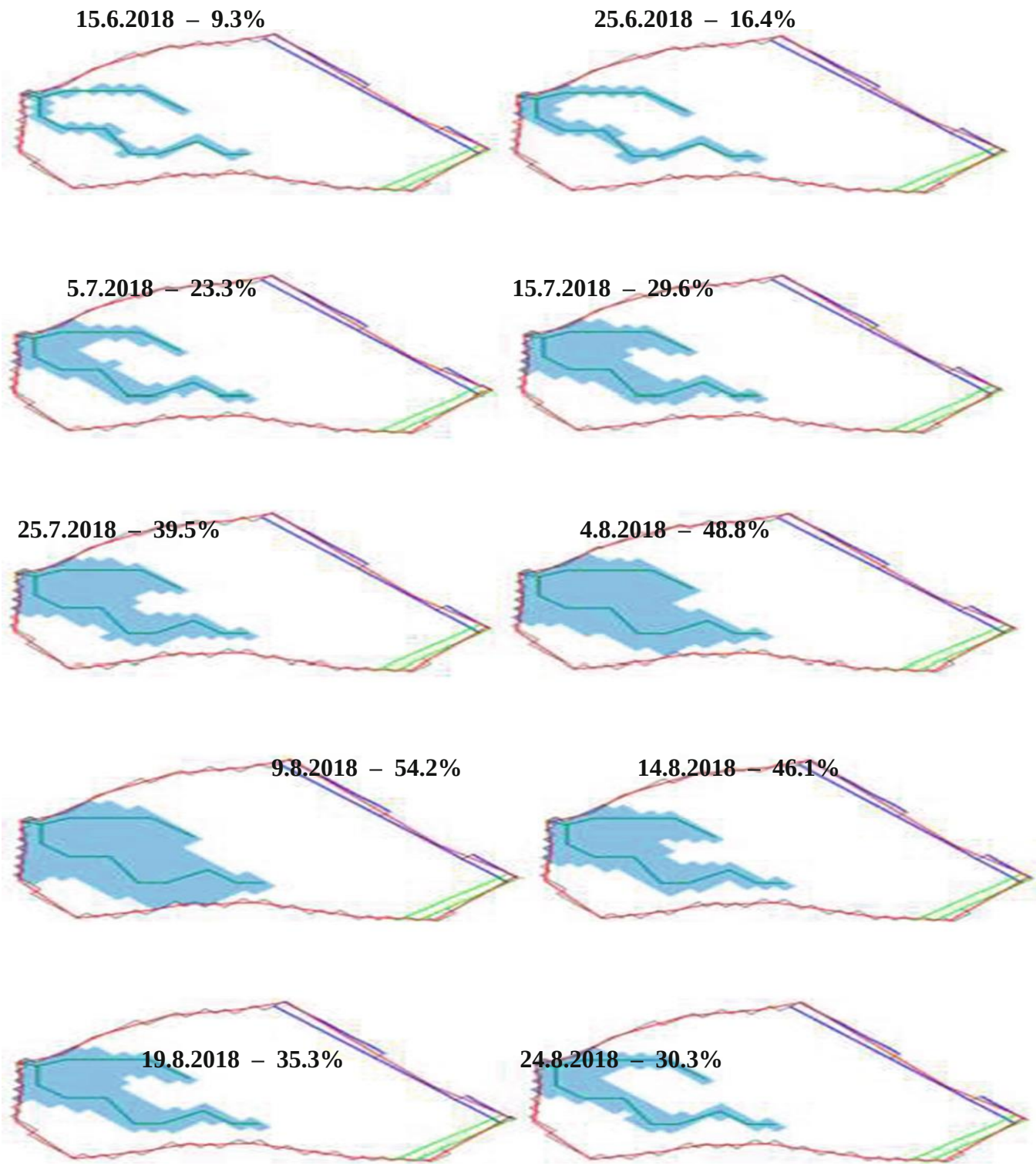

Fig. 10 Variations in the saturated zone in a catchment—the model simulations

Table 4 Growth of saturation zone—the model simulations

Date	Year2011 RF (mm)	Saturated area (%)	2013 RF (mm)	Saturated area (%)	2018 RF (mm)	Saturated area (%)
Up to 15 Jul	1160.7	25.0	2405.9	27.9	2308.1	29.6
25	656.4	29.8	978.3	35.3	760.9	39.5
4 Aug	349.1	37.1	609.8	41.2	331.0	48.8
9	438.9	30.1	198.8	47.1	607.3	54.2
14	194.6	24.7	186.6	37.3	968.0	46.1
19	67.2	18.9	129.6	28.6	840.0	35.3

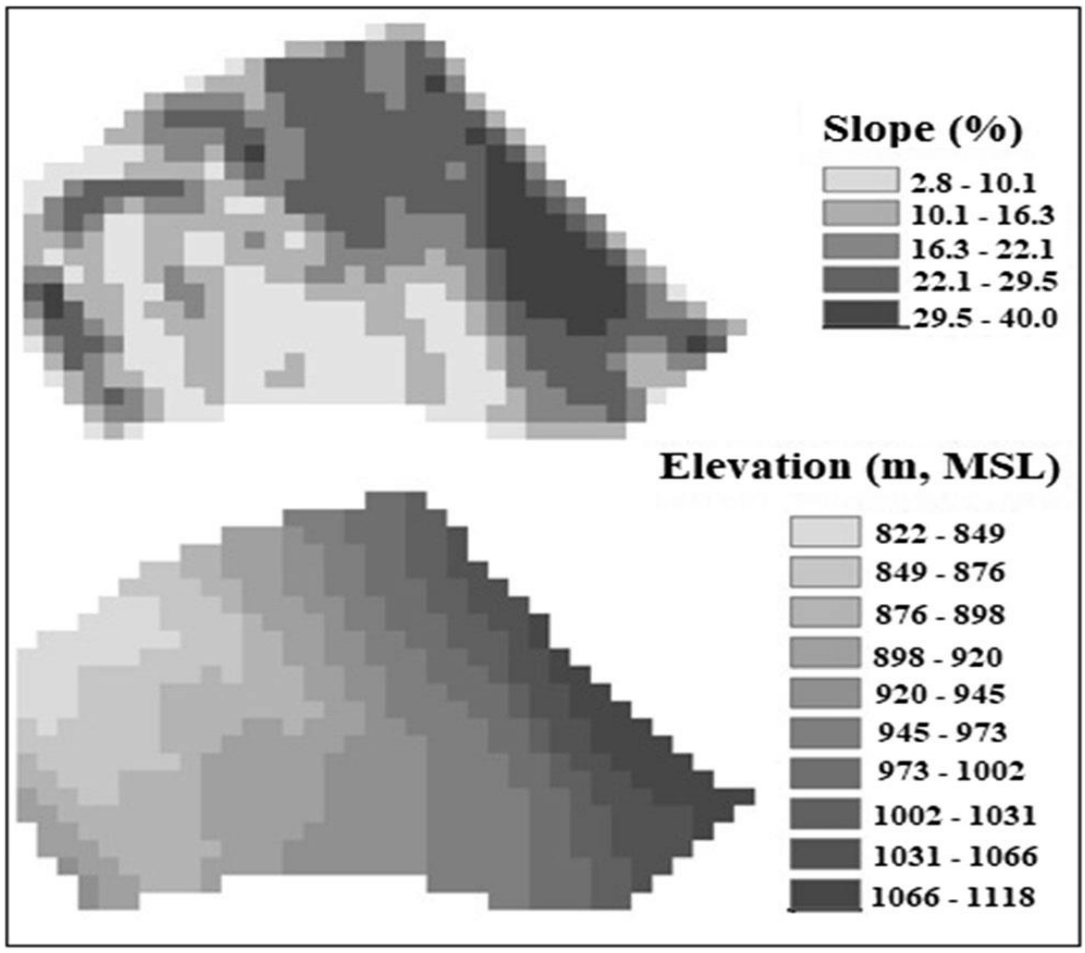

Conclusions

According to DST (2016), investigation of known sites is a thrust area in landslide research. The present work was taken up in order to investigate the events of 2018 that led to extensive and very deep landslides in Kodagu in Karnataka. The interferences drawn from studies on the location of the major landslides, the soil properties at these sites, rainfall characteristics during the year and a model analysis can be summarised into the following conclusions:

- Landslides have occurred on all sorts of land, both disturbed and undisturbed,

implying that anthropogenic activities are not the primary cause of the landslides;

- Very deep and porous soils, characterised by high infiltration rates and a low permeability matrix, are prone to excessive pore pressures due build-up of the ground water table; the exceptionally wet 10 days between 9th and 17th of August, which followed a highly wet 2-month period, seems to have been the factor leading to landslides; 3-day and 5-day extreme rainfall magnitudes during this period have had return periods of around 20 and 50 years, respectively. These extreme rainfall values at Galibeedu, places near which were the worst affected, had return periods of 140 to 2000 years;
- Despite very high magnitudes of daily rain, overland flow is not widespread since short-duration intensities are only moderate and infiltration rates are high; Simulations of the water-shed model indicate that the growth of saturated zones to very steep portions of the valley combined with an unprecedented spell of rain is the most possible triggering factor for the disastrous events in 2018.

Acknowledgements

This investigation was taken up as a part of a major project sponsored by the Ministry of Earth Sciences (MoES), Govt. of India. The authors acknowledge with thanks the authorities of MoES for funding the project. A part of the rainfall data used in the study has been made available by the Karnataka Directorate of Economics and Statistics. The subsurface profile data has been furnished by the Dept. of Mines and Geology, Karnataka. The authors acknowledge with thanks the authorities of these organisations for the help.

Data availability

The datasets generated during and analysed during the current study are not publicly available since they have been procured through intensive field work by the students and will be used by the next batch of students. However, data are available from the corresponding author on reasonable request. Daily rainfall data for Karnataka can be procured on request from Karnataka Directorate of Economics and Statistics, Bengaluru, India.